Supramolecular Assemblies on Surfaces: Nanopatterning, Functionality, and Reactivity

Dominic P. Goronzy,[1,2] Maryam Ebrahimi,[3,a] Federico Rosei,[3,10] Arramel,[4] Yuan Fang,[5] Steven De Feyter,[6] Steven L. Tait,[7] Chen Wang,[8] Peter H. Beton,[9] Andrew T. S. Wee,[4] Paul S. Weiss,[1,2,11,*] and Dmitrii F. Perepichka[*,1,5]

[1]California NanoSystems Institute, University of California, Los Angeles, Los Angeles, California 90095, United States

[2]Department of Chemistry and Biochemistry, University of California, Los Angeles, Los Angeles, California 90095, United States

[3]INRS Centre for Energy, Materials and Telecommunications, 1650 Boul. Lionel Boulet, Varennes, Quebec J3X 1S2 , Canada

[4]Department of Physics, National University of Singapore, Singapore 117542, Singapore

[5]Department of Chemistry, McGill University, Montreal H3A 0B8, Canada

[6]Department of Chemistry, KU Leuven, Celestijnenlaan 200F, Leuven 3001, Belgium

[7]Department of Chemistry, Indiana University, Bloomington, Indiana 47405, United States

[8]National Center for Nanoscience and Technology, Beijing 100190, China

[9]School of Physics & Astronomy, University of Nottingham, Nottingham NG7 2RD, United Kingdom

[10]Institute for Fundamental and Frontier Science, University of Electronic Science and Technology of China, Chengdu 610054, PR China

[11]Department of Materials Science and Engineering, University of California, Los Angeles, Los Angeles, California 90095, United States

"God made solids but surfaces were the work of the devil"

Wolfgang Pauli

[a]Present address: Department of Physics, Technical University of Munich, James-Franck-Str.1, D-85748 Garching, Germany

Abstract

Understanding how molecules interact to form large-scale hierarchical structures on surfaces holds promise for building designer nanoscale constructs with defined chemical and physical properties. Here, we describe early advances in this field and highlight upcoming opportunities and challenges. Both direct intermolecular interactions and those that are mediated by coordinated metal centers or substrates are discussed. These interactions can be additive but they can also interfere with each other leading to new assemblies in which electrical potentials vary at distances much larger than those of typical chemical interactions. Earlier spectroscopic and surface measurements have provided partial information on such interfacial effects. In the interim, scanning probe microscopies have assumed defining roles in the field of molecular organization on surfaces delivering deeper understanding of interactions, structures, and local potentials. Self-assembly is a key strategy to form extended structures on surfaces, advancing nanolithography into the chemical dimension and providing simultaneous control at multiple scales. In parallel, the emergence of graphene and the resulting impetus to explore 2D materials have broadened the field, as surface-confined reactions of molecular building blocks provide access to such materials as 2D polymers and graphene nanoribbons. In this Review, we describe recent advances and point out promising directions that will lead to even greater and more robust capabilities to exploit designer surfaces.

Keywords: self-assembled molecular networks; surface-templated polymerization; two-dimensional polymers; supramolecular assemblies; scanning tunneling microscopy; molecular electronics; graphene nanoribbons

ToC/Abstract Graphic

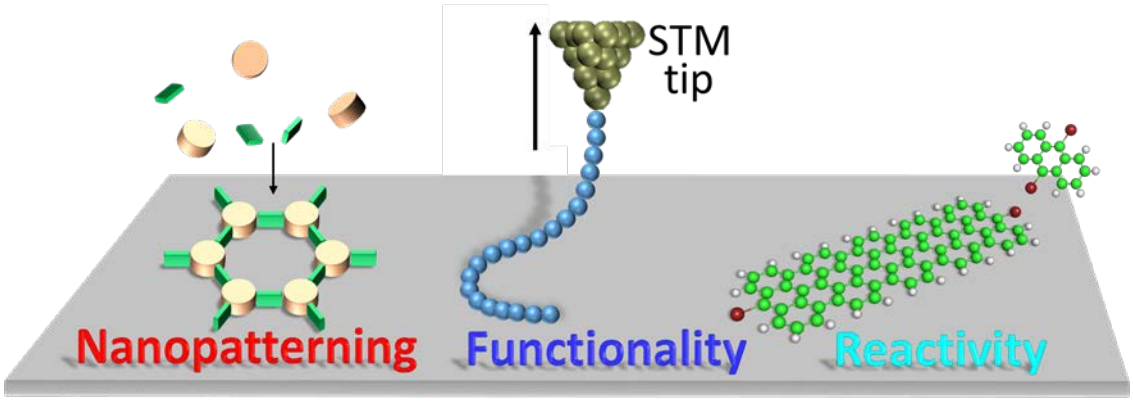

Surfaces and interfaces are particularly important at the nanoscale and often *dominate* the properties of nanomaterials. Fueled by early studies of self-assembled monolayers (SAM),[1,2] surface science has driven many aspects of the 'nano revolution', offering tools and methodologies to advance our understanding of the special properties of low-dimensional nanomaterials and enabling their implementation in a wide range of applications. As a result, the nano revolution has led to the development of new tools critically enabling the field of surface science.[3-5] From a molecular science perspective, surfaces serve as templates that facilitate the organization of molecules. Surfaces actively interact with the molecules at the interface, altering the properties of surface-arranged assemblies and as such have become components of devices that rely on complex molecular arrangements; ranging from thin-film organic field-effect transistors, sensors, to single-molecule diodes, and switches.[6-11]

Technological development, exemplified by scanning probe microscopy (SPM)[12] has opened new perspectives and opportunities in supramolecular chemistry. Through imaging molecules and their assemblies with sub-nanometer resolution, we have learned to guide the assembly process, building designer supramolecular structures. State-of-the-art scanning tunneling microscopy (STM) has given access to the analysis of surfaces with sub-nanometer resolution and enabled visualization of molecular orbitals.[13] Atomic force microscopy (AFM), at its best, can even distinguish between single (C–C) from double (C=C) carbon-carbon bonds.[14,15] This article focuses on new perspectives in the molecular and surface sciences enabled by SPM. As we review new understanding of molecular behavior on surfaces, we will give special emphasis to three subfields: (i) surface *nanopatterning via* molecular self-assembly;[16-21] (ii) surface-confined reactivity, which enables the synthesis of 2D polymers and epitaxially ordered polymeric

wires/ribbons;[22-27] (iii) exploration of *functional properties* of individual molecules (and macromolecules) by taking advantage of their localization/immobilization on surfaces.[28-30] Each of these subfields has been separately reviewed in the past. Here, we provide an overarching perspective focusing on the challenges and opportunities between and beyond these areas.

Discussions on the convergence of these fields began at the scientific gathering "Supramolecular Assemblies on Surfaces: Nanopatterning, Functionality, and Reactivity" in Lanzarote, Spain (February 2012). This initial event was followed by the homonymous symposia during the ACS Spring meeting in Dallas (March 2014), PacifiChem 2015 conference in Honolulu (December 2015), and in a stand-alone event in Hong Kong (December 2016). The discussions and exchanges offered the community a sense of future directions and prospects. Here, we present our vision of this field, selecting recent key achievements and highlighting how understanding molecular interactions at the nanoscale can impact applications of molecular materials and surfaces.

The reviewed material is structured into three sections: (1) self-assembled molecular networks, (2) on-surface reactions and (3) functionality. The first section begins with descriptions of on-surface assembly *via*: hydrogen bonding in biomolecular self-assembly, halogen bonding, dipole-dipole interactions, metal-organic coordination, and charge-transfer interactions. It continues with the discussion of the role of chirality and then kinetic and thermodynamic factors in on-surface assembly. We discuss the applications of these molecular networks in switching, nanotemplating, and as model systems for organic electronic devices, finishing with a less explored, but important for optoelectronic applications, self-assembly on non-conducting substrates. In the second section, we summarize the recent progress in on-surface catalytic and dynamic polymerization, followed by syntheses of graphene nanoribbons and other exotic

molecules. We highlight the practically significant aspect of decoupling the macromolecular structures from the substrate surface. The final part of this section presents an alternative approach to surface reactivity where the new covalent bonds are made *with* the surface, rather than between the molecules. The third section showcases three significant areas where scanning probe microscopy on molecules self-assembled on supporting surfaces enables exploration and elucidation of their functional properties, in nanoelectronic devices, nanomagnets, and catalytic reaction centers.

Self-assembled molecular networks

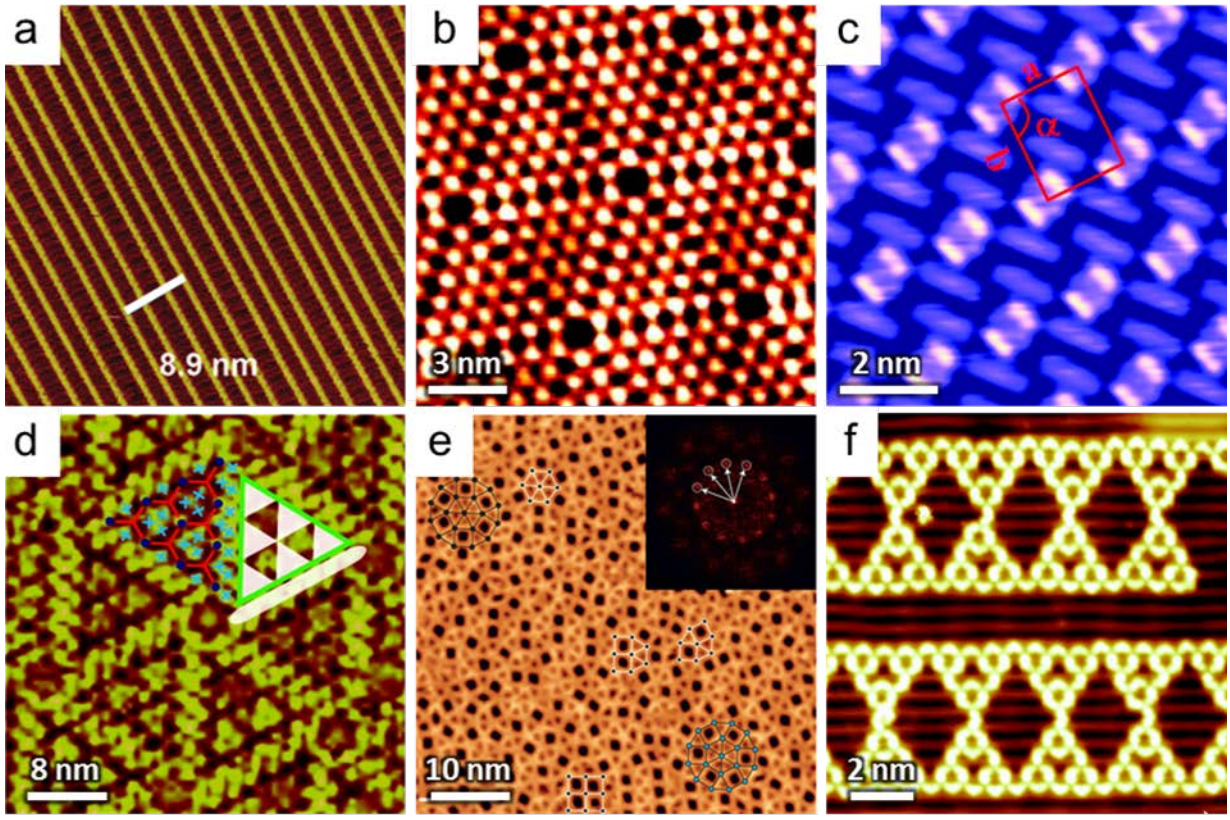

Figure 1. Scanning tunneling microscope images of a) binary self-assembled molecular networks (SAMN) of 1-(2-(10-ethoxydecyloxy)ethyl)-5-(2-(heptadecyloxy)ethyl)anthracene and 1,5-bis((12-methoxydodecyloxy)methyl)anthracene at the phenyloctane-highly oriented pyrolytic graphite (HOPG) interface; b) trimesic acid on Au(111)-(22×$\sqrt{3}$); c) binary SAMN of 3,4,9,10-perylenetetracarboxylic dianhydride and pentacene on Ag(111); d) ternary mixture of 2,3,7,8,12,13-hexahexyloxytruxenone, 1,3,5-tris(10-carboxydecyloxy)benzene, and copper phthalocyanine at the phenyloctane-HOPG interface; e) metal-organic quasicrystalline network formed by coordination of Eu atoms with 4,4'''-dicyano-*p*-quaterphenyl on Au(111); f) Sierpinski triangles patterns formed by coordination of Co with 4,4''-dicyano-*m*-terphenyl on Au(100). Reproduced with permission from refs [31] (a), [32] (b), [33](c), [34] (d), [35] (e), [36] (f). Copyrights 2008 ACS, 2007 ACS, 2010 Wiley, 2011 ACS, 2016 NPG, 2017 RSC, respectively.

In the early 1990s, Rabe and coworkers used STM to observe 2D periodic structures formed through the physisorption of alkanes on the surface of highly oriented pyrolytic graphite (HOPG) at the solid-liquid interface.[37] Ever since, 2D nanostructures with remarkable structural complexity, and rationally tuned symmetry and periodicity have been created using this

approach. Such monolayer structures, often referred to as self-assembled molecular networks (SAMNs), differ significantly from classical SAMs that are composed of chemisorbed molecules such as alkanethiolates on gold (Figure 1). The SAMNs are formed through weak physisorption and non-covalent intermolecular forces, and their supramolecular 2D structure can be tailored by modifying the molecular components. In contrast to SAMs, the molecular constituents of SAMNs lie flat on the surface, giving rise to monolayers with one to a few atoms thickness, although growth off of the surface into the third dimension can be controlled by using more complex molecules[38-40] or through multilayered SAMNs. The long-range order in chemisorbed SAMs is often limited to ~10-100 nm domains due to the reduced mobility of the molecules and restructuring the support surfaces, whereas many SAMNs show single crystalline domains on the micron scale.

Van der Waals (vdW) interactions of long alkyl chains[41,42] and hydrogen bonding (H-bonding)[43-46] are the two most often used interactions to control the structures of SAMNs. However, metal coordination,[47,48] halogen bonding (X-bonding),[49-51] and dipole-dipole interactions[31,52-54] have also been explored in affecting and tailoring their structural configurations. Shape complementarity is another important factor, which has been creatively explored in the design of complex multicomponent SAMNs (see below).[55]

Probing biomolecular self-assembly via scanning tunneling microscopy

This concept has spread into biomolecular self-assembly as a means to explore structural motifs and intermolecular interactions crucial in biology.[56-60] Among many possible hydrogen-bonding

motifs, peptides provide a set of structures for constructing molecular networks with special chemical and biological properties due to their homogeneous backbones and heterogeneous residues. Both inter- and intra-peptide interactions originate from H-bonding of 20 common amino acids. The structure of the peptide networks can thus be precisely programmed by selecting the individual amino acids in the sequences. The known propensities of amino acids to form sequence-dependent secondary structures can provide helpful insights[61] enabling construction of SAMNs with greatly enriched complexity and functionality.[62-65] In a parallel effort, supramolecular networks of nucleobases have been achieved by using complementary Watson-Crick-type H-bonding, as well as non-complementary pairing patterns.[66,67] The documented variations in network structures consisting of peptides and nucleobases manifest the interaction specificity and diversity among the elemental assembly units that are prevalent in the recognition process of biological systems.

A variety of surface-bound peptides, including networks and close-packed structures, have been resolved by STM, providing new insights into the molecular mechanisms of relevant biological properties and biomaterials interfaces.[57-60,67-69] For instance, in an elegant set of STM studies Wang *et al.* have investigated the assembly structures of Aβ42 and other oligopeptides, known to play a role in neurodegenerative diseases. The measured length of the peptides was below the value for fully extended molecules, which was attributed to the formation of hairpin structures. This and other studies showed that STM is a useful tool for the structural analysis of amyloid peptides.[70]

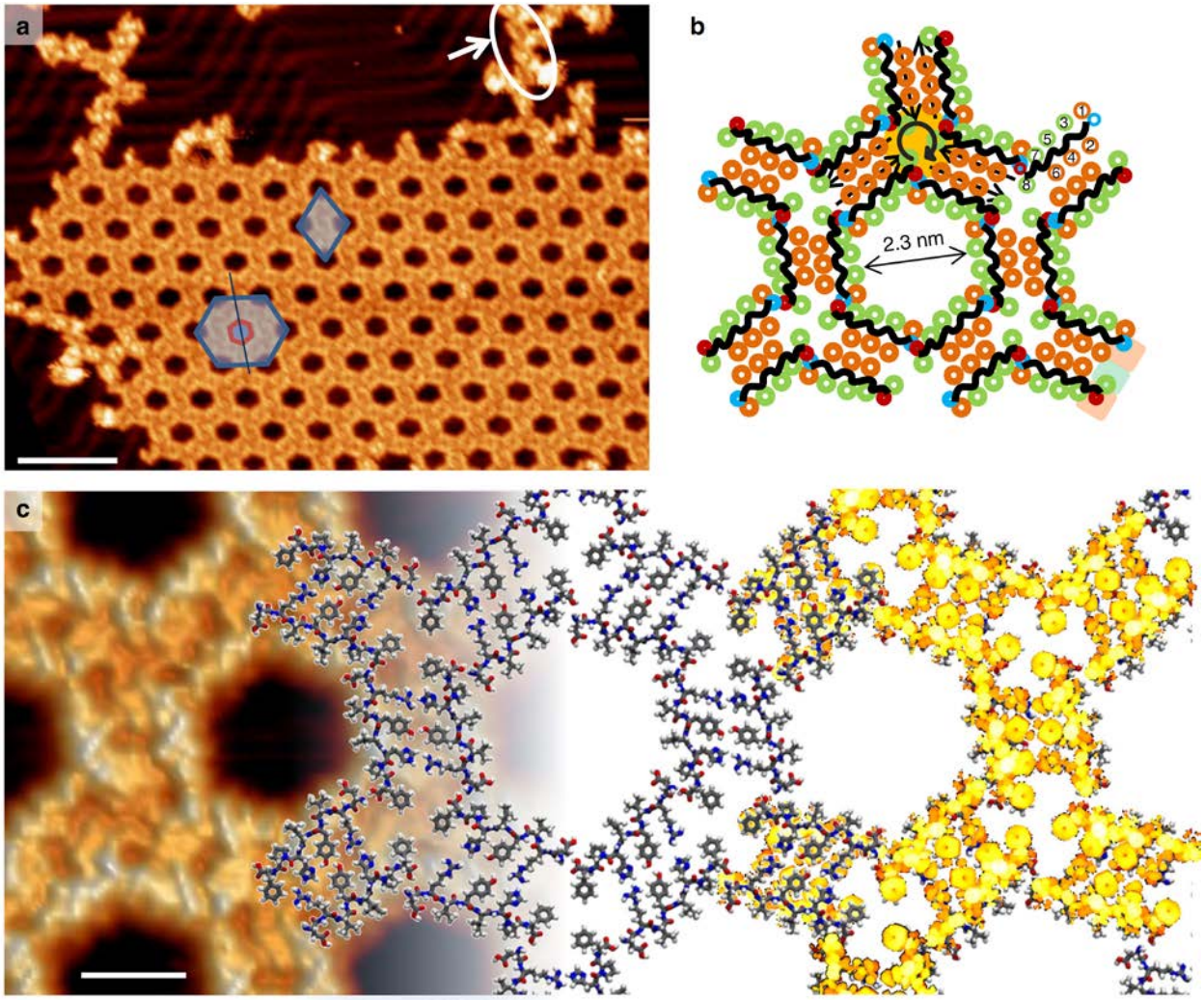

Figure 2. Self-assembled molecular networks of angiotensin II (AT-II) on Au(111). (a) A honeycomb network of the At-II molecules (scale bar 15 nm) is shown with the unit cell indicated by the diamond. The chirality of the network is revealed by a tilt of the hexagonal pore (red) with respect to the hexagonal superstructure (blue). In the upper right corner, a linear arrangement is circled in white. (b) The schematic arrangement demonstrates the nonpolar (green) decoration of the pore with the polar residues (orange) in the inside of the nanostructure. The polar–nonpolar–polar-binding motif at the short edge of the dimer is indicated by a green/orange background in the lower right corner. (c) (Left) Scanning tunneling microscope image (scale bar 2 nm) overlapped with (middle) the molecular dynamics-simulated model, and (right) the calculated electron density for comparison. Adopted from ref [62], copyright 2016 NPG. [Open Access]

Molecularly resolved peptide networks on Au(111) under electrochemical conditions have been demonstrated by STM for alamethicin (Alm), which consists of 20 amino acids.[71] The connectivity

of this peptide is achieved by the H-bonding between the residues of glutamine (Gln), which results in a 2D network with cavities encapsulated by six Alm peptides. These nanometer-sized cavities can be correlated with the formation of porous structures by some transmembrane proteins that define their membranolytic activity. Similar ion channel structures have also been reported for cyclic peptides both at the solid-liquid interface and in vacuum.[72,73] In a recent effort, an octapeptide angiotensin II was shown to form SAMN on Au(111) in vacuum, as shown in Figure 2.[62] The chiral network is formed by peptide dimers in anti-parallel conformations and interconnected by the hydrogen bonds between terminal moieties. These peptide assemblies demonstrate the feasibility of constructing residue-decorated supramolecular structures that could be programmed and engineered for novel material properties such as peptide hydrogels with clinical applications.[74,75]

Co-assembled networks can also be formed by H-bonding of peptides with other organic molecules. Thus, pyridyl moieties can interact strongly with terminal carboxylic groups of the peptide. Co-assembly with oligopyridine molecules affects the peptide transformation of β-sheet conformation, morphology, and biological properties.[63,76] The formation of the organic-peptide networks can be tuned by stoichiometry, as exemplified by the terpyridine and the peptide KLVFF.[63]

Due to the diverse chemical structure of residues, substrate-induced conformational variations should be considered in constructing peptide-based networks. Residue-substrate interactions can contribute appreciably to the peptide-substrate interaction and also affect the structural resolution of the peptides obtained by STM.[68,69,77]

Halogen-bonding interactions

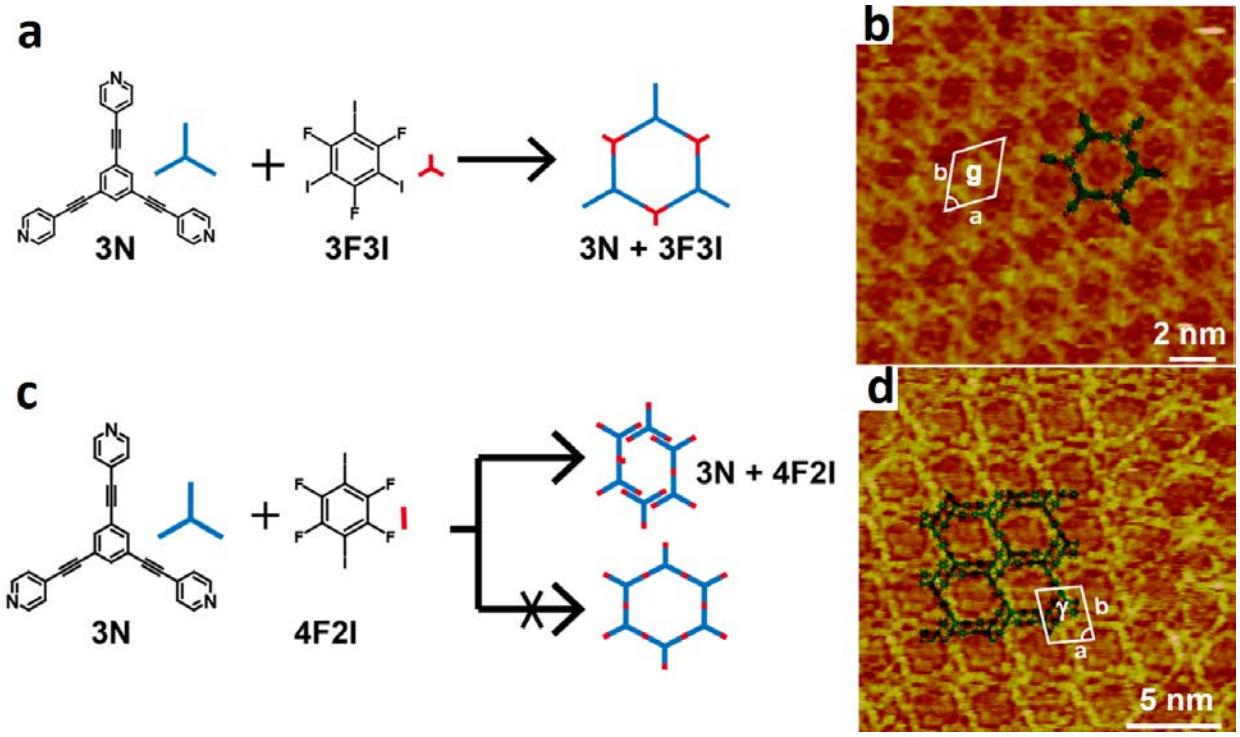

Figure 3. Porous halogen-bonded networks formed by assembly of tripyridine 3N with fluorinated iodobenzenes (a,b) 3F3I and (c,d) 4F2I. Adopted from ref [50], copyright 2015 ACS.

While H-bonding and vdW interactions of long alkyl chains are prevalent tools in constructing supramolecular networks on surfaces, other non-covalent interactions have also been explored. For example, stabilizing halogen bonding (X-bonding) interactions enable control of the monolayer structure of (hetero)aromatic semiconductors[49] and halogenated monomers for on-surface polymerization.[78] Due to relatively weak *homo*atomic X-bonding, these SAMNs tend to adopt close-packed structures to maximize their overall vdW interactions.[49,79-81] Porous X-bonded SAMN can be stabilized at low temperatures: for example, 1,1''-dibromo-*p*-terphenyl on Ag(111) produces SAMNs with square, rectangular and hexagonal X-bonded motifs, but these are

only observed in UHV at below 150 K.[82] Alternatively, stronger heteroatomic X-bonding, *e.g.* between pyridine and fluorinated iodobenzene derivatives can be used to direct the formation of porous networks in ambient at liquid-solid interface (Figure 3).[50] Nevertheless, the strengths of X-bonding interactions are generally weaker than those of H-bonding,[83] and the former can still be partially compromised in favor of maximizing the overall packing density (Figure 3d).

Dipole-dipole interactions

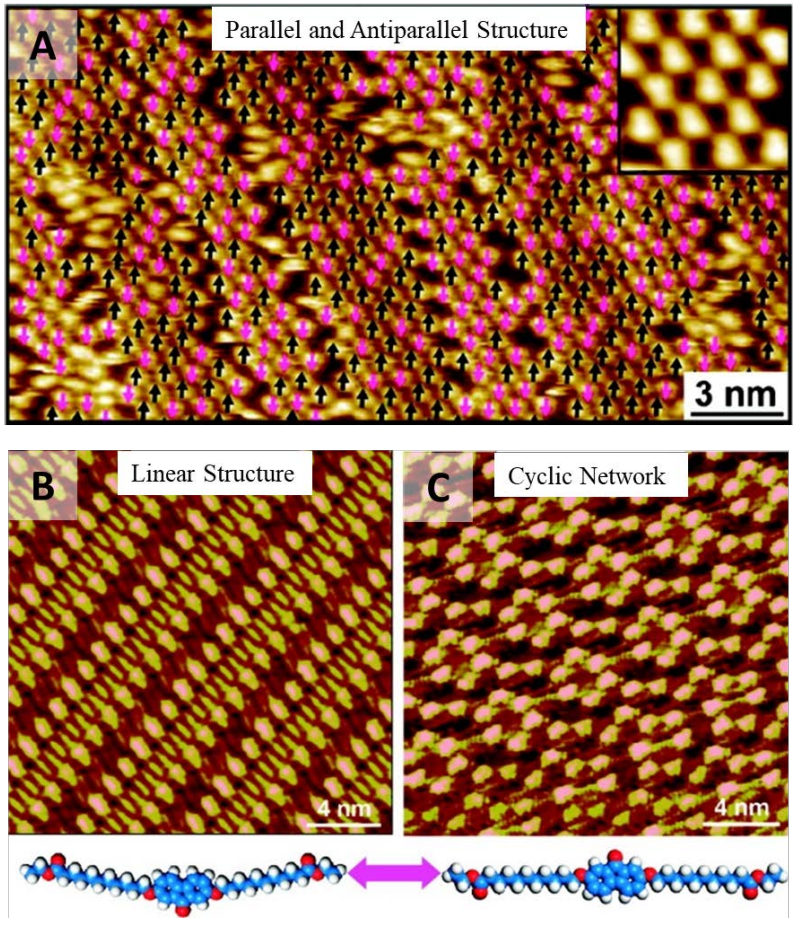

Figure 4: (a) Scanning tunneling microscope (STM) image of a 0.9 monolayer of styrene on Au(111) with molecules pointing up and down, labeled with black and red arrows, respectively. The image shows that molecules are preferentially oriented in one direction within a domain and this orientation alternates between neighboring domains. (b) 2,7-Bis(10-

(ethoxycarbonyl)decyloxy)-9-fluorenone self-assembled on highly ordered pyrolytic graphite in a linear structure and c) in a cyclic network observed *via* STM. A reversible transformation between these two arrangements can be induced in the same assembly by voltage pulses through the STM tip. Adapted from refs [84] and [85],copyright 2007 ACS and 2012 ACS.

Dipole-dipole interactions is another example of less common supramolecular motifs, that nevertheless can have decisive effects on the formation of SAMNs. Sykes and coworkers have shown that even styrene, which has a relatively weak dipole moment, forms local and long-range ordered assemblies dictated by dipole-dipole interaction, Figure 4a.[84] Styrene, when deposited as an almost complete monolayer on Au(111), at low temperature forms local domains with ferroelectric (parallel) ordering. However, long-range order is also observed, with neighboring domains adopting an antiferroelectric (antiparallel) ordering. Dipole-dipole interactions can also operate in conjunction with surface-mediated interactions as demonstrated by Yokoyama *et al*., who showed that the adsorption of uniformly dispersed tris(2-phenylpyridine)iridium(III) on Cu(111) is dominated by strong repulsive forces arising from surface-enhanced dipole-dipole interactions.[86] The dipole location in the sidechain can be used to direct the placement of molecules and control monolayer morphology. Zimmt and coworkers have studied a number of anthracene derivatives with mono-, di- and tri-ether alkyl[53,54] sidechains or ketone and $–CF_2$ dipolar functional groups.[52] The ether alkyl groups result in weak dipole-dipole interactions providing a secondary recognition element between the molecules and allowing to create complex SAMN patterns (Figure 1a).[31] The larger dipole of the ketone, in comparison with the $–CF_2$ group, does not produce a stronger driving force for the assembly as the larger size of the ketone also causes steric hindrance, preventing optimal sidechain packing.

Xu *et al.* used 2,7-bis(10-(ethoxycarbonyl)decyloxy)-9-fluorenone to probe the effect of both the sidechains and the central conjugated moiety in enhancing the dipole-dipole interactions.[85] As a result, the molecule exhibits two assembled phases capable of a reversible interconversion: a linear structure dominated by vdW forces and a cyclic network directed by dipole-dipole interactions (Figure 4b,c).

The above-described studies investigated interactions between molecules with permanent dipole moments that give rise to supramolecular assemblies on surfaces. Perepichka and coworkers recently reported that dipole-dipole interactions can also be employed to drive the assembly of non-polar molecules.[87] They showed that SAMs of pentafluorobenzenethiol on Au(111) form hexagonally packed monolayers of C_{60} fullerene at solid-liquid interfaces, while *no* fullerene adsorption takes place on either benzenethiol or octanethiol SAMs. This observation was attributed to dipole-induced dipole interactions between the polar pentafluorobenzenethiol SAM and polarizable C_{60} molecules.

The use of a SAM to control fullerene adsorption is not the only example of achieving control *via* dipolar interactions between a SAMN and an underlying SAM. Weiss and coworkers have used carboranethiol and –dithiol molecular absorbates to probe the effects of the surface dipole on liquid crystal (LC) orientation.[88] The use of SAMs of isomeric carboranethiols, which are almost solely distinguished by their dipole moments, enables exploration of this specific interaction. Data presented show that both azimuthal orientation and anchoring energy of the LC depend on the direction of the normal component of the dipole, with respect to the surface. The ability to control LC orientation from the nanoscale to the macroscale has a broad spectrum of applications.[89,90] The use of SAMs and this type of dipole-dipole interaction provide high degrees

of tunability, given the large diversity of molecular adsorbates that can be used, as a control mechanism for further SAMN formation.

Metal-organic coordination

Metal-organic coordination provides an alternative to the above-discussed self-assembly strategies, producing highly ordered metal-organic networks on surfaces.[17,91] These systems typically require vapor deposition of two components on the surface in ultrahigh vacuum (UHV), which increases the complexity of the sample preparation compared to the systems discussed above. However, on-surface redox processes have been shown to lead to thermally robust structures[48,92,93] with high degrees of order (due, in part, to directionality of metal coordination bonding),[94] chemical programmability,[95] and high selectivity.[47,96] Extended coordination networks require ligands with diverging geometries, *i.e.*, having binding groups on two or more sides of the molecules. Many metal centers commonly adopt quasi-square planar coordination geometries, although lower coordination numbers have also been observed.[97] There are also examples of systems that employ multiple ligands for coordination around metal centers;[98] these reveal error correction in networks[99] and selectivity of ligands toward specific metal species.[47] Combinations of STM characterization with X-ray photoelectron spectroscopy (XPS) have enabled identification of charge-transfer (redox) processes in the formation of the metal-organic networks at surfaces[94,100] and control of metal oxidation state by ligand design.[95] On-surface redox chemistry has been further supported by vibrational spectroscopy[101,102] and density functional theory (DFT) calculations.[103]

Metal-organic coordination can also be used in the design of quasicrystalline SAMNs. While the 2D quasicrystals were initially discovered in the H-bonded self-assembly of ferrocenecarboxylic acid molecules,[104] a large metal cation is particularly helpful for achieving five-fold coordination. Barth and co-workers achieved these assemblies by using lanthanide metal centers (Figure 1e).[35] There are also examples of molecules with C5 symmetry that do not achieve quasicrystalline ordering, but instead adopt packing-driven interactions that are not sensitive to the molecular shapes.[105,106]

Metal-organic coordination networks at surfaces provide an extensive structural library for nanopatterning of surfaces. Recent studies have begun to explore their chemical activity[102,107,108] to extend these structures to functional applications for catalysis, sensors, and as templates for more complex structures. Further studies are needed to develop these properties and extend the structural library to heterometallic structures[108] and controlled cluster sizes.

Charge-transfer-induced ordering

In recent years, the interactions of monolayer organic molecules on surfaces, with flat-lying polyaromatic species, has become an important topic in the context of 2D supramolecular assemblies. Characterization of these interactions is also important in the ongoing effort to understand fundamental aspects of the critical organic–metal surface interfaces that underlie organic semiconductor technologies. As these studies have progressed, the question of charge transfer between the surface and the organic adsorbates has presented itself and several groups

have reported interesting effects of this charge transfer on the supramolecular self-assembly at the surface.

Understanding the interface between organic semiconductors and metal surfaces is an ongoing challen96ge. In many cases, the interactions can be presented as a combination of relatively weak adsorbate-substrate interactions with some electronic effects, which can be modulated by perturbed surface electronic structure.[21,109-116] Models of level alignment and charge transfer have been presented in the literature.[117,118] Charge transfer from the surface depends on a choice of molecular adsorbate with orbital energy close to the surface work function.

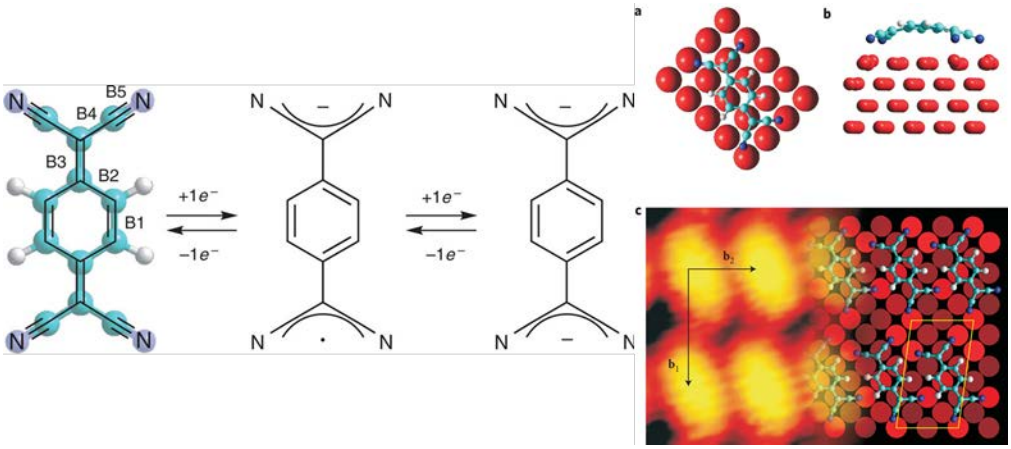

Figure 5**.** Assembly of tetracyanoquinodimethane (TCNQ) on the Cu(100) surface mediated by charge-transfer interactions. Reproduced from ref[119], copyright 2010 NPG.

Charge transfer can have a significant impact on molecular assembly as the electronic state of the molecule can affect its *shape* and thus its ability to interact with (bond to) the surface. This effect of substrate-mediated interactions has been demonstrated in multiple studies of the broadly used electron acceptor TCNQ. Kamna *et al.* determined that on Cu(111), the assembly of TCNQ is dictated by a combination of favorable intermolecular interactions and molecule-

induced electronic perturbations of the Cu surface.[112] At low coverage, TCNQ forms close-packed molecular chains at the Cu(111) step edges, an orientation that maximizes the interaction between the molecule and the favorable electronic structure of the step edge.[120] At full (monolayer) coverage, TCNQ assembles into orthogonally packed ordered structures on the Cu(111) terraces in two possible unit cells, an assembly that is more strongly influenced by the intermolecular interactions. A study by Tseng *et al.* showed that two-electron charge transfer from the Cu(100) surface to TCNQ leads to rearrangement of the π-bonds in the molecule (Figure 5).[119] The reduced bond order between the central benzene ring and diacyanomethylene moieties allows cyano groups to bend towards the Cu surface enhancing molecule-surface interactions, as determined by a combination of STM, near-edge X-ray absorption fine structure spectroscopy (NEXAFS), XPS, and DFT calculations. A more recent study involving STM and X-ray standing wave spectroscopy reported significant flexibility in TCNQ when co-adsorbed with K atoms, which act as positive counterions.[121] In that case, the terminal groups are tilted such that one cyano group was oriented toward the surface and the other is oriented upward toward K. Charge transfer to TCNQ impacts molecular structure and interaction with the surface and thus

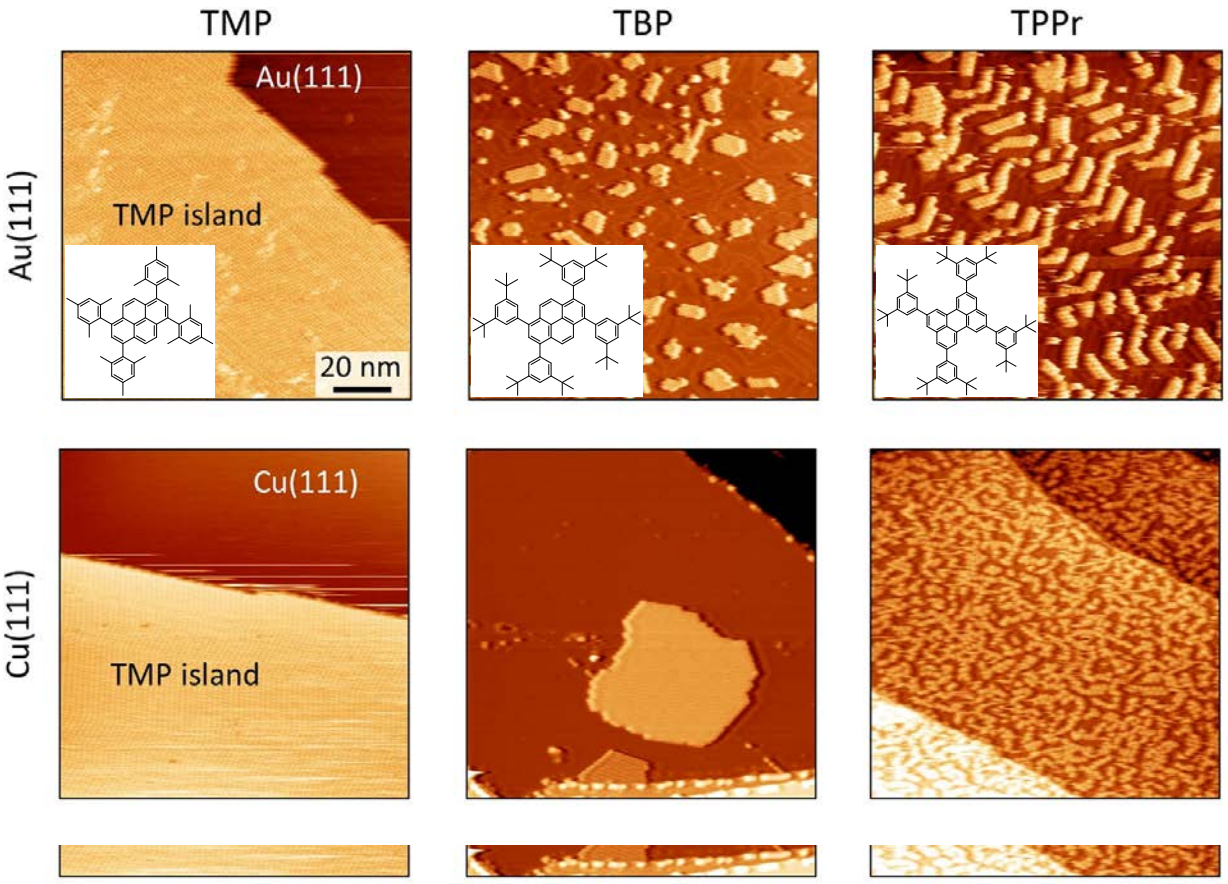

Figure 6. Scanning tunneling microscope images of three organic molecules: (left) 1,3,6,8-tetramesitylpyrene (TMP), (middle) tetrakis[1,3-di(tert-butyl)phenyl]pyrene (TBP), and (right) 2,5,8,11-tetrakis-(3,5-di-tert-butylphenyl)perylene (TPPr), (top) on Au(111) and (bottom) on Cu(111). Reproduced from ref [122], copyright 2014 ACS. [ACS AuthorChoice Article]

Charge transfer to or from adsorbates introduces new intermolecular interactions impacting self-assembly of the molecular layer. The resulting supramolecular structure is defined by the interplay between intermolecular repulsion due to the surface-adsorbate dipole and intermolecular attraction due to vdW interactions. Charge transfer affects island sizes in the submonolayer regime, producing dramatic differences in self-assembly on Au(111) and Cu(111) surfaces (Figure 6), where the former allows molecular charging and the latter has neutral

adsorbates.[122] On the Au(111) surface TBP displays an "anomalous coarsening" that is manifested in co-existence of large and small molecular islands. This behavior was explained by reversible charge transfer at the organic/metallic interface due to TBP effective ionization potential being close to the work function of Au(111) (5.3 eV). The growth of TBP was contrasted with that of TMP and TPPr, which have higher and lower adsorption heights than TBP, respectively. While TMP does not experience charge transfer and grows in large islands, TPPr is closer to the surface and experiences stronger charge transfer than TBP, only forming small domains.

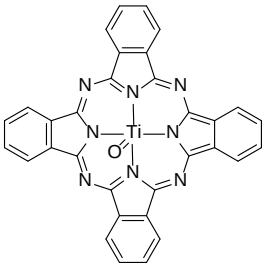

TiOPc

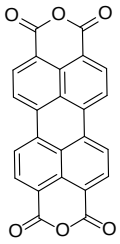

PTCDA

The assembly due to the charge-transfer-induced dipole interactions can be compared to the assembly of molecules with intrinsic dipole moments normal to the surface. For example, titanyl phthalocyanine (TiOPc) has a molecular dipole moment normal to the plane of the molecule and adsorbs on both sides.[123] "O-down" molecules tend to adsorb at step edges due to the higher mobility and to attractive interactions with the intrinsic dipole of the step edges.[124] These molecules have intrinsic dipoles that are not acquired by charge transfer from the surface. At low coverages, there is little aggregation, possibly due to dipole repulsion. At higher coverages, Cu adatoms are involved in interactions with molecules to form 1D aggregates.[123]

Molecular adsorption on metal surfaces typically involves the extension of the molecular wave function within the substrate and charge back donation, which lead to spectroscopic broadening

and formation of 2D bands at the interface due to substrate-mediated intermolecular interactions. Interestingly, these strong electronic interactions and overlap can lead to lower charge transfer than that on less interacting surfaces.[125] Weak molecule-substrate interaction, where little or no hybridization or charge back donation occurs, can allow integer charge transfer. This effect was reported for perylenetetracarboxylic dianhydride (PTCDA) adsorbed on conductive *n*-doped ZnO surfaces although the charge transfer is restricted to the first layer.[125] PTCDA adsorbed on Ag(111) experiences charge transfer that was estimated to be only about 0.35 electrons, although this value is difficult to quantify because of the electron overlap with the surface.[126] It has been also argued that the PTCDA herringbone pattern on Ag and Ag@Si includes molecules of two different charge states, which have been resolved experimentally by measurement of local variations in the surface dipole.[127]

Fluorinated fullerene $C_{60}F_{18}$ has an intrinsic dipole moment, *i.e.*, it does not require charge transfer from the surface.[128] $C_{60}F_{18}$ island growth is different from the standard Ostwald ripening that would be observed with pristine C_{60}. Estimates similar to those of ref. [122] for the contributions of the two competing effects (gas phase HOMO level *upshift* due to the electrostatic screening by the metal substrate and *downshift* due to the intrinsic ~10 D dipole moment of $C_{60}F_{18}$), show that the HOMO of $C_{60}F_{18}$ molecule appears more than 1.2 eV below the Au(111) Fermi level. As a result, there is no charge transfer from the molecule to the substrate in the $C_{60}F_{18}$/Au system. The absence of Oswald ripening was therefore attributed to the dipole–dipole repulsion rather than to charging of the molecules. This result highlights the important roles that intrinsic dipole moments play in intermolecular and molecule–substrate interactions.

Chirality

For all of the above-described non-covalent interactions, on-surface molecular assembly can and often does lead to chiral organization. This is an obvious outcome for assembly of enantomermically pure chiral molecules, but can also can happen for prochiral molecules[129] (which become chiral upon adsorption) and even achiral ones[46] providing they associate *via* chiral supramolecular motifs. The combination of chirality and surfaces is prominent in materials science and catalysis,[130] *e.g.* the stereoselectivity of many heterogenous reactions is controlled by interactions of reagents or products with surfaces. In this context, SPM studies of chirality in surface-supported SAMN can bring insight into the mechanisms of resolution of enantiomers and evolution of chirality in 3D systems. Last, but not least, chirality can itself be used as another tool in engineering the SAMNs.

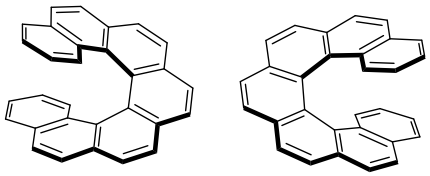

R and S **[7]H**

Among the many molecules that have been investigated on surfaces, helicenes have a special place because they serve as a model for chiral crystallization. They are fascinating chiral objects, and their self-organization has been investigated in detail on a variety of metallic substrates.[131,132] Lacking polar functional groups, unsubstituted helicenes are expected to interact *via* vdW interactions. One typical helicene, [7]H, adsorbs in such a way that as many benzene rings as possible are (near) parallel to the surface. The parts of the molecules close to the surface are thus responsible for stereochemical molecule-surface recognition. This assembly is surface dependent

and major differences in their behavior can be traced back to molecular structural differences. Thus, cyano-functionalized racemate [7]H undergoes spontaneous separation on Cu(111), *i.e.*, forms domains that are exclusively composed of one enantiomer. However, on the same surface, the unsubstituted [7]H self-assembles in alternating rows of opposite enantiomers. These helicenes show a cooperative response to a small chiral bias, leading to large magnification effects in supramolecular systems. Two such cooperative responses are the (i) "sergeant-and-soldiers" effect: in a mixture of achiral and enantiopure analogues the enantiopure ones dictate the chiral organization of *all* molecules, and (ii) the "majority rules" effect: in a non-racemic mixture the chiral induction is non-linear (*vide infra*). For example, at an enantiomeric excess of one enantiomer of [7]H by at least 8%, a single enantiomorph is observed despite the fact that the composition within a domain in still racemic. The excess of one of the enantiomers allows only one of the two possible arrangements of the pairs of both enantiomers.[131] Another interesting observation relates to the formation of multilayers by this helicene.[132] In contrast to the SAMNs with monolayer coverage, where the domains are composed of both enantiomers, the second layer in bilayer films is revealed to be homochiral. This effect is explained by transition from a 2D to a 3D racemate in multilayer films, which are composed of alternating homochiral layers of two opposite enantiomers.

Interesting chirality phenomena are often observed at solid-liquid interfaces under enantio-enriched conditions. Co-assembly of a chiral molecule in a SAMN composed of achiral molecules was shown to lead to homochiral layers. When enantio-enriched mixtures of the chiral molecule were used, instead of domains reflecting the initial ratio of the enantiomers, homochiral surfaces were formed. This is a demonstration of the "majority rules" effect, attributed to entropy-driven

mechanisms. Furthermore, after the formation of the chiral SAMN, the chiral inducers can be replaced dynamically by achiral analogues, while maintaining the initial surface chirality, due to strong memory effects.[133]

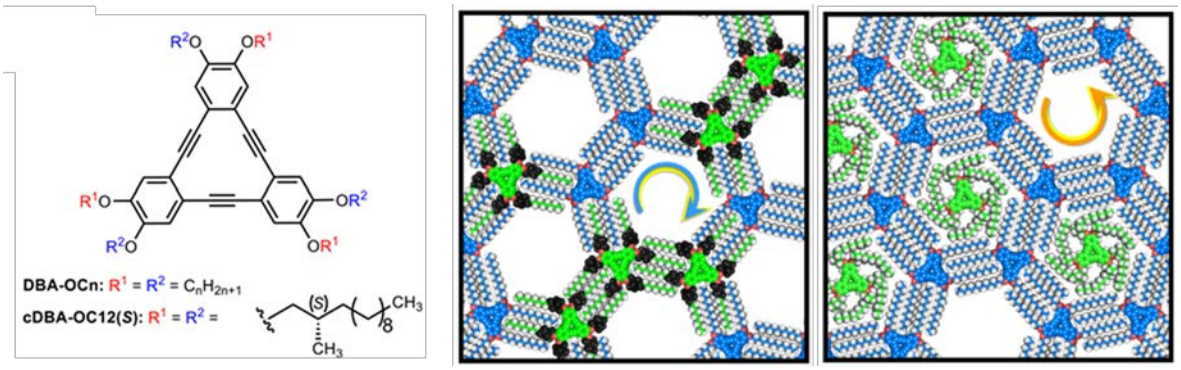

Figure 7: Left: Chemical structures of achiral (DBA-OCn) and chiral (DBA-OC12(*S*)) dehydrobenzo[12]annulene derivatives studied in ref [134]. Center: model of honeycomb network formed by DBA-OC12 (blue) and DBA-OC12(*S*) (green) molecules. The chiral centers are highlighted in black. Co-adsorption of DBA-OC12(*S*) leads to the preferential formation of clockwise nanowells (see arrows), according to a "sergeant-soldiers" mechanism. Right: model of honeycomb network formed by DBA-OC12 (blue); some nanowells contain co-adsorbed DBA-OC12(*S*) molecules (green). Preferentially, counter clockwise nanowells are filled and stabilized. Both the "sergeant-soldiers" mechanism and "host-guest" mechanism act simultaneously as competitive chiral induction pathways.

In a recent study, the expression of chirality at solid-liquid interfaces was used as a probe to distinguish between competitive self-assembly pathways that simultaneously act as opposite chiral induction pathways. Both pathways act at different stages of the self-assembly process, *i.e.*, nucleation *versus* ripening. Therefore, the chiral outcome of self-assembly can be tuned and controlled, leading to homochiral surfaces of opposite chirality under optimized conditions.[134]

It is also worth noting that the solvent itself can be used as a chiral inducer. When dissolved in enantiopure solvents, certain prochiral molecules can form homochiral SAMN at a liquid-solid

interface.[135] A growing amount of evidence suggests that the chiral discrimination in many of these cases occurs at the monolayer nucleation phase.[136]

Kinetics versus thermodynamics

Most often, molecular engineering of SAMNs relies on the rules of thermodynamics. The majority of molecular design strategies aims at accounting for the subtle balance of molecule-molecule, molecule-substrate, molecule-medium, and substrate-medium interactions and generally assumes a sufficiently fast reversible dynamics. The self-assembling system will often evolve on a rather shallow energy landscape but is hoped to reach the minimum energy state. Sometimes not a unique pattern, but several polymorphs can be formed. Convergence to a single polymorph upon extending the assembly time or annealing at elevated temperatures supports, though does not ensure, that the thermodynamic minimum is reached, as will be discussed below. However, certain strategies have been developed to "select" a certain supramolecular pattern (polymorph), for instance, by controlling the solute concentration at the liquid/solid interface.[137] Not surprisingly, low density polymorphs phases are favored at low solute concentration and *vice versa*.

Despite its impact being long underestimated, it is now well established that kinetics plays a major role in the outcome of self-assembly processes.[138-140] The fact that many systems do not reach thermodynamic equilibrium is not necessarily a drawback, but can be turned to advantage.[20] Indeed, out-of-equilibrium structures can possess properties different from their low-energy analogues. Understanding the roles of kinetics is therefore essential to control the

outcome of self-assembly. This effect was recently demonstrated at the solid-liquid interface for a mixture of two porphyrins, cobalt (II) octaethylporphyrin (CoOEP) and NiOEP.[141] When their solution in phenyloctane is brought in contact with a gold surface, a highly regular pattern is formed almost immediately. Both porphyrins can be identified on the surface by their specific image contrast revealing that the surface composition is identical to the ratio of both porphyrins in solution. Nevertheless, this regular pattern is *not* a result of thermodynamic equilibrium. This effect was elegantly shown by studies of temperature dependence, in which the sample was heated and allowed to cool to room temperature for imaging while tracking changes in surface composition. Heating at 135 °C for several hours was required to induce noticeable desorption in this system. An important practical implication of these results is the realization that noncovalent adsorption can lead to exceedingly strong molecular binding on surfaces. Even at 135 °C, the rate of desorption of CoOEP from an Au(111) in contact with phenyloctane solution was orders of magnitude slower than that of a covalently bound alkanethiol at 25 °C.

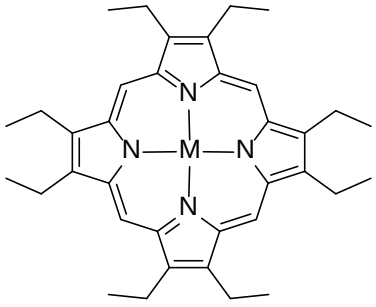

NiOEP (M = Ni)
CoOEP (M = Co)

Building up complexity: multicomponent assemblies

Multi-component assembly is critically important to the grand challenge of rational design and bottom-up fabrication of complex materials and devices.[142] It could greatly expand the fabrication of functional molecular nanostructures,[143] but the great diversity of the available building units is inevitably accompanied by enormous complexity in assembly mechanisms. Confining the interaction space to 2D (surface ad-layers) and imaging of the self-assembly pathways by SPM, has enabled rational control of highly complex (2, 3 and 4-component) structures, that is not easily achievable in 3D.

As documented in various multi-component SAMNs, complementarity and compatibility of intermolecular interactions of suitable chosen molecular building blocks can lead to pronounced selectivity and specificity. Selectivity can be demonstrated in preferential interactions between building units, mostly originating from specific interactions such as H-bonding, steric, and electrostatic interactions. Specificity in multi-component assemblies is manifested in the characteristic network topology and symmetry that can be uniquely assigned to interactions of a given series of building blocks, while their chemical structures may vary in size, terminal moieties, *etc*.

Selectivity is particularly important as it enables molecular building units to recognize each other in the formation of multi-component assemblies. Such site-specific selectivity in intermolecular interactions could enable precise control of the assembly composition and topology. In one of the early examples, formation of a 2D co-crystal between metallated tetraphenylporphyrin and perfluorophthalocyanine was attributed to specific H…F interactions that occur only in the

coassembled phase.[144] Selectivity has also been realized in many anthracene derivatives by manipulating the chain length, chain shape and dipole interactions.[31,145] Such side-chain based selectivity has been manifested in a variety of multicomponent SAMNs, including those with perfluoroalkyl chains.[146]

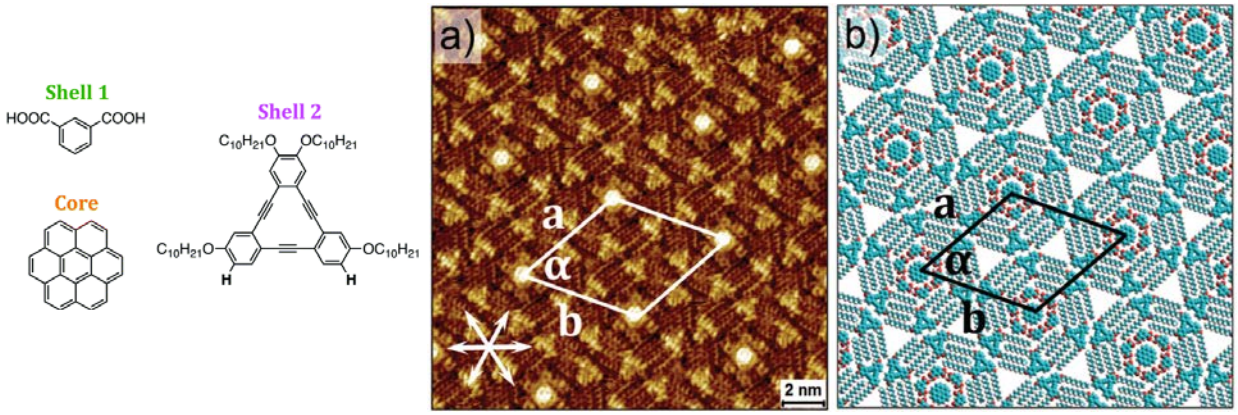

Figure 8. (a) Scanning tunneling microscope image showing the three-component network obtained at the octanoic acid/highly oriented pyrolytic graphite interface. Graphite symmetry axes are shown in the lower left corner. (b) Molecular model for the three-component system. Individually, each of these components forms different 2D patterns. Reproduced from ref [147], copyright 2017 RSC. [Open Access]

The multiple component strategies greatly enrich the scope of structural and chemical design of supramolecular networks. Such chemically decorated SAMNs with defined dimensions and geometries can be further pursued as the host structures to accommodate guest species with desired functionalities. The selectivity in the host-guest assemblies originates from the constituent components in host networks. Guest molecules such as fullerenes and coronene can be selectively encapsulated in the host molecular networks. In some cases, the guest molecules can also transform the host networks as shown in Figure 8.[147] While it can be seen as a porous SAMN in which the pores are filled by a supramolecular complex of coronene surrounded by six

isophthalic acid molecules, the alkylated annulene molecule, apparently forming the porous host network, does so only in presence of the other components.

Switching structures

The responsiveness of SAMNs to environmental stimuli provides important insights into thermodynamic and kinetic aspects of polymorphism, which are essential to the molecular-level design of stability and functionality in these systems. For example, H-bonded networks can be destabilized and transformed by thermal annealing. Isomerization of molecular moieties with temperature, light, or electric field stimuli can also induce structural reconfiguration of the networks. A range of SAMNs have exhibited pronounced responses under external stimuli including solvent, temperature, light, electric field, and molecule-substrate interactions. Photoisomerization has been documented for the transformation of molecular assemblies with various isomers, such as derivatives of azobenzene,[148] terthiophene,[149] diarylethene,[150] and porphycene.[151] The irradiation wavelength spans from the visible to the UV, covering photon energies approximately between 1.0 to 4.0 eV. These studies provide the structural basis for constructing photoactive molecular networks.

The electric field is an example of an external stimulus that can lead to dramatic variations in supramolecular networks due, in part, to the wide range of fields that can be applied experimentally. The dependence of the molecular conformation on the electric field originates from the structure-related electron density distribution. The non-planarity and non-centrosymmetry in molecular structures can result in net dipole moments that are one of the

main contributors for the responsivity to external electric fields.[152-154] The effects of electric fields can also lead to field-induced isomerization[155] and interfacial charge transfer.[156] The strength of the electric field within a STM junction can be as high as 10^8 V/m. Such high field strength can significantly alter the adsorption of the dipolar molecular adsorbate. Reports of reversing molecular orientations upon changing the tunneling voltage illustrate the predominant effect of the electric field on the orientation selectivity of adsorbed molecules. The dominance of the electric field effect on molecular conformations is reinforced by the fast response of collective supramolecular networks. In addition, the conformation selectivity due to the electric field is inevitably reflected in the network configurations. The energetics of network polymorphism can be dramatically affected by the electrostatic energies of molecular dipoles in the presence of an electric field. The field-dependent polymorphs should be based on the energetically favored molecular conformations.

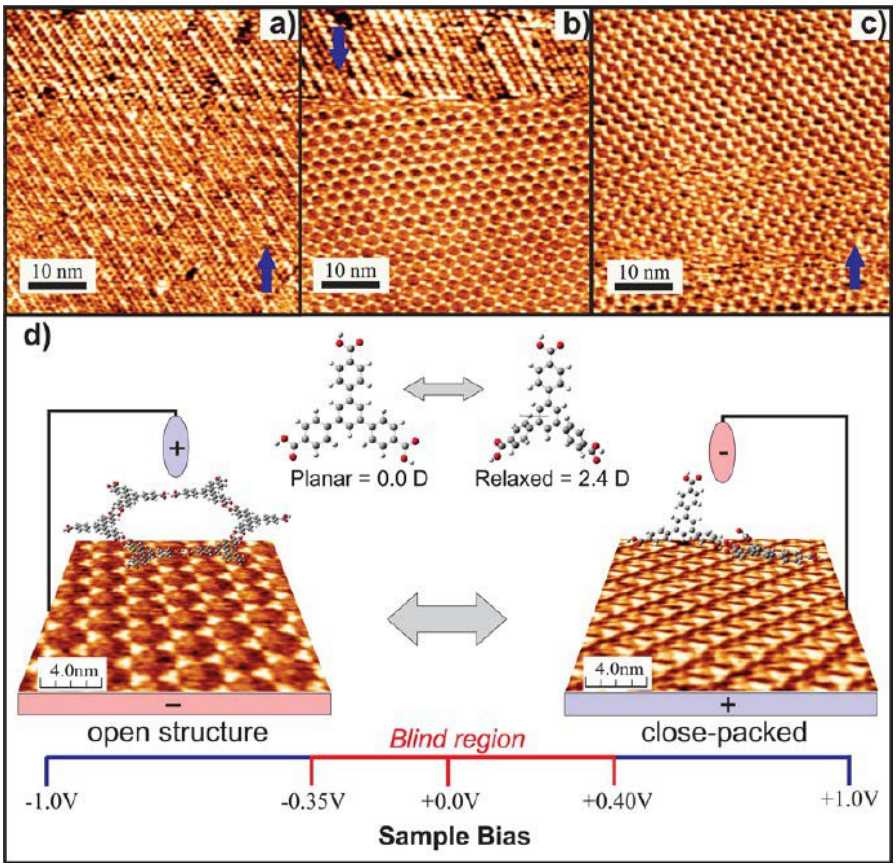

Figure 9. (a-c) Sequential scanning tunneling microscope images of 1,3,5-tris(4-carboxyphenyl) benzene (BTB) self-assembled molecular networks showing the voltage-induced phase transformation. (d) A schematic representation of the corresponding structural change with the applied bias-voltage. Reproduced from ref [156], copyright 2015 ACS.

The electric field effect is also manifested in the electrostatic interactions between adsorbed molecules and the substrate. Interactions between atoms and/or molecules and substrate lead to site-dependent interactions between molecules in the supramolecular networks.[110,113,115,157-163] The presence of an external field or surface charge can affect the periodicity of the supramolecular networks by affecting the electrostatic interactions between adsorbate and substrate.[112,164] The charge transfer between molecule and surface can also lead to selectivity of molecular conformations under an applied electric field, as demonstrated in the orientational

effects of 1,3,5-tris(4-carboxyphenyl) benzene (BTB) on graphite surfaces, as shown in Figure 9. It was proposed that the dipole orientation of BTB can be defined by the electron transfer between the graphite surface and the benzene ring and the carboxylic oxygen. As a result, field-induced reversible changes can be observed between open and close-packed 2D supramolecular networks.[156] The molecular networks at solid-liquid interfaces can also be tuned by electrical potential under electrochemical (EC) control. In the EC-STM studies of a charged polycyclic aromatic compound, 2-phenylbenzo[1,2]quinolizino[3,4,5,6-*fed*]phenanthridinium perchlorate, the molecular packing density could be reversibly and continuously changed by adjusting the substrate potential to compensate the surface negative charge by the polyaromatic cations. As a result, the porous network could be transformed between close-packed and bilayer structures.[165]

Even though the electrostatic interactions between molecular dipoles are long range,[166] the interaction magnitude is significantly attenuated by intermolecular separations determined by the network's periodicity and can be amplified by the external field. The addition of metal ligands to supramolecular networks provides the potential for novel catalytic properties. The atomic precision of periodicity and geometry of SAMNs provide a convenient platform for investigation of molecular mechanisms in heterogeneous catalysis.[48,167] The tilt angles of molecules can also be controlled with electric field.[7,168-170] In a closely related study, the reversible switching of intramolecular structures due to proton transfer was demonstrated by controlling the atomic and molecular environments.[171] Such intramolecular switching capability can extend the molecular basis for activating network structures.[172]

The above results illustrate that inclusion of stimuli-responsive moieties in the building unit can lead to collective structural responses of the supramolecular networks and provide the basis for

functional systems.[173,174] Due to the inherently different structures and chemistry of the constituent moieties, it should be possible to tune the networks' energetics and kinetics by temperature, intermolecular interaction strength, and other environmental stimuli.

Self-assembled molecular networks as nanotemplates

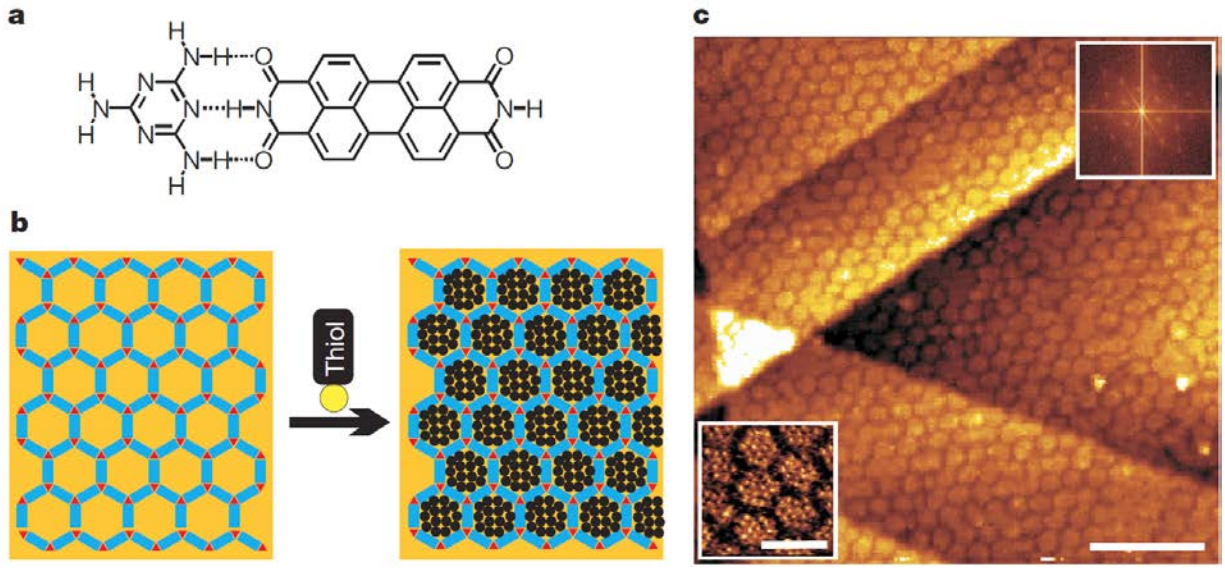

Figure 10. Templating of alkanethiol adsorption on Au(111) by a H-bonded self-assembled molecular network. (a) Structures of melamine and perylenetetracarboxydiimide. (b) Scheme of 2D assembly. (c) Scanning tunneling microscopy image of the resulting structure. Adopted from ref [175], copyright 2008 NPG.

Tunable symmetry, periodicity, and interactions of SAMNs make them attractive as nanoscale templates for patterning functional materials on surfaces. Since the emergence of this field, the porous nature of SAMNs has been widely explored to probe interactions with large π-conjugated molecules, for example, coronene and heterocirculenes, resulting in the formation of host-guest systems.[176] Specificity of binding in host/guest systems is primarily dictated by matching shape

and size between the guest molecules and the SAMNs' pores, although more specific interactions such as charge transfer could also play roles in stabilizing the guest molecules.[129] In addition, the surface of the underneath substrate can provide the additional interactions necessary for templating the guest molecules. For example, porous H-bonded molecular networks formed by melamine and perylediimide on Au(111) have been used to pattern thiol-based SAMs (Figure 10).[175,177] In this case, the chemisorption of thiol molecules on gold is modulated by blocking the surface with H-bonded networks.

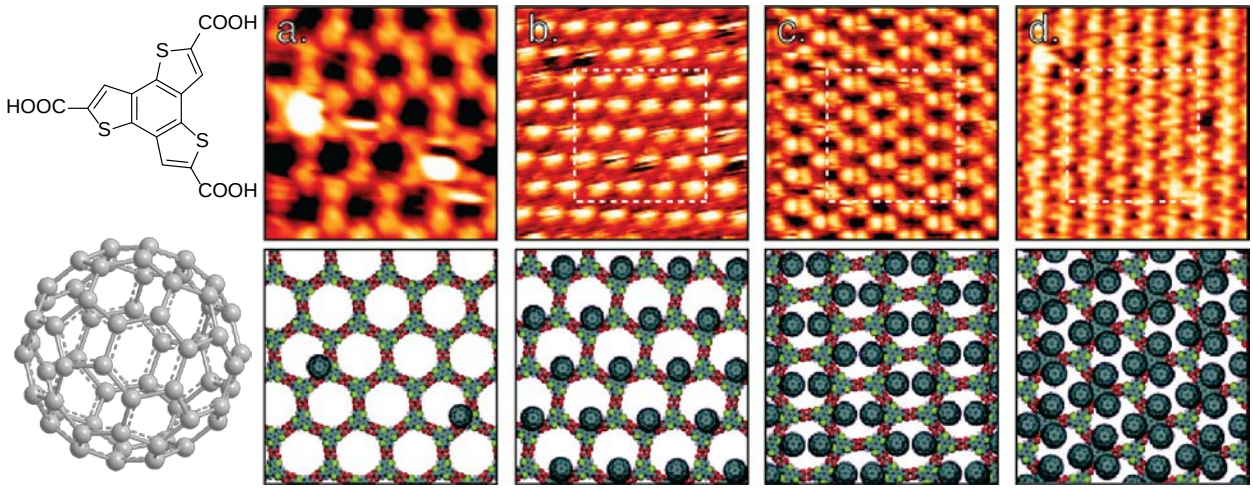

Figure 11. Incorporation of C_{60} fullerene guest molecules into a network host of terthienobenzenetricarboxylic acid with (a) sparse fullerene coverage, (b) one, (c) two, and (d) three fullerenes per unit cell. Molecular models are shown below each image. Image area sizes are (a) 10.7 nm × 10.7 nm and (b-d) 18 nm × 18 nm. Reproduced from ref [129], copyright 2009 ACS.

Due to its role as an electron acceptor/*n*-type semiconductor in organic electronics, C_{60} is the most widely explored guest molecule templated by SAMNs.[178,179,180] A partially phase-separated mixture of C_{60} derivatives with electron-donor polymers as a "bulk heterojunction" is the key material in solution-processable photovoltaics. The nanoscale structure/morphology of bulk heterojunction films is one of the most important factors defining the efficiency of solar cells,

and is the most difficult feature to control. In this respect, molecular networks can provide a means to control the structure of bulk heterojunction with molecular-level precision. This concept was exploited by MacLeod *et al.* who reported that at solution/graphite interface, the tricarboxylic acid derivative of oligothiophene (terthienobenzenetricarboxylic acid) forms a porous network through dimeric H-bonding.[129] The cavities of the network structure can efficiently host C_{60} molecules, which form ordered domains with one, two, or three fullerenes per cavity, depending on their surface concentrations (Figure 11). Specific fullerene-thiophene interactions increase the efficiency of fullerene adsorption, as determined by comparison with similar SAMNs of trimesic acid on HOPG, which lack such interactions.[181]

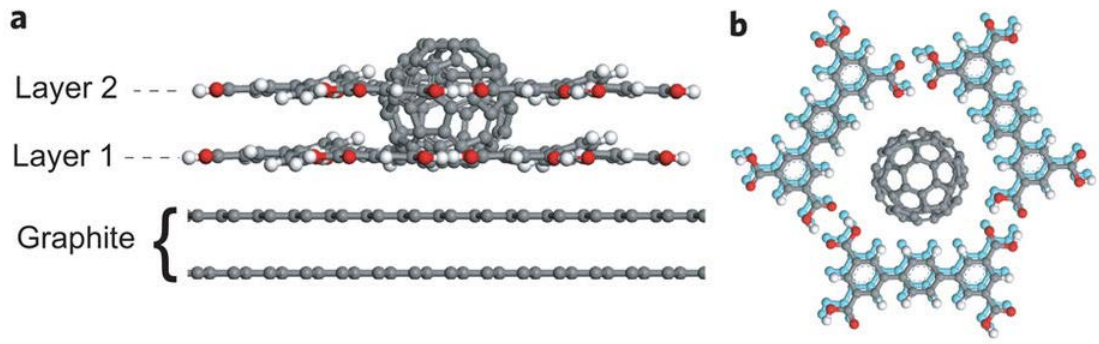

Figure 12. (a) Side-view and (b) top-view of the molecular model of terphenyltetracarboxylic acid (TPTC) - C_{60} bilayer self-assembled molecular network. Adsorption of C_{60} in the pores H-bonded TPTC network promotes the growth second layer. Reproduced from ref [182], copyright 2011 NPG.

To be relevant for photovoltaic device applications, such templated donor-acceptor monolayer would have to grow in the third dimension creating vertically oriented *p*- and *n*-type conducting channels. Blunt *et al.* showed that this might be possible.[182] Due to the different thicknesses of aromatic terphenyltetracarboxylic acid (TPTC), ~0.35 nm and fullerene, ~1 nm, adsorption of the latter in the TPTC monolayer host subsequently promotes the growth of a second layer of host

molecules, extending self-assembly in the vertical direction (Figure 12)**.** Other groups have also demonstrated stacking of organic molecules into multiple layers, while maintaining crystalline order.[183-186]

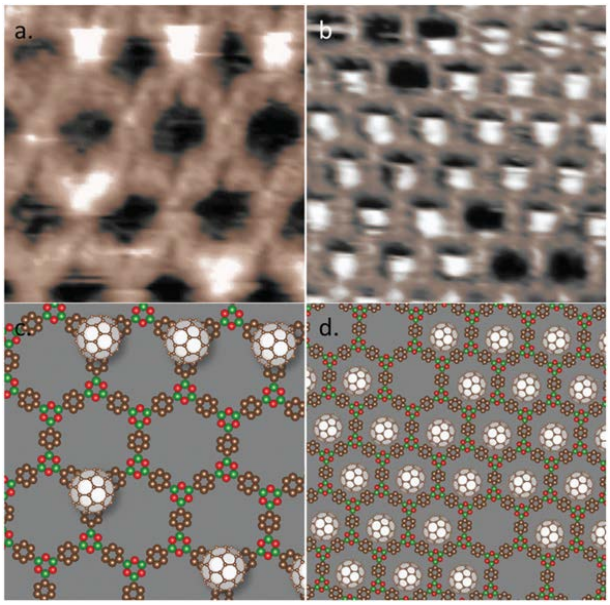

Figure 13. Host/guest structures formed by boroxine-based covalent organic framework COF-1 and C_{60} at the solution/solid interface. The scanning tunneling microscopy images in (a) and (b) show the observed C_{60} adsorption geometries, denoted as top site and pore site, respectively. The respective molecular models are displayed in (c) and (d). Reproduced from ref [187], copyright 2015 RSC. [Open Access]

The dynamic nature of self-assembled supramolecular structures is an advantage in designing highly ordered domains, however, their poor stability under ambient conditions is a drawback. On the other hand, surface supported covalent organic frameworks (COFs), created through dynamic covalent chemistry, can have remarkable degrees of order yet are much more robust.[188-190] The well-defined composition and porosity of COFs make them suitable for host-guest applications, as illustrated in the formation of COF-1 (produced by self-condensation of 1,4-benzenediboronic acid) on HOPG, which was used as host/guest system to accommodate C_{60}

molecules.[187,191] Cui *et al.* observed two distinctive COF-1 adsorption sites for fullerene molecules, denoted as the top site and the pore site.[187] The STM images show both the fullerene molecules and COF frameworks, revealing the adsorption sites of C_{60} guest molecules (Figure 13). In subsequent studies, the authors have applied the same COF-1 template for 3D self-assembly of fullerene films. The structural arrangements of C_{60} in the third dimension is determined by co-adsorption of solvent (trichlorobenzene *versus* heptanoic acid).[192]

All of the above examples deal with SAMNs templating adsorption of other molecular species, but this concept can be extended to other nanoscale materials. Thus, favorable vdW interactions of alkyl chains of dialkoxybenzene SAMN and alkanethiol-protected gold nanoparticles (AuNPs) can be used to guide the adsorption of the latter on HOPG surfaces.[193] The alignment and periodicity of AuNPs are determined by the SAMN template, but only when the lengths of the alkyl chains in the host and guest match one another.

Model systems to understand and to control the organic/metal interface in organic electronic devices

Controlling molecular adsorption at the organic/metal interface is essential[194,195] for designing molecular electronic devices, in which individual molecules are employed as wires, switches, sensors, current rectifiers, and transistor components.[7,196-200] Investigating the structural and chemical properties of such interfaces also has major implications in organic electronics,[201] in which molecular thin films are used as semiconducting layers or band-alignment interlayers of light-emitting diodes, transistors, memories or solar cells.[202-204] Specifically, the local structure of

the metal/insulator/organic interface plays major roles in determining charge injection or collection at the electrodes, yet it is still poorly understood. In this context, STM has been widely used to image SAMNs and organic/metal interfaces in real space, with the aim of understanding and improving the performance of organic electronic devices. Likewise, device measurements determine the effectiveness of the molecular layers.

As discussed above, TCNQ adsorption is a notable example of modification of the surface structure by adsorbed organic molecules.[119] Due to strong charge transfer induced across the interface, both the substrate and the molecule can undergo significant structural rearrangements. The TCNQ is a prototypical π-electron acceptor that has given rise to many organic metals and magnets. TCNQ/copper interface is an important model for doping and band-alignment layers in organic semiconducting devices. In this case, charge transfer induces strong chemical bonding between the lone pairs of the nitrogen atoms and the d_z^2 orbital of copper atoms. In addition, the stress field created around the reconstructed copper atoms strongly affects the self-assembly of TCNQ molecules. Such changes can significantly affect the charge injection at the metal/organic semiconductor interface.

Charge transport at the organic/metal interface could also affect the chemical reactivity of the molecules, inducing dissociation reactions on metal surfaces brought about by hot electrons, that is, electrons excited above the Fermi level of the metal then transferred to the unoccupied states of the molecule. Bond dissociation induced by injected electrons from the STM tip has been studied in various reactions[205,206] including the dehydrogenation of the benzene rings of cobalt phthalocyanine (CoPc),[207] dissociation of C-Cl in chlorobenzene[208] and C-I in iodobenzene,[209] and dissociations of C-S bond in a conjugated thiol derivative.[210]

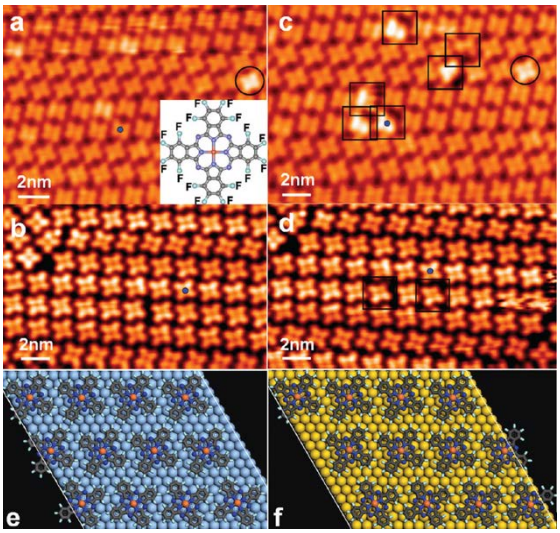

Figure 14. Scanning tunneling microscope images of F_{16}CuPc (structure in inset) on (a) Ag(111) and (b) Au(111) before pulsing. (c,d) Same images after a pulse at -3.0 and -3.2 V on top of a molecule, respectively; the blue dot, rectangles, and circles represent the pulsing position, reacted molecules, and bright molecules not induced by pulsing, respectively. Proposed structure models of F_{16}CuPc on (e) Ag(111) and (f) Au(111). Reproduced from ref [211], copyright 2009 ACS.

By using hot electrons from a STM tip, Chen *et al.* demonstrated different nonlocal chemical reactions in one monolayer of copper perfluorophthalocyanine (F_{16}CuPc) adsorbed on Ag(111) and Au(111).[211] Figure 14 shows that F_{16}CuPc adsorbs in a flat-lying configuration with its molecular π-plane parallel to the metal surface. On both surfaces, the molecules appear as four-leaf features corresponding to F-substituted benzene rings. After electron injection by STM pulses, one of the molecule's four arms appeared shortened, which was attributed to its chemical decomposition, most likely dissociation of the C–F bond(s). Interestingly, the reaction was observed to occur as far as 12 nm distance from the tip (Figure 14c). The statistical analysis of the radial distribution of reaction events shows that such non-local reactions are induced by lateral propagation of hot electrons.

Such transformations could also plausibly occur during normal device operations; they are extremely difficult to detect using common analytical techniques yet could be detrimental to device longevity.

Assembly on non-conducting substrates

While metallic (or HOPG) surfaces have been the prime substrates for the majority of STM studies of supramolecular self-assembly, assembly on non-conducting surfaces is highly essential for most optoelectronic applications of the SAMNs. Indeed, conducting substrates can readily quench the fluorescence and mask semiconducting properties displayed by many aromatic molecules explored in such studies. There has been excellent progress in forming SAMNs on the surfaces of bulk alkali halide crystals in vacuum[212-215] and it is possible, using AFM, to identify molecular ordering within adsorbed monolayers. In some cases, for example PTCDA on alkali halides[216], molecules are adsorbed in a face-on orientation, similar to the geometry on metal surfaces.[217] However, a weaker interaction of molecules with the surface can alternatively result in a morphology dominated by intermolecular forces. This can lead to an edge-on orientation as demonstrated by Maier and coworkers who used non-contact AFM (nc-AFM) to study cyanophenyl-substituted porphyrin derivative on KBr(001).[212] These molecules assemble in π-stacked 'molecular wires' with ~0.5 nm spacing, preferentially arranged along the step edges of the substrate.

The growing interest in two-dimensional materials has attracted attention to hexagonal boron nitride (hBN), a layered insulator which is isostructural to graphite/graphene, but contains a

boron and a nitrogen atom instead of two carbon atoms in its 2D unit cell. This substrate provides an atomically smooth surface with almost no dangling bonds and large terraces (up to tens of microns).[218] hBN is available in two common forms: as exfoliated flakes with thicknesses from a monolayer up to tens of nanometres, or as monolayers grown by chemical vapor deposition (CVD) on metal surfaces. hBN grown on metals commonly exhibits a moiré pattern[219] that provides a unique template for the preferential adsorption of atoms,[220,221] atomic clusters,[222] or molecules.[220,223,224] In this latter form, the hBN is sufficiently electronically transparent to support STM investigations of surface structure and supramolecular arrangements. While hBN monolayers on metals promote significant electronic decoupling of the molecules from the underlying substrates, the properties of the latter are nonetheless affected by the metal substrate. For example, Joshi and coworkers studied the effect of the hBN/Cu(111) substrate in templating the growth of molecular arrays of free-base porphyrin donors and TCNQ acceptors.[225] Porphyrin exhibits the smallest electronic bandgap at the “hills” and the largest bandgap at the “valleys” of hBN due to subtle modulation of screening.[225]

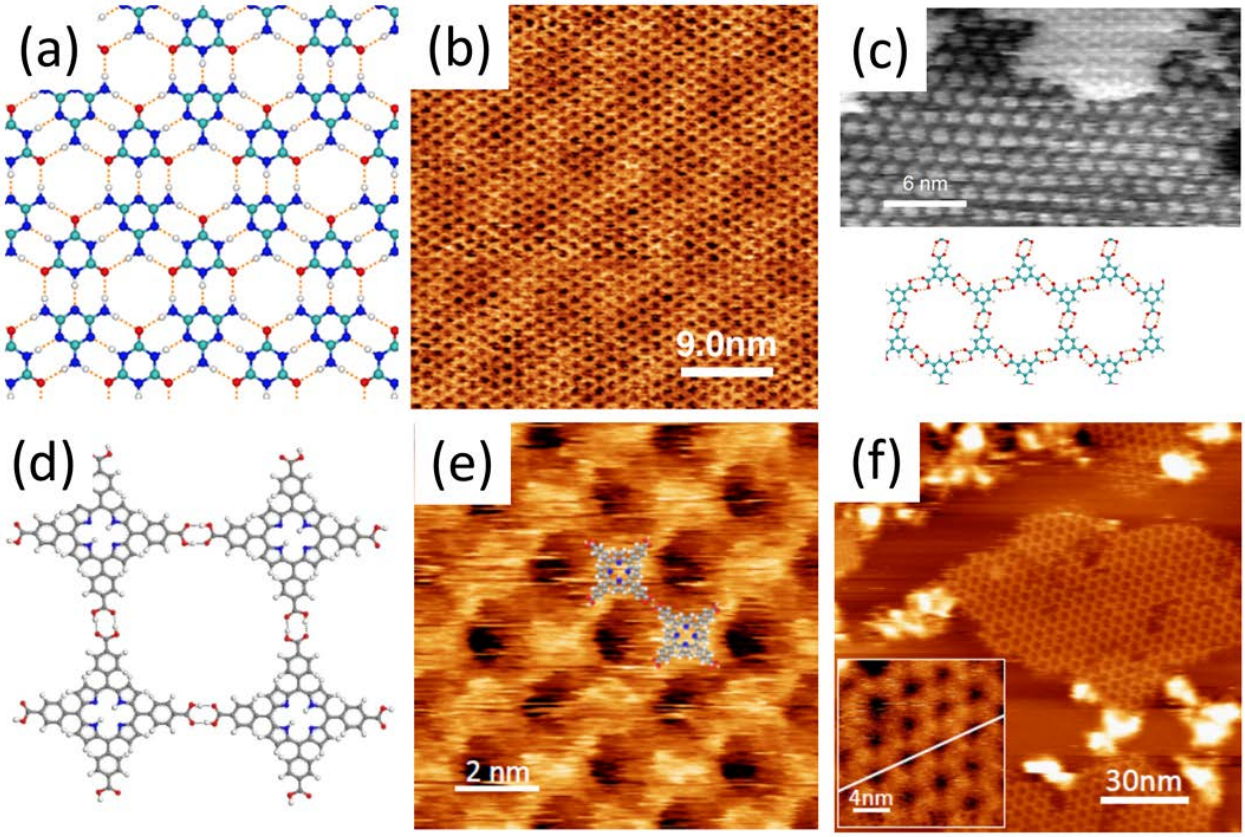

Figure 15**.** Hydrogen-bonded self-assembled molecular networks on hexagonal boron nitride (hBN). (a) Molecular model and (b) atomic force microscopy (AFM) image of melamine cyanurate formed by co-assembly of cyanuric acid and melamine; the observed moiré pattern is due to interface with hBN. (c) Heterostructure formed from by nanoporous array of trimesic acid (period ~ 1.6 nm, lower half of AFM image – see also schematic structure below) on melamine cyanurate (period ~ 1 nm, top centre); image in inverted contrast. (adapted from ref[226], copyright 2017 NPG) (d) Molecular model and (e) AFM of a self-assembled square phase of 5,10,15,20-tetrakis(4-hydroxycarbonylphenyl)porphyrin on hBN. (f) Minority hexagonal network co-existing with square phase (adapted from ref [227], copyright 2015 ACS [ACS AuthorChoice Article]).

In contrast, exfoliated hBN flakes with thicknesses greater than 5-6 layers are too resistive for STM, and AFM must be used to image surface structures. It has been demonstrated that highly ordered thin films of organic semiconductors, including rubrene and pentacene can be grown on exfoliated hBN, and, further, that these flakes can act as a dielectric layer in a planar organic field effect transistor geometry, thus realising devices with high carrier mobility.[228-230] While these

organic layers were grown from the vapour phase it has also been shown that molecular assemblies can be deposited on hBN from solution, and that AFM under ambient conditions provides sufficient resolution to characterise the molecular arrangements within the resulting monolayer and multilayer films. The availability of hBN as an insulting substrate compatible with SAMN formation under standard atmospheric conditions greatly extends the range of relevant materials and potential applications. Several examples of SAMNs on hBN deposited from solution have now been demonstrated including a porous bimolecular network formed from perylenetetracarboxydiimide (PTCDI) and melamine[178,231], as well as large monolayer and multilayer islands of melamine cyanurate.[226] Figure 15a and b show, respectively, a structural diagram and high resolution AFM images of melamine cyanurate which forms a honeycomb SAMN with a lattice constant of 0.98 $\pm$ 0.02 nm. Interestingly, moiré patterns may be clearly resolved at the melamine cyanurate/hBN interface (Figure 15c), and furthermore, the formed melamine cyanurate islands can be used as a substrate for the growth of further supramolecular layers, for example of trimesic acids, giving rise to highly ordered organic heterointerfaces.

SAMNs of not completely planar molecules such as 5,10,15,20-tetrakis(4-carboxyphenyl)porphyrin (TCPP, Figure 15d) can also be formed on hBN.[227] Two typical supramolecular structures are observed, namely the square and hexagonal arrangements presented in Figure 15e,f. These structures are stabilized by vdW interactions between the molecules and the underlying hBN and by intermolecular hydrogen bonding. Measuring the fluorescent properties of TCPP on hBN revealed a significant red shift of the emission peak compared to these molecules in solution, which was attributed to conformational changes due to molecular deformation mediated by substrate-molecule interactions. The correlation between

optical properties and molecular organization within a 2D layer has also been investigated recently under vacuum conditions using both fluorescence[232,233] and STM-induced luminescence.[234,235] In these studies, chromatic shifts have been attributed to the coupling of transition dipole moments of neighboring molecules, and can be engineered either through supramolecular organization or by manipulating individual molecules using the tip of a scanning probe microscope.

Calcite ($CaCO_3$) provides an alternative insulating substrate that can support the formation of well-ordered SAMNs *via* vacuum sublimation.[236] The interactions of adsorbed layers with photons have also been investigated on this surface, including light-induced changes in conformation of a photochromic molecule 4-methoxy-3,3',5,5'-tetra-*t*-butylazobenzene.[237]

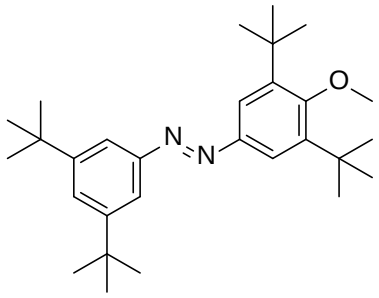

4-methoxy-3,3',5,5'-tetra-*t*-butylazobenzene

Together these results highlight the possibilities of the combined study of the fluorescence, photochemistry and spatial ordering of molecular assemblies with potential applications in optoelectronics, integration with other two-dimensional materials such as metal dichalcogenides, and fundamental optical studies relevant to organic photovoltaics and sensing.

On-surface reactions

The templating effect of crystalline surfaces in pre-organizing reactive molecules creates special opportunities for manipulating the direction of coupling reactions,[238] controlling the structure and order of covalent macromolecular systems. This approach was used in 1997 by the De Schryver[239] and Aono[240] groups in photo- and STM-tip induced[241] 1,6-addition of diacetylene derivatives in monolayers on HOPG. Unlike the many cases of diacetylene polymerization in 3D (occurring through topotactic single-crystal-to-single-crystal transformation), the reaction was much less efficient on HOPG, as the polymer size was limited by frequent "chain-termination" defects. Another notable early attempt of on-surface polymerization is electrooxidative growth of conjugated polythiophenes on iodine-covered Au(111) electrodes by Sakaguchi *et al.*[242] In contrast to diacetylene polymerization, the thiophene monomers are not preorganized on the surface, but the adsorption of the growing oligomers from solution leads to ordered domains of polythiophenes oriented along [111] directions. This growth results in crystalline domains of polythiophenes aligned along one of the three crystallographic axes of Au(111). Subsequent work from the same group has also demonstrated epitaxial growth of diblock copolymers (containing thiophene units with different substituents).[243] While the electrochemical growth of thick and usually amorphous polythiophene films is straightforward, carrying out this reaction controllably is challenging.

Catalytic on-surface polymerization

The game-changing reaction that has enabled much of the explosive growth of the field of on-surface polymerization is Ullmann coupling, which links halogenated aromatic rings with a C–C bond. Initial STM insight into Ullmann coupling was provided by Weiss and coworkers who showed alignment of the surface-bound phenyl intermediates and pairs formed from iodobenzene on the Cu(111) surface.[111] In the early 2000s, Hla *et al.* reported the STM-tip controlled coupling of iodobenzene on Cu(111), to produce biphenyl.[209] Weiss and coworkers demonstrated that depositing of *p*-diiodobenzene on Cu(111) at 77 K leads to the growth of lines of *protopolymers*.[244] This protopolymer was later identified by Lipton-Duffin *et al.* as an organometallic intermediate linked *via* C-Cu-C bonds, which converts to covalent poly(*p*-phenylene) (PPP) by annealing at 470 K (Figure 16).[245] In 2007, Grill *et al.* showed that C-C coupling of aromatic halides can also be initiated on Au(111) at above 600 K.[246] They demonstrated the growth of a two-dimensional network from 5,10,15,20-tetrakis(4-bromophenyl)porphyrine, highlighting the new opportunities offered by on-surface chemistry. A number of 2D conjugated polymers were synthesized by coupling various polyhalogenated aromatics on Au, Ag and Cu surfaces.[247-250] In addition to its catalytic effect, the surface plays a crucial role in templating the 2D growth of the polymers, which would otherwise collapse into disordered 3D crosslinked networks.

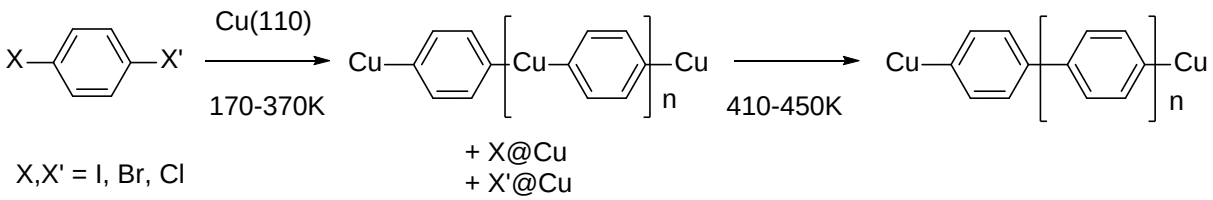

Figure 16. Ullmann polymerization of dihalobenzene on Cu.

The templating role of the substrate is also important in 1D Ullmann polymerization on strongly interacting surfaces such as Cu and to a lesser extent on Au[251] (as one measure of the interactions on Au(111), unlike more strongly bound adsorbates, benzene does not even lift the surface reconstruction).[252] Both organometallic intermediates and the final polymer can maintain strong epitaxial relationships with the substrate and at low coverage, the reaction intermediates can interact *via* perturbation of the substrate electrons.[111,244] Depending on the size and surface density of the monomer, and the crystallographic orientation of the substrate, polymer chains adopt different yet strictly fixed orientations on the Cu surface. On the other hand, the mismatch between the periodicity of the surface along these directions and the polymer creates strain in the latter, suppressing polymer growth or even quenching polymerization. Thus, the length of the PPP chains formed from 1,4-dibromobenzene polymerization on Cu surfaces varies along different directions, with the longest being oriented along the <1–1±2> direction, which has the closest epitaxial match.[253]

A mechanistic understanding of the Ullmann polymerization is essential for developing approaches for structural control of the resulting polymers, which thereby has been the subject of various recent theoretical and experimental studies.[248,254-256] On Cu surfaces, the C–X bond dissociation happens readily below room temperature for I, Br (and slightly above for Cl[257,258]), while the subsequent formation of C–C bonds between metal-linked carbons is the rate-limiting step (Figure 16). In aromatics with multiple halogens, which C-X bonds are broken can thus be controlled thermally.[258-260] While C-C coupling typically occurs at 150–200 °C, the rate of the

coupling reaction depends on the nature of the halogen.[258] The halogen could, in principle, stabilize the organometallic intermediate by binding to the bridging metal center (C-Cu-C) and thereby affect the reaction rate.[111,261]

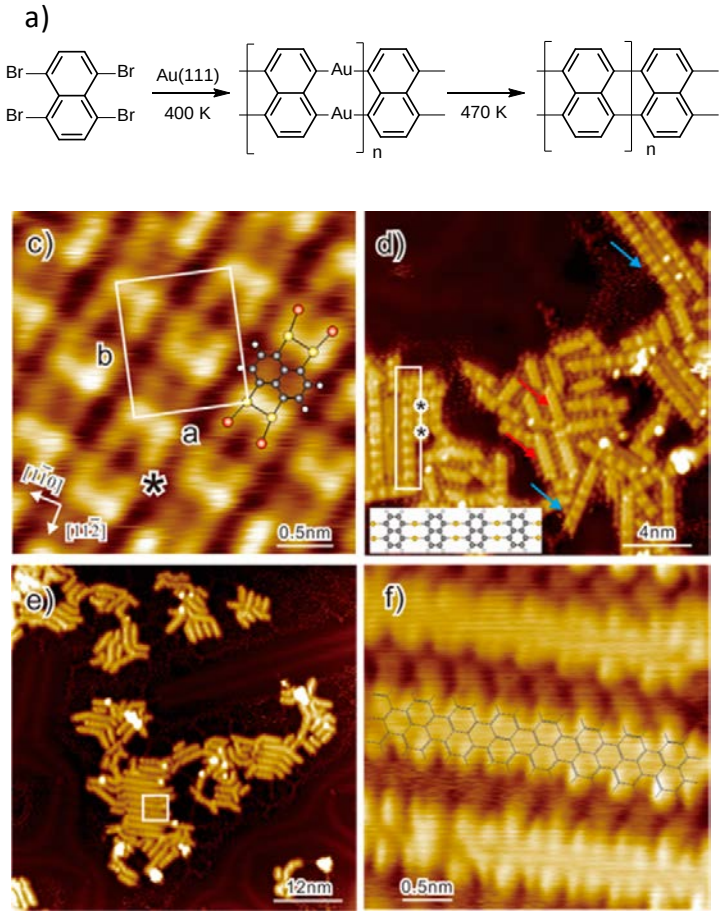

Figure 17. On-surface synthesis of fused polyrylene (5-GNR) on Au(111). (a) The reaction scheme; (c,d) organometallic intermediates formed at 400 K; (e,f) covalent polymers formed upon annealing at 470 K. Adopted from ref [262], copyright 2015 ACS.

In the abovementioned examples, Ullmann coupling links aromatic building blocks with single C–C bonds. The relative flexibility of this connection allows for sterically induced out-of-plane deformations in the polymer, including twisting (non-zero dihedral angle between the aromatic rings), which limits the electron delocalization as well as bending,[263] which results in structural

defects in 2D polymers (*e.g.*, pentagon/heptagon defects in hexagonal networks[250]). These defects could be suppressed by connecting the building blocks with two bonds, as demonstrated by Chi and co-workers in converting tetrabromonaphthalene in fully fused polyrylene on Au(111) (Figure 17).[262] The latter represents the narrowest graphene nanoribbon (5-GNR) obtained *via* molecular precursor route.

Due to its selectivity, predictability, and broad applicability for both the monomers and surfaces (Cu, Ag, Au), dehalogenative Ullmann coupling has become the most general and useful method for surface-confined synthesis of macromolecular structures. The methodology has also been extended to the coupling of non-aromatic alkynylbromides,[264] alkenylidenedibromides,[265] and alkylbromides[266] (Wurtz reaction). Its main limitations are the need for pre-functionalizing the monomer with the active halogen group, the reduced volatility of the halogenated monomer and the formation of metal halide side products. The latter can block the reactive surface and limit the growth of the polymers, although the low thermal stability of some halide adlayers (*e.g.*, bromine on gold) allows cleaning the surface by annealing at moderate temperatures. Non-halogen functional groups can also be used in on-surface polymerization (*e.g.*, polydecarboxylation of naphthalene-2,6-dicarboxylic acid[267]), but they remain subject to the above limitations.

In this respect, direct CH activation on metal surfaces followed by C-C coupling provides an interesting alternative to the Ullmann reaction. On-surface polymerization *via* CH activation was serendipitously discovered by Veld *et al.* upon annealing (~450 K) of tetrakis(*p*-tolyl)porphyrin on Cu(111).[268] More recently, a similar dehydrogenative C-C coupling was reported for octaethyltetraazaporphyrin on Au(111). Controlling the precursor deposition process, the

authors were able to steer the reaction to either *inter*molecular coupling, producing polymer chains fused by newly formed naphthalene rings, or *intra*molecular coupling, resulting in selective formation of phthalocyanine.[269] While in the above examples, the ease of dehydrogenative coupling could be intuitively attributed to the activating role of the aromatic rings, this functionality is not a precondition for on-surface coupling. Indeed, even linear alkanes can undergo dehydrogenative polymerization *via* terminal CH_3 groups forming polyethylene chains, when heated to 150-200 °C on high-index Au surfaces.[270]

Several groups reported dehydrogenative C-C coupling of terminal alkynes, resembling Glaser-Hay solution-based reaction. Despite substantial progress,[271-273] this approach is not nearly as efficient as Ullmann coupling. The polymer networks formed by this method suffer from both topological defects, brought about by the high flexibility of the resulting butadiyne links as well as structural defects, due to competing alkyne addition reactions,[274] forming benzene, diene and enyne connections.

Only a few examples of on-surface polymerization proceeding through CH-activation of aromatic precursors are known.[275] Surface-catalyzed cleavage of C_{sp2}-H bonds is more difficult than that in both alkanes (sp^3) and alkynes (sp), due to their low acidity and high strength. Also, selective activation of just one of the many CH bonds present in typical aromatic precursors is an additional challenge. Nevertheless, *intramolecular* dehydrogenative coupling leading to ring fusion and planarization of sterically congested aromatics has been widely used in on-surface chemistry,[276] and is an essential part of the on-surface synthesis of graphene nanoribbons described hereafter. *Intermolecular* dehydrogenative coupling was recently demonstrated for *p*-quaterphenyl connecting these monomers into polyphenylene chain *via meta*-positions of terminal phenyls.[277]

The reaction was also extended into 2D by using cobalt phthalocyanine as a precursor.[278] In classical organic synthesis, regioselectivity of dehydrogenative coupling is most often provided by directing groups. On-surface implementation of this approach was reported by Chi and coworkers who showed C-C coupling of 4-hydroxyphenyl-terminated monomers, *via* one or both *ortho*-positions of the hydroxyphenyl moiety, on Ag(111) or Au(111), respectively.[279] Interestingly, the XPS results suggest that the directing hydroxyl groups are removed from the resulting polymers upon annealing at 250-300 °C, although the mechanism of such dissociation and the termination of the corresponding carbons atoms, are not understood.

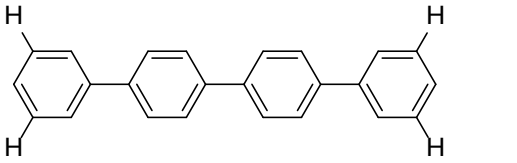

p-quaterphenyl

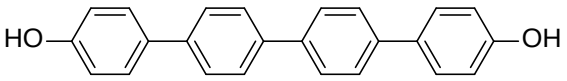

4,4'''-dihydroxy-p-quaterphenyl

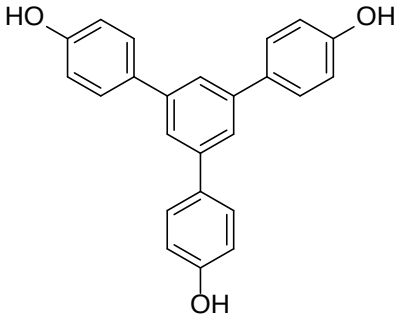

1,3,5-tris(4-hydroxyphenyl)benzene

On-surface dynamic covalent polymerization

Despite significant progress in improving the order of on-surface synthesized covalent networks, their structural quality is limited and does not compare to that of graphene prepared by high-temperature CVD. This difference is likely an intrinsic limitation of synthesis under "kinetic control", where the (entropically favored) defects, once formed, remain a part of the structure. Dynamic covalent chemistry (DCC) offers a possible solution to this problem: reversible formation

of covalent bonds enables error-checking and self-healing, as was demonstrated by Yaghi and coworkers in preparation of crystalline covalent organic frameworks (COFs).[280] Potentially, COF monolayers could combine the self-assembly of SAMNs with robustness and strong electronic coupling of covalent polymers.

On-surface DCC has been applied for the synthesis of 2D polymers *via* polycondensation of boronic acids,[281-286] polycondensation of aldehydes with amines (Schiff base reaction),[89,287-289] as well as combinations of both.[290] Experiments performed on Ag (111) in a UHV-STM chamber led to highly disordered networks because the condensation by-product (H_2O) necessary for the reverse reaction, does not remain on the surface in UHV.[281] In order to provide dynamic equilibrium conditions in on-surface polymerization both solid-liquid and solid-gas interfaces have been explored, primarily on HOPG.

Polymerization at solid-liquid interfaces is appealing because of its simplicity and dynamic surface/solution exchange, which can select for adsorption of ordered 2D polymers while leaving small molecular impurities and 3D macromolecular structures in solution. However, the selective adsorption makes control of stoichiometry in multicomponent reactions more difficult.[284,287] Avoiding competing in-solution polymerization, which can result in precipitation of disordered COF particles on the surface, is another challenge. Some studies suggest that it might be possible to suppress in-solution-polymerization because the "local concentration" effect upon on-surface adsorption can accelerate the condensation reaction by four orders of magnitude.[291] Indeed, partially ordered COF monolayers have been prepared at solid-liquid interfaces by controlling the solution concentration[289] and the pH.[287] The solution concentration was also reported to steer the structure of the imine-linked COF monolayers, between Kagome and oblique 2D lattices.[292]

The most ordered COF monolayers have been prepared at the solid-gas interface, where the reactive components are delivered either by prior casting from solution[89] or by evaporation;[286] annealing at increased temperature in high-humidity atmosphere is used to accelerate the self-healing process. The use of hydrated salts ($CuSO_4 \cdot 5H_2O$) in humidity-controlled chambers allows control of the release of water upon heating and its reabsorption during the cooling process, thus accelerating the dynamics of the reaction and shifting the equilibrium towards the COF.[283] Furthermore, the reactive monomers can be delivered to the surface dynamically, *via* gas-phase.[288] This strategy works best for copolymerization of monomers with different volatilities and results in highly ordered COF monolayers (Figure 18). However, the reaction temperature appears to have a dramatic effect on the uniformity of the resulting COF.

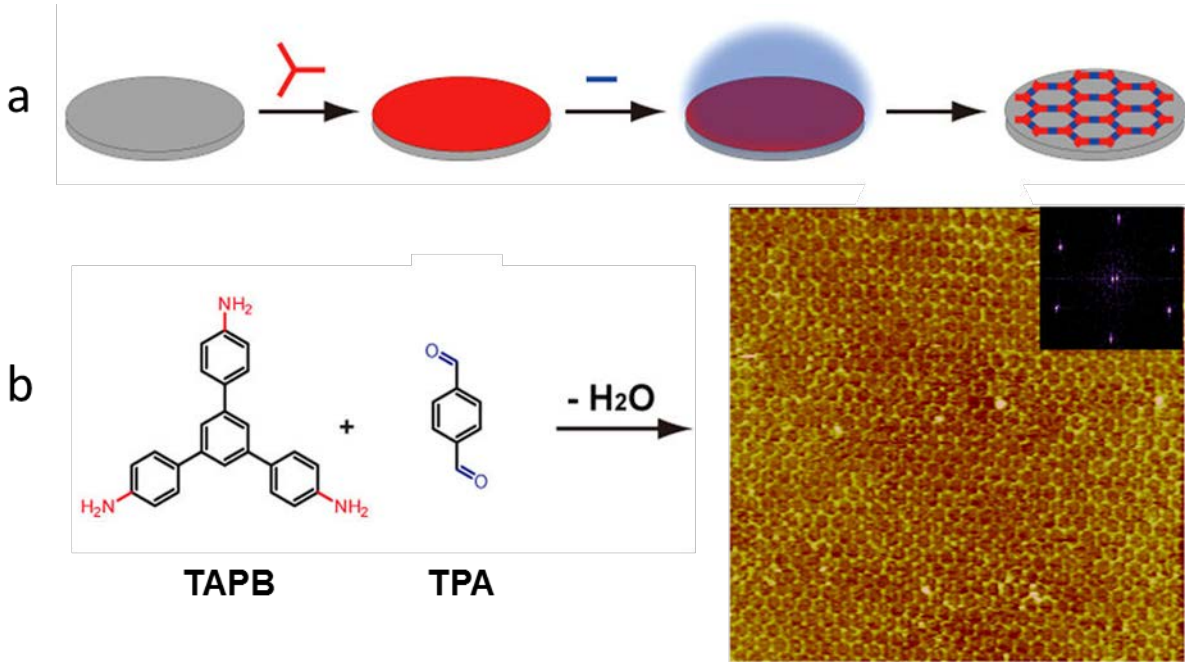

Figure 18. On-surface synthesis of an imine covalent organic framework (COF) *via* solid–vapor phase strategy. a) Schematic diagram showing sequential drop-casting and *in situ* dynamic vapor deposition of the monomers followed by annealing-induced polymerization. b) Reaction of tris(4-

aminophenyl)benzene (TAPB, drop-casted) and terephthalic aldehyde (TPA, introduced from the gas phase) forming a long-range ordered hexagonal COF imaged by STM (inset: a two-dimensional fast Fourier transform (2D-FFT) of the image). Adapted from ref [288], copyright 2013 ACS.

Graphene nanoribbons

Templating effect of surface has also been paramount in synthesis of quasi-one-dimensional materials such as graphene nanoribbons (GNRs). The GNRs can exhibit intriguing physical properties such as width-dependent electronic bandgaps,[293,294] photoconductivity,[295] and superlubricity.[296] A topic of interest in the condensed matter community is how to exploit the precise control of GNR width and edge geometry to modulate its electronic properties. In particular, the edge state of GNRs can determine their electronic structure and result in low-dimensional magnetism at zigzag edge GNRs.[297] There are two general strategies for the synthesis of GNRs: top-down and bottom-up. The former was first developed with an emphasis on device fabrication using micrometer length GNRs; the latter bottom-up methods can form GNRs with well-defined width and edge structures.[27,298-308]

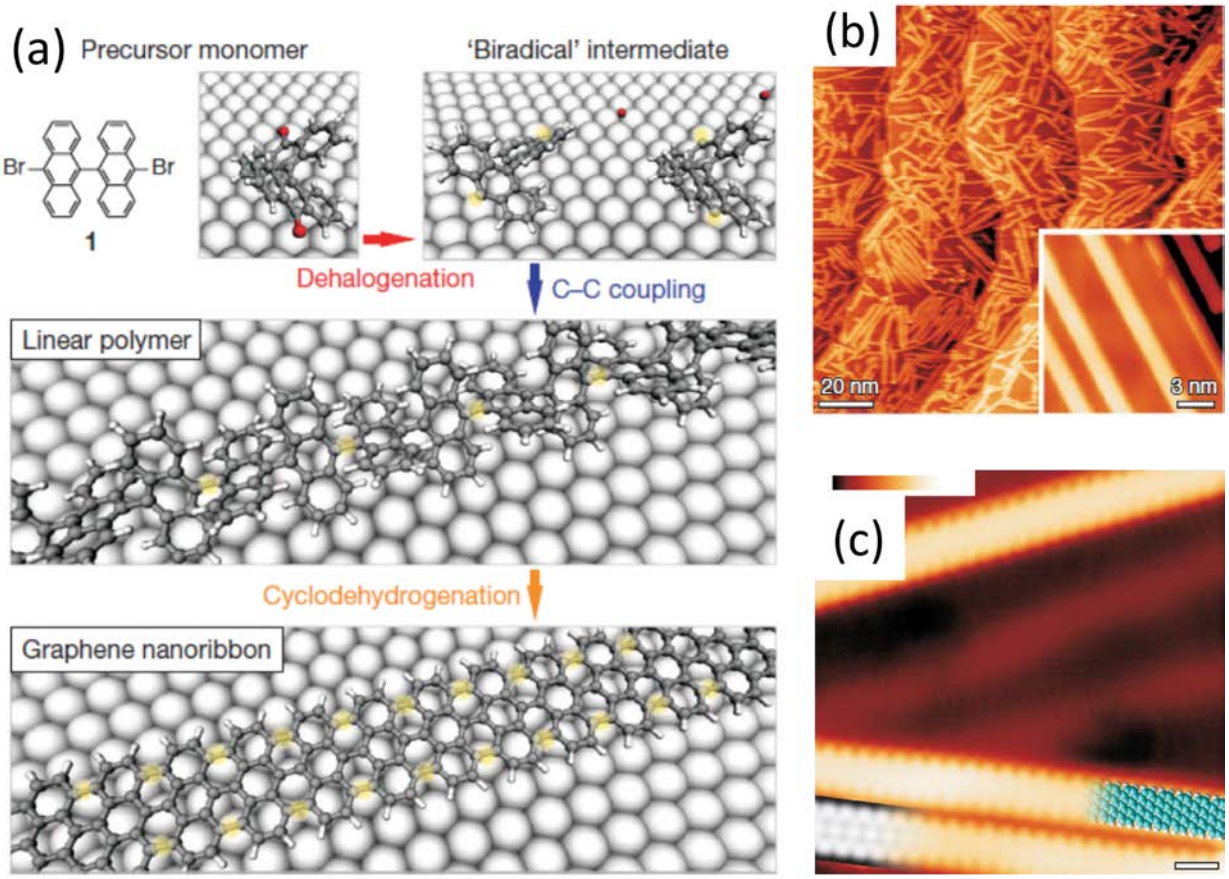

Figure 19**.** Bottom-up synthesis of graphene nanoribbons (GNRs). (a) A scheme showing the precursor monomer showing its halogenation, polymerization and cyclodehydrogenation forming GNR. (b) Scanning tunneling microscope (STM) image of linear 7-GNRs after cyclodehydrogenation at 400 °C. (c) High-resolution STM image showing GNR nanostructure with overlaid molecular model (blue). Adapted with permission from ref [300], copyright 2010 NPG.

So far, the bottom-up synthesis of GNR has been mainly limited to UHV conditions, although recently Sakaguchi *et al.* demonstrated the large-scale growth of armchair-edged graphene nanoribbons (AGNRs) using CVD in low vacuum.[309] In all cases, such syntheses are based on surface-assisted polymerization of molecular precursors on coinage metals followed by 'fusion' of the resulting linear polymer into GNR. This approach was pioneered by Cai *et al*.[300] and is illustrated in Figure 19a. This two-step thermally activated conversion of the molecular precursor

10,10'-dibromo-9,9'-bianthracene (DBBA) forms linear polyphenylenes, and the subsequent cyclodehydrogenation reaction results in GNRs with well-defined widths and arm-chair edges (Figure 19b and c). Recent updates of bottom-up GNRs fabrication can be found in the reviews of Narita *et al*.,[310] Talirz *et al*.,[27] and Xu *et al*.[311] The former two reviews highlight GNR synthesis with heteroatoms such as nitrogen at atomically defined positions. The latter describes recent progress on the scalable template growth of GNRs on SiC, as well as the directed growth of GNRs on nickel nanostructures.

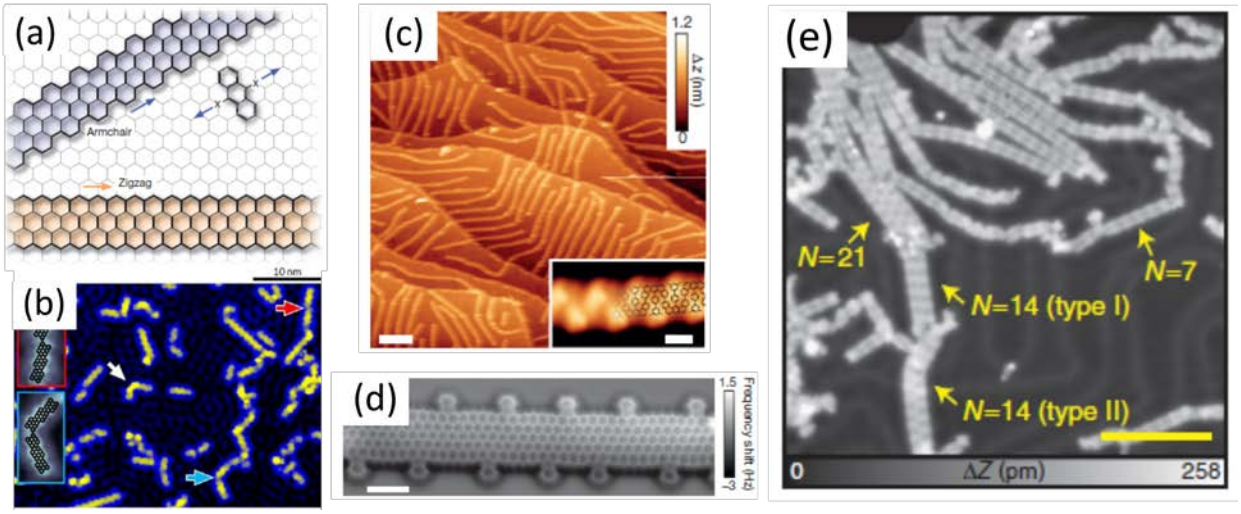

Figure 20**.** (a) Models of the armchair and zigzag graphene nanoribbons (GNRs) showing edge structures (reproduced from ref [312], copyright 2016 NPG). (b) Scanning tunneling microscope image of (3,1)-GNR on Cu(111); the white arrows represent the connected GNR with continuous π-conjugation, the red and blue arrows display regions in which the π-conjugation is not continuous (reproduced from ref [305], copyright 2015 ACS). (c) High coverage of 6-zigzag GNR (ZGNR)-decorated Au(111) surface; scale bar 20 nm; the inset shows alternation of bright features, which indicates the zigzag nature of the structure. (d) Non-contact atomic force microscope (AFM) frequency-shift image of edge-modified 6-ZGNR; scale bar 1 nm (reproduced from ref [312], copyright 2016 NPG). (e) Atomic force microscope image of boron-doped GNRs with different lengths (adapted from ref [313], copyright 2015 NPG [Open Access]).

A reliable protocol for the mass production of GNRs should ultimately achieve the desired practical application. For example, the precise control of GNR width and edge type allows the direct integration of GNRs on insulating or semiconducting substrates for device fabrication. In particular, proper selection of the precursor monomers allows one to assemble specific GNRs selectively with either armchair or zigzag edge structures (Figure 20a).

The reactivity of the metal substrate is also important for surface-assisted molecular self-assembly of GNR, and other metals besides Au(111) have been used, such as Cu(111),[305,302] Cu(110),[314] and Ag(111).[300] For example, Han *et al.* reported that DBBA precursor, which leads to AGNR on Au(111) at 400 °C,[300,305] affords isomeric (3,1)-GNRs when the reaction is carried out on Cu(111) at 500 °C (Figure 20b).[305] This result was attributed to cross-dehydrogenative polymerization *via* 6,6‘-positions of DBBA instead of dehalogenative Ullmann polymerization *via* 10,10‘-positions.

The importance of surface reactivity was further demonstrated by Simonov *et al.*[314] who compared the assembly of DBBA on two Cu surfaces with different crystallographic orientations. On Cu(110), the self-assembly of DBBA is hindered due to the strongly anisotropic feature of Cu(110) that suppresses the covalent coupling of DBBA fragments, and consequently no polyanthracene chains are formed. In contrast, Ullmann coupling is facile on Cu(111). Chen and colleagues expanded the width of AGNRs by employing a π-extended DBBA derivative in polymerization on Au(111).[301] Huang and coworkers used the Ag(111) substrate to extend the width of DBBA-derived GNRs through dehydrogenative ring fusion, affording the ribbons with double (14-AGNR) and triple (21-AGNR) width.[315]

The fabrication of zigzag GNRs (ZGNRs) has proved more challenging, and Ruffieux *et al*. demonstrated the self-assembly of well-defined 6-ZGNRs using surface-assisted aryl–aryl coupling on Au(111) (Figure 20c).[312] Non-contact atomic force microscopy imaging confirmed that the observed width and edge morphology correspond to the 6-ZGNR structure (Figure 20d). Substitutional doping of GNRs by boron and nitrogen atoms has also been demonstrated.[313,316,317] For example, boron atoms can be introduced into the GNR structure as a BC_3 Lewis acidic site at the center of the AGNRs. The STM image contrast is typically used to identify the perturbed electronic structure since boron atoms serve as electron-accepting sites. Further annealing of the substrate at 510 °C results in B-doped GNRs with different widths (Figure 20e).

The scope for structural diversity and control of GNR prepared *via* on-surface polymerization is almost as limitless as the variety of possible building blocks. By combining several building blocks, even more functionally complex structures such as atomically precise GNR heterojunctions can be realized.[318] Likewise, it should be possible to use STS to test connections to determine how to create optimized contacts with aligned electronic bands. This study could be done by selecting combinations of precursors and reaction conditions known to result in a range of products.[304,319] That is, reactants (graphene precursors) and reaction conditions can be selected to yield a range of junctions upon reaction. These connections (contacts) can then be measured individually (on the same substrate surface) with STS to test if the molecular orbital structure is continuous and node-free. Ultimately, it will be the mesoscale control of these structures (the lengths of GNRs and their relative positions on the surface) that will determine our ability to integrate these materials into functional electronic devices.

On-surface discovery of new reactions and new molecules

Most current efforts in on-surface synthesis have relied on adopting well-established solution chemistry, which is challenged by dramatic differences in the kinetics and mechanisms of chemical reactions in solution and on solid surfaces. In addition, SPM studies of molecules adsorbed on reactive surfaces have also led to the discovery of new reactions and preparation of exotic molecules, which are not possible to synthesize *via* standard solution chemistry.

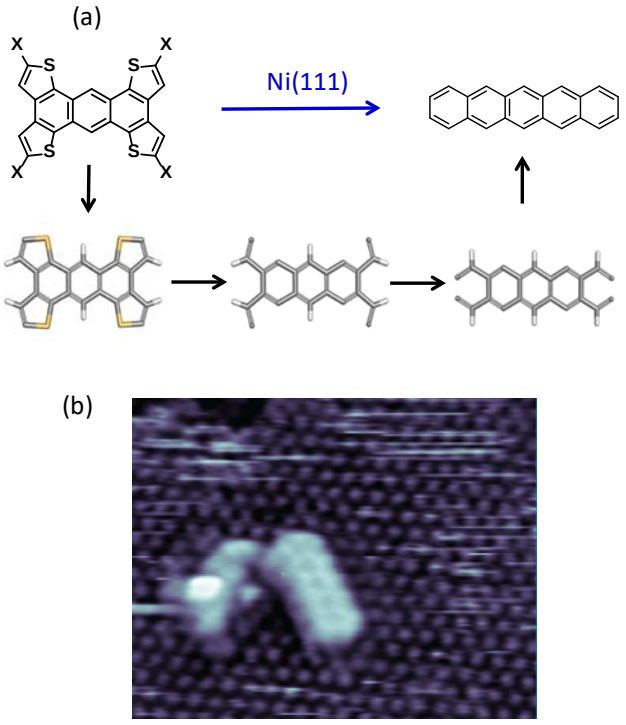

Figure 21**.** (a) Reaction scheme and (b) Scanning tunneling microscopy image of pentacene formed from tetrathienoanthracene on Ni(111); X = Br or H. Adopted from ref [320], copyright 2013 ACS.

In an attempt to use a Ni surface to initiate Yamomoto-type polymerization, Dinca *et al.* reported the formation of pentacene $C_{22}H_{18}$ on Ni(111), starting from a tetrathienoanthracene precursor (Figure 21).[320,321] The reaction occurs *via* nickel-induced sulfur abstraction from the thiophene

rings followed by C–C coupling resulting in the fusion of two benzene rings to the anthracene core. The structure of the product was established *via* a combination of STM imaging with secondary-ion mass spectrometry (SIMS) analyses. Note that as-prepared pentacene misses several hydrogen atoms and the desulfurized/debrominated carbons are presumed to bond covalently with the Ni. These carbons, however, are spontaneously protonated upon exposure of the surface to atmospheric moisture, as confirmed by SIMS analyses of isotope distribution in samples exposed to D_2O vapor.

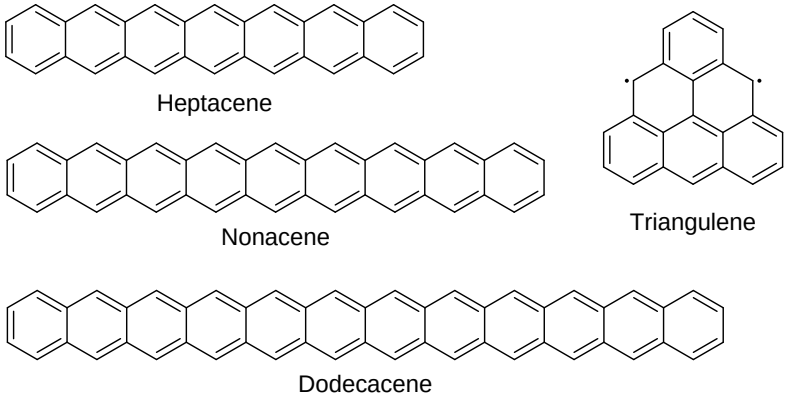

Surface immobilization and UHV conditions have enabled synthesis and SPM characterization of exotic molecules that are not accessible by traditional organic synthesis. Thus, unsubstituted acenes longer than hexacene are not stable and cannot be isolated under ambient conditions. However, heptacene,[322] and even (previously unknown) nonacene[323] and dodecacene[324] have been recently synthesized on Ag(111) and Au(111) surfaces by retrocyclization or dehydrogenation of their stable precursors. In a similar approach, synthesis of a triangulene biradical *via* dehydrogenation on Au(111) and its detailed characterization *via* nc-AFM, STM, and STS have been reported.[325]

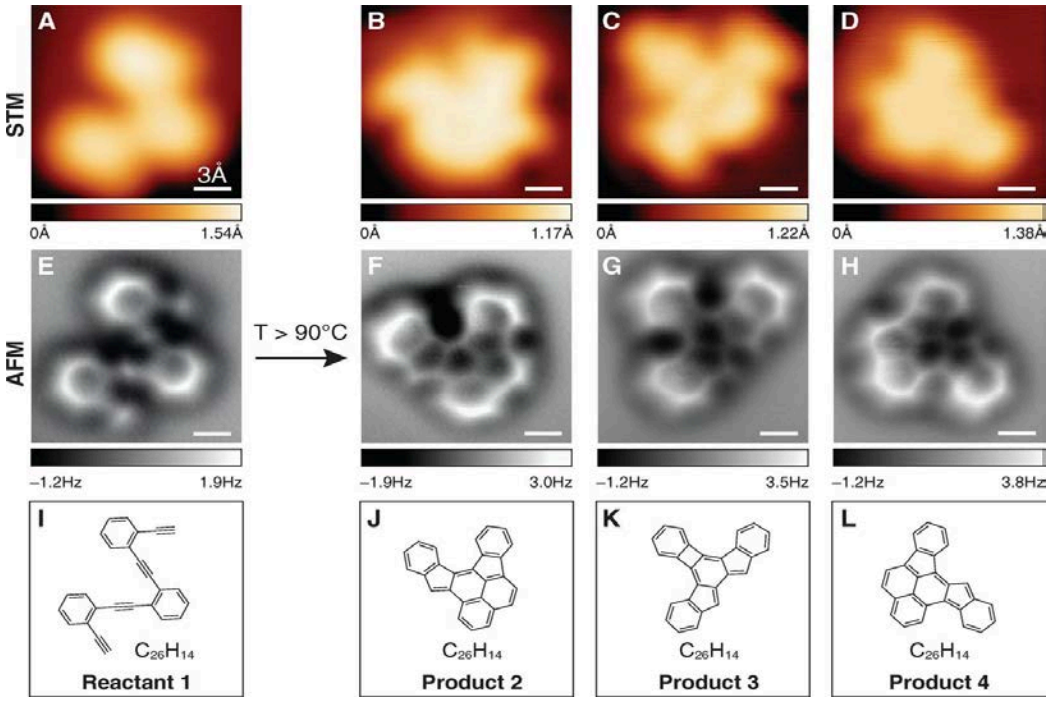

Figure 22. Transformation of oligo(*o*-phenylene ethynylene) (Reactant 1) into isomeric polycyclic aromatic hydrocarbons *via* a combination of 1,5- and 1,6-cyclization reactions on Ag(100). Reproduced from ref [326], copyright 2013 AAAS.

High-resolution nc-AFM provides impressive opportunities in discovering the unusual on-surface reactivity of organic molecules. Thus, de Oteyza *et al.* showed the Bergmann-like cyclization of oligo-*o*-phenyleneethynylene (Reactant 1) on Ag(100), leading to a variety of new polycyclic aromatic hydrocarbons (Figure 22).[326] The molecular diversity results from a combination of 1,6- and 1,5-cyclization pathways. While both of these cyclization pathways have precedence in solution chemistry, the structural identification of the produced isomers would have been extremely challenging without direct imaging by nc-AFM.

From the concept of reaction dynamics to surface reactions

By combining STM imaging with theoretical calculations of model cases of molecular dissociation, Polanyi's group has brought the fundamental concepts of reaction dynamics and kinetics to the study of surface reactions.

A fundamental finding in reaction dynamics is that the location of the crest of the potential energy barrier, attributed as "early" or "late", along the reaction coordinate in simple atomic-transfer reactions can be a useful index of the dynamics.[327-329] The location of the crest lies along the approach coordinate for the reactants, and the retreat coordinate for the products, for "early" and "late" barriers, respectively. Polanyi and coworkers applied this concept to simple dissociation reactions, of H_2 or HCl adsorbed on Si(100)-2×1, in which the location of the energy barriers were linked to the final surface reaction products.[330] The "early" barrier, whose activation energy is lower than the "late" barrier, is driven by the translation energy, while the "late" barrier is led by the vibrational energy. This finding suggests a means for steering reactions by reagent translation or vibration, leading to the dissociative attachment at closer or further separations on a surface.

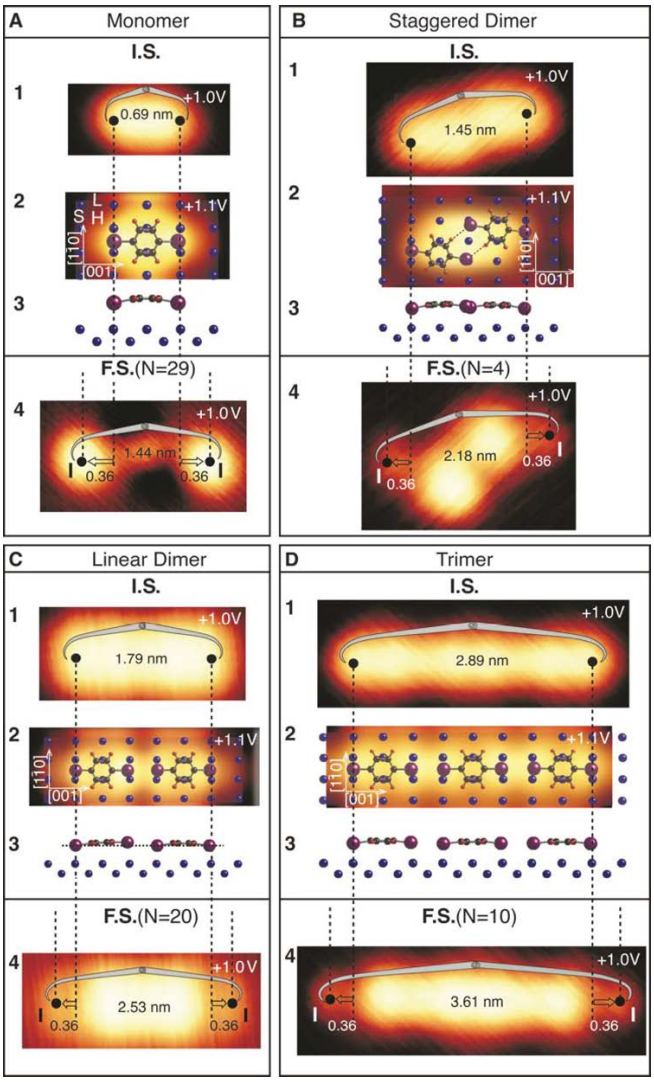

Figure 23. Scanning tunneling microscopy images obtained before (Panels 1) and after (Panels 4) electron-induced reaction from a (A) monomer, (B) staggered dimer, (C) linear dimer, and (D) linear trimer. The calculated adsorption geometries are shown in Panels 2 (top view) and Panels 3 (side view). Sites on the copper substrate are indicated in panel 2 of (A): long bridge (L), short-bridge (S) and 4-fold hollow (H). The diagrammatic calipers indicate the terminal I to I distances in nanometers in both the Initial state (I.S.) and Final state (F.S.) In panels 4, the distances in nanometers are the F.S. separations between the I-atoms. On average the I-atoms were displaced 0.36 nm from their initial positions. The number of observed cases is indicated as N in each panel. Reproduced from ref [331], copyright 2011 ACS.

A number of experiments explore the reaction path and kinetics of dissociative reactions of haloalkanes and haloarenes on Cu(110).[331-333] The STM can be used to follow the adsorbed

molecules from the physisorbed (self-assembly) state to chemisorbed (imprinting) state. In the case of *p*-diiodobenzene, the initial separation of the two terminal iodine atoms of the monomer, dimer, or trimer assembly imprints the final product. The terminal iodine atoms, which undergo electron-induced dissociation induced by the STM tip, will move 0.7 nm further apart from the initial separation. Therefore, the physisorbed molecule(s) acts as a "molecular caliper", which determines the final local separation of its terminal iodine atoms (Figure 23).[331]

Decoupling from the substrate

Once molecular systems adsorb on surfaces, their intrinsic electronic and optical properties are modified by their interactions with the substrate, which can lead to quenching of an excited state or metallization of the semiconducting structure. Electronic decoupling of adsorbates from the substrate would be required for most of the anticipated applications of on-surface synthesized 2D polymers or GNR. One solution to decouple the organic layer from Ag(111), is the addition of iodine, that forms a monolayer on the surface underneath the organic nanostructures. Upon exposure to I_2 vapor, the synthesized covalent organic nanostructures are less coupled to the surface and structurally relax.[334]

Alternatively, non-metallic surfaces could potentially be used as catalytic templates in growing such structures. For instance, dehalogenative (Ullmann-like) coupling of diiodobenzoic acid (DIBA) and even dichlorobenzoic acids (DCBA) was reported to take place on a surface of calcite at temperatures as low as 260 °C. The carboxylic groups deprotonate and chemisorb to the calcite surface, preventing desorption of the molecules in UHV.[335] Using larger (less volatile)

diiodoterfluorene monomer (DITF), polymerization was also achieved at 260 °C on a reduced TiO_2(011)-(2×1) surface, and its efficiency was correlated with the density of surface hydroxyl groups. Reportedly, polymerization does not occur on surfaces without hydroxyl groups, and is most effective with a moderate amount of hydroxyl groups.[336] However, the mechanism of this coupling reaction is not known, and subsequent studies on TiO_2(110)-(1×1) suggest efficient polymerization of dibromo-*p*-terphenyl despite "negligible" amounts of hydroxyl groups.[337]

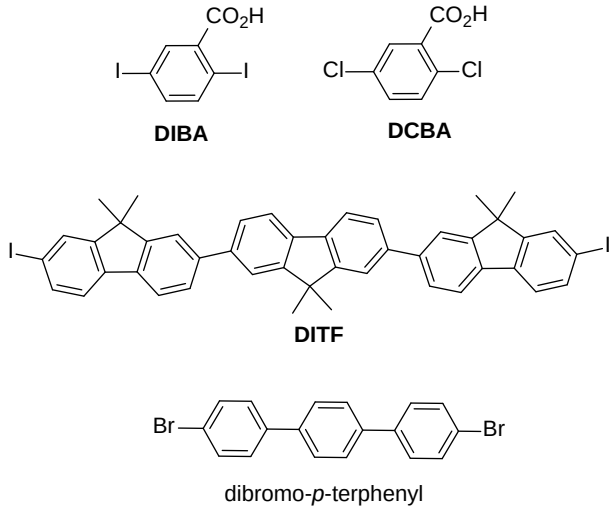

Perhaps even more promising is the use of non-conducting substrates to template polymerization *via* non-catalytic reactions. Thus, conversion of diacetylene monomers into polydiacetylene, that has been studied by STM on HOPG since the 1990s,[239,240] has recently been re-examined on calcite surfaces, using thermal initiation.[338] This same reaction has also been realised on hBN[240] and, importantly, an increased efficiency of polymerization on hBN *versus* HOPG was found.[339,340]

Reactions with the substrate

The interaction strength of the adsorbate with the substrate ranges from weak physisorption to strong chemisorption with significant covalent character. Strong covalent interactions with the surface can impede the above discussed supramolecular assembly as well as polymerization by arresting the diffusion of the molecules. On the other hand, the resulting chemisorbed molecular monolayers are more robust and generally more effective in tuning the properties of the *substrate*. Thus, many applications of graphene are limited by its zero band gap. Non-covalent modification of graphene with SAMN can generate a periodic electrostatic potential and change some of its properties (*e.g.*, polarity of the major charge carrier),[341] but is less likely to open the gap significantly in its band structure. Introducing sp^3 defects in a controlled manner is a promising strategy towards this objective. Thus, self-assembly of long aliphatic chain molecules with a aryldiazonium group on graphene leads to an ordered monolayer.[342] After transferring to an aqueous electrolyte, the aryldiazonium cation can be converted electrochemically into an aryl radical, which grafts covalently to the substrate thus transforming physisorbed adsorbates into covalently bound species (Figure 24). The STM images of the products reveal that molecular order is retained upon self-assembly, and it controls the periodicity of spatially defined sp^3 defects in the substrate.

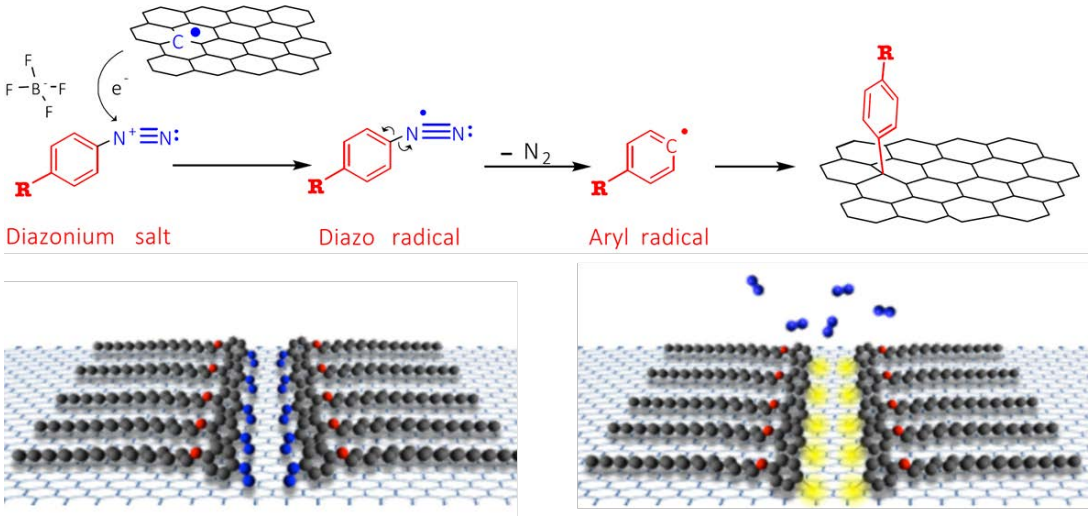

Figure 24. Top: Electroreduction of a diazonium salt leads to aryl radicals that bind covalently to graphitic surfaces. Bottom: Self-assembly of an alkylated aryldiazonium salt (left). Upon electroreduction, the aryl radical binds to the graphitic substrate (right). Adopted from ref [342], copyright 2016 ACS.

Molecules grafted on surfaces can also serve other purposes. The formation of supramolecular assemblies in two dimensions normally employs (nearly) defect-free surfaces. However, real surfaces are not defect-free. To gain insight into the presence of certain types of defects on the formation of supramolecular assemblies, such defects can be introduced deliberately. This approach was recently taken in grafting molecules on graphite.[343] Covalently modified graphite is a convenient and powerful testbed for the investigation and control of 2D crystallization at solid-liquid interfaces. Grafted aryls act as surface defects and create barriers to supramolecular self-assembly. They locally disrupt supramolecular networks and can alter the nucleation, growth, and ripening of 2D crystals. Easily tunable grafting densities enable the systematic study of the effects of such defects on supramolecular self-assembly. These defects could be locally removed, triggering monolayer reconstructions and allowing *in situ* investigation of thermodynamically unstable or metastable morphologies.[343]

Controlled removal of high-density covalently bound or grafted molecules by STM-induced nanoshaving was exploited for the formation of nanocorrals of well-defined size and shape. These nanocorrals serve as confined areas for the formation of supramolecular assemblies. It was shown that self-assembly of 10,12-pentacosadiynoic acid occurs exclusively in the nanocorrals. The probability of monolayer formation reduced upon decreasing the size of the nanocorrals. Alignment effects were evident where the nanocorral nanoshaving occurred at the solid-liquid interface.[344]

Functionality: a perspective from scanning probe microscopy measurements

Apart from templating self-assembly of molecules into supramolecular and macromolecular structures, atomically flat surfaces played a pivotal role in exploring their functionality, at the sub-nanometer scale. Most of single-molecule conductance,[345] switching,[168] and electrically driven actuation[346] studies have been enabled by the use of scanning probe techniques on single-crystal metals. Scanning probe studies also contribute to our understanding of catalytic transformations, addressing the important role of surfaces in molecular reactivity.[347] Much of this work has already been reviewed; here, we highlight some of the recent developments in this area.

Exploring polymer chain conductivity

A key challenge in molecular electronics is to develop methods to make nanoscale connections so as to probe conductivity and charge transport through individual molecular devices. Various approaches such as scanning probe techniques (STM and conductive probe AFM), liquid-metal (Hg and GaIn eutectic) drop electrodes, nanopores, mechanical break junctions, and electrodeposited electrodes have been used to measure the conductivity of individual molecules and assemblies. These methods can be divided into two broad categories: statistical[345,348-353] and non-statistical[354-358] approaches. The former category explores the conductance of an ensemble of molecules located within a two-electrode junction, in which the conductance of a single molecule is deduced from a statistical analysis. Statistical measurements are generally less experimentally demanding, but the results are obscured by broad distributions of data. In non-statistical approaches, measurements are conducted on single molecules or assemblies, which can provide deeper atomic-scale physical insight in the charge transport *via* "molecular wires".

In this context, scanning tunneling spectroscopy (STS) enables tunneling current measurements across the molecules as two-terminal conductors attached between two conductive materials (the tip and the substrate). These measurements can be conducted in a statistical manner in ambient, using a STM tip to create and to probe thousands of break junctions repeatedly.[349] Such measurements can also be performed on individual molecules, which generally requires low temperature UHV-STM but also enables high-resolution *in-situ* imaging of the interrogated molecules.

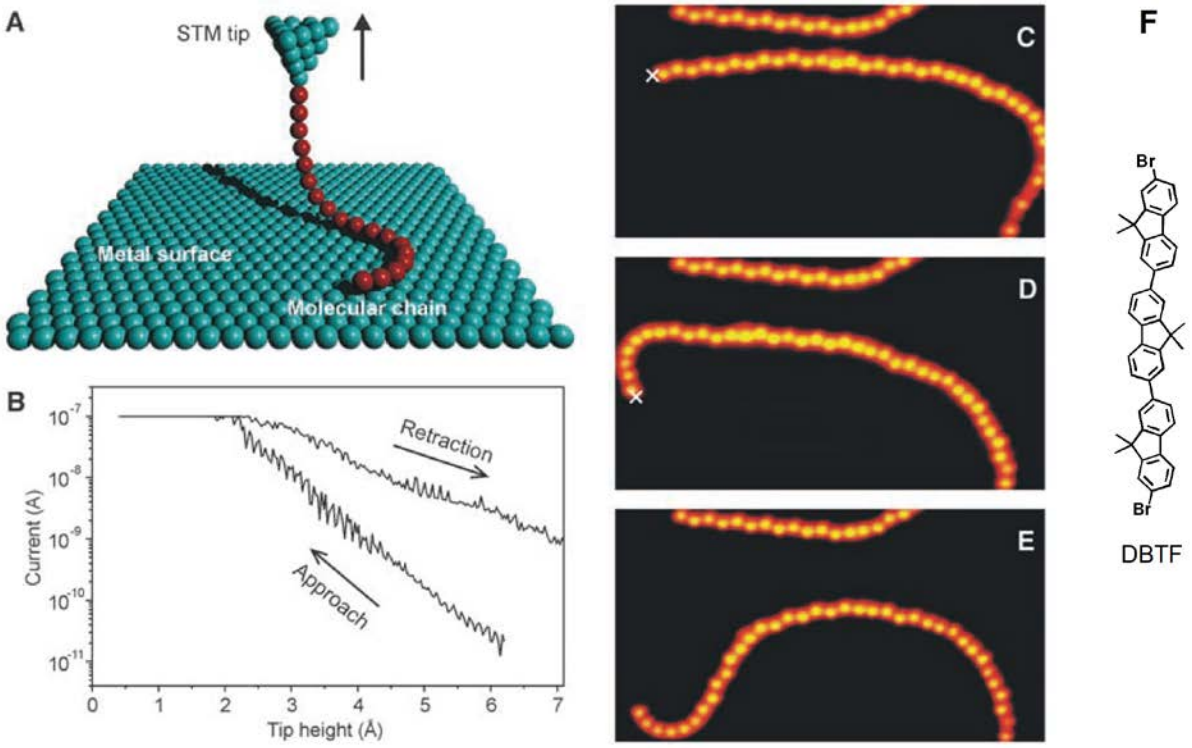

Figure 25. Lifting a single molecular chain with the scanning tunneling microscope (STM) tip. (A) Scheme of the chain pulling procedure (B) Tunneling current as a function of the tip height during a vertical manipulation (approach and retraction). (C-E) Scanning tunneling microscope images (25.4 nm × 13.7 nm) of the same surface area during a vertical manipulation series. The short chain at the upper images serves as a reference, while the longer chain is manipulated, and changes its shape during the pulling processes. (F) Chemical structure of dibromoterfluorene (DBTF). Reproduced from ref [357], copyright 2009 AAAS.

Grill, Hecht, and coworkers reported the conductance measurements of polymeric molecular wires using an original approach where the polymer chain is "pulled out" from surface by a STM tip.[357,358] They first prepared individual polyfluorene wires on Au(111) by *in-situ* Ullmann-like polymerization of dibromoterfluorene (DBTF) at 520 K (Figure 25).[357] The out-of-plane methyl substituents on the fluorene ring weakens the interactions with the surface resulting in fast diffusion of the monomers. This mobility leads to the formation of extended polymeric chains

>100 nm long, which are sufficiently mobile on Au(111) and can be manipulated by a STM tip without any rupture of the chemical bonds.

The manipulation procedure starts with the STM tip approached and positioned at one end of the chain, and the tip is then progressively retracted, so as to lift the polymeric chain from the surface (Figure 25a). Simultaneously, the tunneling current is recorded with a higher measured current for the retraction than the approach step for the same tip-surface distance (Figure 25b). The chain can be then released, and comparing the STM images before and after the pulling-release sequence shows the change of the curvature and displacement but preservation of its structural integrity (Figure 25c-e). Chains up to 20 nm length were pulled out of the surface, with measured conductances of ~10^{-12} S. Assuming the cross section of a polyfluorene "wire" is 0.2 nm^2, this value corresponds to conductivity of *ca*. 10^{-3} S/cm, which is >8 orders of magnitude below that of copper wire. The through-chain conjugation/electron delocalization in polyfluorene is limited by aromatic stabilization of electron sextets in its benzene rings, which explains the rather large band gap (~3 eV) and low electrical conductivity.

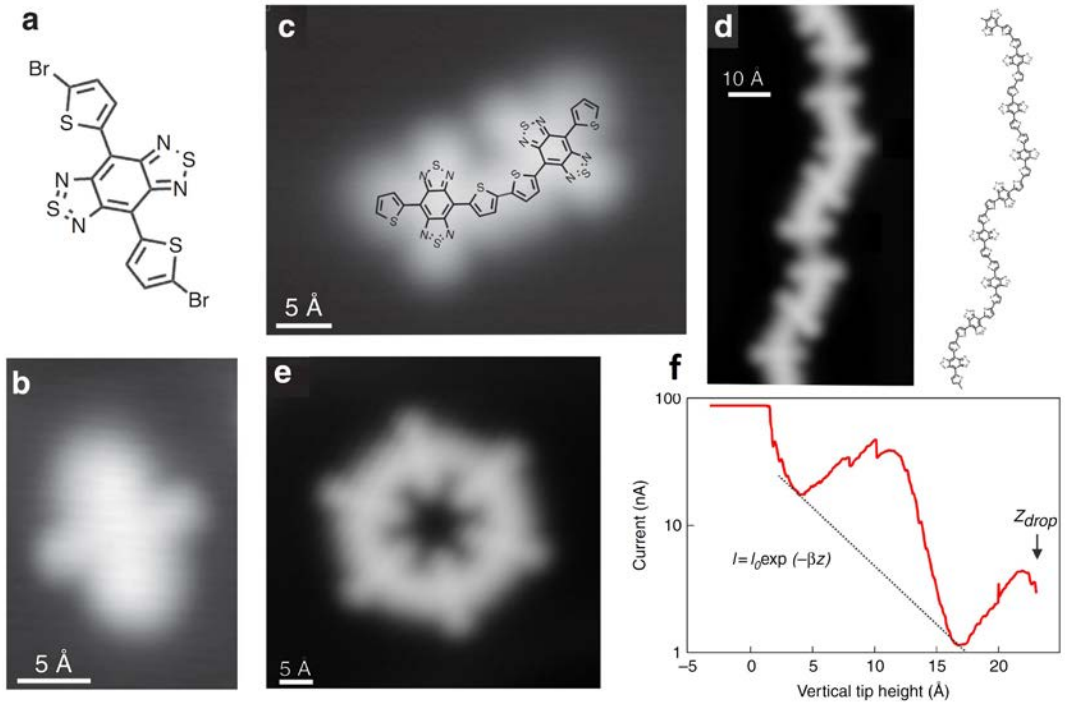

Figure 26. (a) Chemical structure and (b) scanning tunneling microscope image of bis(5-bromo-2-thienyl)-benzobis(1,2,5-thiadiazole) monomer Br-DAD-Br and products of its coupling on Au(111) into (c) dimer $(DAD)_2$, (d) longer chains $(DAD)_n$, and (e) macrocycle $(DAD)_6$. (f) Tunneling current as a function of the tip height upon the polymer chain. Adopted from ref [358], copyright 2015 NPG. [Open Access]

In bulk polymer semiconductors, alternation of donor and acceptor units is commonly applied to reduce the band-gap and enhance the device performance. In this context, the same group has reported on-surface synthesis and conductance measurements of a low band-gap bithiophene-*co*-benzobisthiadiazol oligomers $(DAD)_n$.[358] The polymer was synthesized from brominated monomer Br-DAD-Br by the same Ullmann-type coupling on Au(111), as a mixture of chains of different length, up to ~23 nm and some macrocycles (Figure 26). The conductance of individual wires was measured by performing STM tip pulling experiments, as described above for polyfluorene (Figure 26f). Based on the decay constant (β) measurements, the conductance of

$(DAD)_n$ chains was found to be higher than that reported for other polymeric molecular wires such as polyphenylene, polyfluorene or polythiophene.[357] The presence of alternating donor and acceptor groups in the monomer was suggested to be the key towards obtaining high conductance in $(DAD)_n$. This conclusion is in agreement with the fact that almost all high charge mobility polymers are based on alternating donor-acceptor motifs.

Spintronics

Recent interest in single-molecule magnet (SMM)-based spintronics paved the way for the investigation of intriguing physical phenomena such as spin states, magnetic anisotropy, quantum tunneling of magnetization, and the spin Kondo effect.[223,359,361] However, such magnetic characteristics can be strongly influenced by the contact between individual molecules with the external circuit in SMM-based spintronic devices. This presents a major challenge for practical applications. In particular, the dissociation or deformation of the adsorbed SMM on the electrode surface may change its properties. Therefore, in-depth studies of adsorbed SMMs are needed to understand the SMM self-assembly mechanism and its interaction with the substrate. The goals in this field include control of the orientation of SMMs on various surfaces, intramolecular organization of spins, and site-directed magnetic anisotropy.

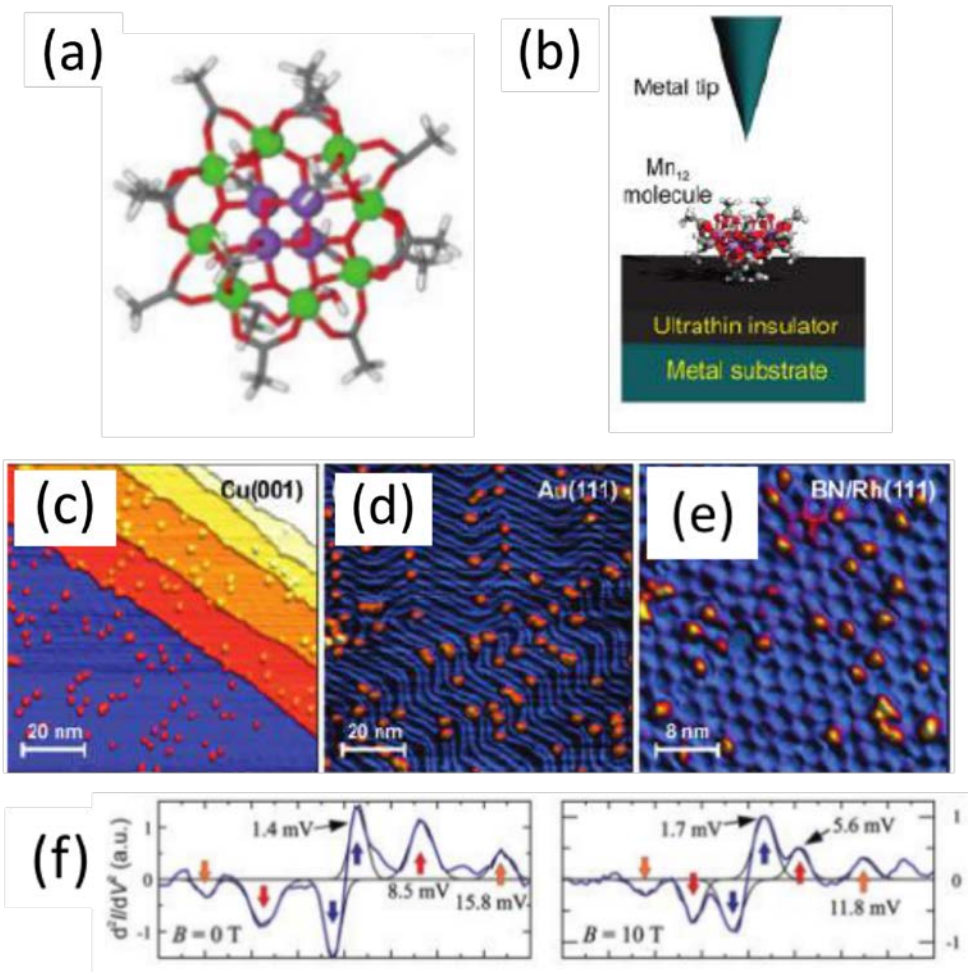

Figure 27**.** Magnetic behavior of Mn_{12} molecules on surfaces. (a) Ball and stick model of Mn_{12} molecules. Manganese atoms has two different charge and spin states: green, Mn^{3+} (S= 2); violet, Mn^{4+} (S= 3/2). Red (gray, white) sticks represent bonds to oxygen (carbon, hydrogen). (b) The tunneling scheme geometry. Scanning tunneling microscope topographic images of Mn_{12} molecules evaporated on (c) Cu(001), (d) Au(111) and (e) hexagonal boron nitride (hBN) on Rh(111) surfaces. (f) d^2I/dV^2 spectra of a Mn_{12} molecule adsorbed on a BN/Rh(111) surface at B = 0 T (left) and B = 10 T (right) show peaks in the d^2I/dV^2 spectrum (blue lines) that associated to low energy spin-flip excitations. Adapted from ref [223], copyright 2012 ACS.

The field of SMM was pioneered by the development of polymetallic manganese acetate (Mn_{12}) molecules.[223,362] These studies primarily encompass the magnetization behavior of SMM molecules at low temperature, and typically reveal magnetic hysteresis. Kahle *et al*. demonstrated the preservation of the magnetic properties of Mn_{12} molecules (Figure 27a) by

depositing them on ultrathin insulating hBN.[223] The experimental schematic is shown in Figure 27b. The substrate influences the adsorption site preference of the Mn_{12} molecule; a random distribution of adsorbed molecules on Cu(001) is observed at room temperature (Figure 27c) and on Au(111) at low temperature (Figure 27d). The inert hBN interlayer is used for magnetically decoupling the substrate, and randomly distributed Mn_{12} molecules were observed at the BN corrugation sites (Figure 27e).

To demonstrate that SMMs preserve their magnetic properties upon adsorption, inelastic tunneling spectroscopy (IETS) was performed at T = 1.5 K (Figure 27f). A step-like feature dominates the d^2I/dV^2 spectra when the SMMs were adsorbed onto hBN. The innermost step is observed at 1−2 meV, while the outer steps are observed up to 16 meV.[223] These peaks are attributed to the presence of spin-flip excitations across the manganese-12-acetate on hBN interface. In contrast, on metal surfaces, such features are absent and the d^2I/dV^2 spectra close to the Fermi energy indicate that the ultrathin BN insulator effectively screens the underlying metallic state and prevents the spin quenching of Mn_{12} molecules.[223]

Controllable switching of the spin Kondo effect at the single-molecule level is needed for bistable dynamic switching in molecular magnetic devices. Recent research has focussed on the chemical control of magnetic molecules interacting with nonmagnetic surfaces, manifested by the presence of the Kondo resonance state.[363,367] Tsukuhara *et al*. have shown that an unpaired electron contributes significantly to the observed sharp Kondo signature.[368] Moreover, this interesting feature can be selectively manipulated *via* chemical stimuli. A combined low-temperature STM and DFT study by Tsukuhara *et al*. demonstrated the persistence of the spin Kondo resonance when the iron(II) phthalocyanine molecule on Au(111) was coordinated to a

NO molecule.[368] The physical origin of the spin Kondo resonance effect is driven by the remnant magnetic moments that involve the d_{z2} orbital of the Fe atom and the lone pair of the NO. This method offers means for the orbital-selective manipulation of many-body quantum states through the chemical coordination of small molecules.

Heterogeneous catalysis

Scanning tunneling microscopy is an excellent tool to study surface catalysis at a single molecule level. Many of these studies have been traditionally performed under UHV conditions,[347] but it is also possible to explore catalytic reactions at liquid-solid interface. In a series of studies, Elemans *et al*. revealed alkene oxidation catalyzed by individual manganese porphyrin molecules, in real time, at the interface between tetradecane and Au(111).[369] Small molecular weight alkene substrate (stilbene) that diffused in the liquid phase to the liquid-solid interface was oxidized to the corresponding epoxide. It was found that oxygen atoms that were incorporated in the stilbene originated from O_2 molecules that were previously bound to adjacent porphyrin catalysts. Differences in the appearance of the manganese porphyrins as a function of their oxidation state were also revealed on graphite, where it was shown that it is possible to discriminate different states of a reactive species with STM and to monitor complex multistep reactions at the submolecular level.[370] Furthermore, STM was not only used for imaging purposes but played an active role in inducing such reactions in a spatially resolved fashion.[371]

Conclusions and Prospects

During the last two decades, scanning probe microscopies have become a major research tool at the interface of molecular and surface sciences. Direct imaging with submolecular resolution, easily achieved with STM, provides a unique approach to investigate molecular assemblies on surfaces, to probe non-covalent supramolecular interactions, and to discover new chemical reactions. Recent advances in non-contact AFM provide stunning resolution that allows direct identification of chemical structure at a single-molecule level.[14,372] While such remarkable resolution requires highly controlled conditions (cryo-temperature, UHV) and is only available in a few laboratories in the world, continuing instrumental development will inevitably accelerate the adoption of these methods in broad areas of molecular science. One of the major handicaps of SPM is its limited chemical sensitivity. It is not currently possible to determine the exact atomic structure/composition of molecules using SPM alone, and thus on-surface characterization of new molecules and reactions generally requires auxiliary spectroscopic studies (XPS, NEXAFS, SIMS, infra-red and high resolution electron energy loss spectroscopy (HREELS), *etc*.), which can conclusively test hypotheses made on the basis of SPM images.[373] Also, important additional information on the molecular structures can be obtained from scanning probe-based measurements such as STS (molecular orbitals and vibrational signatures of the molecules *via* inelastic energy tunneling spectroscopy), tip-enhanced Raman, and force-distance or current-distance measurements.[30,374-376] The resulting fundamental insights from SPM studies into complex phenomena such as biological recognition, chirality, crystallization phenomena, host-guest interactions, and chemical reactivity, extend across many disciplines. [105,347,377] The ability

to interrogate chemical systems by direct imaging with sub-nm resolution has opened new dimensions in many fields, from biochemistry[378] to CO_2 capture.[379]

On-surface molecular assembly has already become a reliable method to engineer surface patterns with (sub)nanometer features and easily controlled symmetry, periodicity and unit cell structure. Historically, the rational design of these ordered structures was predicated on achieving thermodynamic equilibria. The use of kinetic stabilization of non-equilibrium phases opens the possibility of engineering even more complex nanoscale architectures.[380] In addition, highly ordered yet aperiodic (quasicrystalline) SAMNs have also been reported.[35,104] These molecular networks in turn can serve as templates to assemble other functional materials. We envisage that the further progress in this direction will enable molecularly controlled *epitaxial* growth of multilayer films[183-186] that display a spectrum of new optical and electronic properties. There is also a rapidly growing interest in molecular assembly on inorganic 2D materials including graphene, semiconducting metal dichalcogenides, and others.[381,382] The resulting heterojunctions can harness the advantages of both 2D and molecular materials, whereby the special optoelectronic properties of the former are easily tuned by the choice of molecular components. We also expect that layered assemblies of such hybrid organic-inorganic 2D materials could be engineered in robust flexible devices.

At the same time, dynamic interactions between molecular building blocks, that are essential prerequisites for self-assembly, including error correction, also limit the stability of the resulting structures. Achieving chemically, thermally, and mechanically robust patterns *via* molecular self-assembly remains a major challenge. Surface-confined covalent organic frameworks, formed *via* dynamic covalent chemistry, are emerging as a plausible solution to this problem.[283] We expect

that the remarkable flexibility in molecular design and long-range order already realized in SAMNs can be attained for surface-confined COFs in the near future. One upcoming challenge will be applying this "bottom-up" patterning to device fabrication method, *i.e.*, developing reliable scale-up strategies that maintain the high efficiency and design capability of molecular self-assembly, to replace or at least to improve/enhance conventional top-down lithographic methods.

Surface-confined polymerization has become a synthetic tool for the realization of macromolecular architectures, unimaginable *via* standard, solution-based chemistry. The last ten years have seen an explosion in reports on epitaxially ordered conjugated polymer "wires", graphene nanoribbons of atomically precise width and controlled topology, and atomically thin two-dimensional conjugated polymers prepared from rationally designed molecular building blocks. The new chemistry learned from these studies has challenged our understanding of organic reactivity, contributing to the important knowledge base of heterogenous catalysis. For example, the highly efficient dehalogenative and dehydrogenative C-C aromatic coupling on Au(111),[300] and dehydrogenative alkane polymerization on stepped Au surfaces,[270] were highly counterintuitive considering the common notion of gold being "most noble of all metals".[383]

Most on-surface synthesis experiments have been performed on single crystal metals, which facilitated these studies by catalyzing the needed coupling reaction and enabling STM monitoring of the reactions. However, decoupling of GNR or 2D polymers from the surface, ideally without mechanically detaching them,[384] is essential for almost any imagined application of these materials in nanoelectronics. Chemical solutions to this problem are possible; for example, selective "etching" of the top-most layers of metal below the macromolecular semiconductor

could be elaborated to grow metal-insulator-semiconductor structures *in situ*.[334] Alternatively, polymerization reactions executable on non-metallic surfaces could be developed. Apart from adopting the common metal-catalyzed C-C coupling chemistry for non-metallic surfaces,[337] other already studied surface-confined polymerization approaches, such as polycondensation or light-induced polymerization, could enable the growth of 2D polymer on non-catalytic (dielectric) surfaces.

Equally significant is the challenge of establishing an effective electrical contact to such nanomaterials, which has been a major bottleneck in the field of molecular devices.[385] Thus, while the field-effect transistors with on-surface synthesized GNR have already been reported, the electrical current in such nanoscale-channel devices appears to be limited by contact tunneling,[384] and a roadmap for implementing on-surface synthesized semiconductors in practical thin-film devices, is as yet undefined.

Overall, the field of molecular surface science is on the verge of transition; remarkable structural control has already been achieved for a broad range of structures and systems, on *planar crystalline* surfaces. Could equally fine supramolecular-level control be implemented on curved or faceted surfaces, *e.g.*, on nanoparticles? Could the unique functionality offered by on-surface controlled supra- and macromolecular structures be harvested in *manufacturable* functional devices? So far, the field was fueled mainly by the curiosity of chemists and physicists. It might be time for engineering researchers to join. What are the engineering challenges that need to be addressed? What new applications can be enabled by molecular level programming of surfaces? The long-range order, particularly in the most interesting materials such as GNR or 2D conjugated polymers, is currently limited to relatively small (~10-100 nm) domains. Can we grow much larger

defect-free domains or can we use finite domain size to the advantage of some applications (such as organic photovoltaics)? Implementation in large-scale manufacturing will favor a transition away from UHV processing of materials, which will push the field to develop assembly strategies amenable to ambient environments, including solution processing.

The remarkable opportunity of programming surface structure and functionality by the design of simple molecular building blocks has captured the imagination of scientists around the world. In the coming years, we will see this field further ripen to new applications and technologies, as well as new nanometer-scale science and discovery.

Acknowledgments

We thank Profs. Tomas Base and Alex Kandel for useful discussions as well as all the attendees of the meetings that contributed to the work described in this Review. DFP and FR are thankful to Fulbright Canada and California NanoSystems Institute for the visiting Fulbright Canada Chairs at UCLA. PSW thanks the Department of Energy (grant #SC-1037004) for support of past and continuing work in this area and the Institut National de la Recherche Scientifique (INRS) for the Chaire d'excellence Jacques-Beaulieu at the Centre for Energy, Materials and Telecommunications. SLT acknowledges support from the National Science Foundation (DMR 1533988) and the Department of Energy (DE-SC0016367). DFP acknowledges funding from US-ARO and NSERC. FR is supported by a Discovery Grant from NSERC and is grateful to the Canada Research Chairs program for funding and partial salary support. SDF thanks the Fund of Scientific Research–Flanders (FWO), KU Leuven Internal Funds, the European Research Council under the European Union's Seventh Framework Programme (FP7/2007-2013)/ERC Grant Agreement No. 340324, and Future and Emerging Technologies Action (FET Open) under Grant Agreement No. 664878 (2D-INK). ATSW and A acknowledge funding support from the MOE Tier 3 grant MOE2014-T3-1-004.

AUTHOR INFORMATION

Corresponding authors

*dmitrii.perepichka@mcgill.ca, psw@cnsi.ucla.edu

ORCID

Dominic P. Goronzy: 0000-0003-2856-4732

Maryam Ebrahimi: 0000-0003-1421-2971

Arramel: 0000-0003-4125-6099

Yuan Fang: 0000-0002-4846-1725

Steven De Feyter: 0000-0002-0909-9292

Steven L. Tait: 0000-0001-8251-5232

Peter Beton: 0000-0002-2120-8033

Federico Rosei: 0000-0001-8479-6955

Andrew T. S. Wee: 0000-0002-5828-4312

Paul S. Weiss: 0000-0001-5527-6248

Dmitrii F. Perepichka: 0000-0003-2233-416X

Glossary

AFM: atomic force microscopy

BTB: 1,3,5-tris(4-carboxyphenyl)benzene

COF: covalent organic framework

CVD: chemical vapor deposition

DBTF: dibromoterfluorene

DBBA: 10,10'-dibromo-9,9'-bianthracene

DFT: density functional theory

EC: electrochemical

F_{16}CuPc: hexadecafluorophthalocyanine

GNR: graphene nanoribbon

H-bonding: hydrogen bonding

HOPG: highly oriented pyrolytic graphite

LC: liquid crystal

nc-AFM: non-contact atomic force microscopy

NEXAFS: near-edge X-ray absorption fine structure spectroscopy

PTCDA: perylenetetracarboxylic dianhydride

PTCDI: perylenetetracarboxydiimide

TCPP: 5,10,15,20-tetrakis(4-hydroxycarbonylphenyl)porphyrin

TCNQ: tetracyanoquinodimethane

TBTTA: terthienobenzenetricarboxylic scid

TBP: tetrakis[1,3-di(*tert*-butyl)phenyl]pyrene

TPTC: *p*-terphenyl-3,5,3’’,5’’-tetracarboxylic acid

SAM: self-assembled monolayer

SAMN: self-assembled molecular network

SIMS: secondary ion mass spectrometry

SMM: single molecule magnet

SPM: scanning probe microscopy

STM: scanning tunneling microscopy

STS: scanning tunneling spectroscopy

UHV: ultrahigh vacuum

vdW: van der Waals (force)

X-bonding: halogen bonding

XPS: X-ray photoelectron spectroscopy

ZGNRs: zigzag graphene nanoribbons

Supporting Information Available:

Structural diagrams of the discussed molecules. This material is available free of charge via the Internet at http://pubs.acs.org

References and Notes

1. Sagiv, J. Organized Monolayers by Adsorption. 1. Formation and Structure of Oleophobic Mixed Monolayers on Solid Surfaces. *J. Am. Chem. Soc.* **1980,** *102*, 92-98.
2. Nuzzo, R. G.; Allara, D. L. Adsorption of Bifunctional Organic Disulfides on Gold Surfaces. *J. Am. Chem. Soc.* **1983,** *105*, 4481-4483.
3. Binnig, G.; Rohrer, H. Scanning Tunneling Microscopy. *Helv. Phys. Acta* **1982,** *55*, 726-735.
4. Binnig, G.; Quate, C. F.; Gerber, C. Atomic Force Microscope. *Phys. Rev. Lett.* **1986,** *56*, 930-933.
5. Weiss, P. S. New Tools Lead to New Science. *ACS Nano* **2012,** *6*, 1877-1879.
6. Casalini, S.; Bortolotti, C. A.; Leonardi, F.; Biscarini, F. Self-Assembled Monolayers in Organic Electronics. *Chem. Soc. Rev.* **2017,** *46*, 40-71.
7. Pathem, B. K.; Claridge, S. A.; Zheng, Y. B.; Weiss, P. S. Molecular Switches and Motors on Surfaces. *Annu. Rev. Phys. Chem.* **2013,** *64*, 605-630.
8. Rivnay, J.; Inal, S.; Salleo, A.; Owens, R. M.; Berggren, M.; Malliaras, G. G. Organic Electrochemical Transistors. *Nat. Rev. Mater.* **2018,** *3*, 17086-17099.
9. Katz, H. E.; Huang, J. Thin-Film Organic Electronic Devices. *Annu. Rev. Mater. Res.* **2009,** *39*, 71-92.
10. Wu, X.; Mao, S.; Chen, J.; Huang, J. Strategies for Improving the Performance of Sensors Based on Organic Field-Effect Transistors. *Adv. Mater.* **2018**, 1705642-1705648.
11. Shirai, Y.; Morin, J.-F.; Sasaki, T.; Guerrero, J. M.; Tour, J. M. Recent Progress on Nanovehicles. *Chem. Soc. Rev.* **2006,** *35*, 1043-1055.
12. Binnig, G.; Rohrer, H. Scanning Tunneling Microscopy—From Birth to Adolescence. *Rev. Mod. Phys.* **1987,** *59*, 615-625.
13. Gross, L.; Moll, N.; Mohn, F.; Curioni, A.; Meyer, G.; Hanke, F.; Persson, M. High-Resolution Molecular Orbital Imaging Using a *p*-Wave STM Tip. *Phys. Rev. Lett.* **2011,** *107*, 086101-086104.
14. Gross, L. Recent Advances in Submolecular Resolution with Scanning Probe Microscopy. *Nat. Chem.* **2011,** *3*, 273-278.
15. Gross, L.; Mohn, F.; Moll, N.; Liljeroth, P.; Meyer, G. The Chemical Structure of a Molecule Resolved by Atomic Force Microscopy. *Science* **2009,** *325*, 1110-1114.
16. Mali, K. S.; Adisoejoso, J.; Ghijsens, E.; Cat, I. D.; De Feyter, S. Exploring the Complexity of Supramolecular Interactions for Patterning at the Liquid–Solid Interface. *Acc. Chem. Res.* **2012,** *45*, 1309-1320.
17. Barth, J. V. Molecular Architectonic on Metal Surfaces. *Annu. Rev. Phys. Chem.* **2007,** *58*, 375-407.
18. Love, J. C.; Estroff, L. A.; Kriebel, J. K.; Nuzzo, R. G.; Whitesides, G. M. Self-Assembled Monolayers of Thiolates on Metals as a Form of Nanotechnology. *Chem. Rev.* **2005,** *105*, 1103-1170.
19. Smith, R. K.; Lewis, P. A.; Weiss, P. S. Patterning Self-Assembled Monolayers. *Prog. Surf. Sci.* **2004,** *75*, 1-68.
20. Claridge, S. A.; Liao, W.-S.; Thomas, J. C.; Zhao, Y.; Cao, H. H.; Cheunkar, S.; Serino, A. C.; Andrews, A. M.; Weiss, P. S. From the Bottom Up: Dimensional Control and Characterization in Molecular Monolayers. *Chem. Soc. Rev.* **2013,** *42*, 2725-2745.
21. Barth, J. V.; Costantini, G.; Kern, K. Engineering Atomic and Molecular Nanostructures at Surfaces. *Nature* **2005,** *437*, 671-679.
22. Franc, G.; Gourdon, A. Covalent Networks through On-Surface Chemistry in Ultra-High Vacuum: State-of-the-Art and Recent Developments. *Phys. Chem. Chem. Phys.* **2011,** *13*, 14283-14292.
23. Dong, L.; Liu, P. N.; Lin, N. Surface-Activated Coupling Reactions Confined on a Surface. *Acc. Chem. Res.* **2015,** *48*, 2765-2774.
24. Fan, Q.; Gottfried, J. M.; Zhu, J. Surface-Catalyzed C–C Covalent Coupling Strategies Toward the Synthesis of Low-Dimensional Carbon-Based Nanostructures. *Acc. Chem. Res.* **2015,** *48*, 2484-2494.
25. Lackinger, M. Surface-Assisted Ullmann Coupling. *Chem. Commun.* **2017,** *53*, 7872-7885.

26. Held, P. A.; Fuchs, H.; Studer, A. Covalent-Bond Formation *via* On-Surface Chemistry. *Chem. Eur. J.* **2017,** *23*, 5874-5892.
27. Talirz, L.; Ruffieux, P.; Fasel, R. On-Surface Synthesis of Atomically Precise Graphene Nanoribbons. *Adv. Mater.* **2016,** *28*, 6222-6231.
28. Palma, C.-A.; Samori, P. Blueprinting Macromolecular Electronics. *Nat. Chem.* **2011,** *3*, 431-436.
29. Nitzan, A.; Ratner, M. A. Electron Transport in Molecular Wire Junctions. *Science* **2003,** *300*, 1384-1389.
30. Claridge, S. A.; Schwartz, J. J.; Weiss, P. S. Electrons, Photons, and Force: Quantitative Single-Molecule Measurements from Physics to Biology. *ACS Nano* **2011,** *5*, 693-729.
31. Wei, Y.; Tong, W.; Zimmt, M. B. Self-Assembly of Patterned Monolayers with Nanometer Features: Molecular Selection Based on Dipole Interactions and Chain Length. *J. Am. Chem. Soc.* **2008,** *130*, 3309-3405.
32. Ye, Y.; Sun, W.; Wang, Y.; Shao, X.; Xu, X.; Cheng, F.; Li, J.; Wu, K. A Unified Model: Self-Assembly of Trimesic Acid on Gold. *J. Phys. Chem. C* **2007,** *111*, 10138-10141.
33. Chen, W.; Li, H.; Huang, H.; Fu, Y. X.; Zhang, H. L.; Ma, J.; Wee, A. T. S. Two-Dimensional Pentacene : 3,4,9,10-Perylenetetracarboxylic Dianhydride Supramolecular Chiral Networks on Ag(111). *J. Am. Chem. Soc.* **2008,** *130*, 12285-12289.
34. Liu, J.; Chen, T.; Deng, X.; Wang, D.; Pei, J.; Wan, L.-J. Chiral Hierarchical Molecular Nanostructures on Two-Dimensional Surface by Controllable Trinary Self-Assembly. *J. Am. Chem. Soc.* **2011,** *133*, 21010-21015.
35. Urgel, J. I.; Ecija, D.; Lyu, G.; Zhang, R.; Palma, C.-A.; Auwaerter, W.; Lin, N.; Barth, J. V. Quasicrystallinity Expressed in Two-Dimensional Coordination Networks. *Nat. Chem.* **2016,** *8*, 657-662.
36. Li, N.; Gu, G. C.; Zhang, X.; Song, D. L.; Zhang, Y. J.; Teo, B. K.; Peng, L. M.; Hou, S. M.; Wang, Y. F. Packing Fractal Sierpinski Triangles into One-Dimensional Crystals *via* a Templating Method. *Chem. Commun.* **2017,** *53*, 3469-3472.
37. Rabe, J. P.; Buchholz, S. Commensurability and Mobility in Two-Dimensional Molecular Patterns on Graphite. *Science* **1991,** *253*, 424-427.
38. Du, P.; Jaouen, M.; Bocheux, A.; Bourgogne, C.; Han, Z.; Bouchiat, V.; Kreher, D.; Mathevet, F.; Fiorini-Debuisschert, C.; Charra, F.; Attias, A.-J. Surface-Confined Self-Assembled Janus Tectons: A Versatile Platform Towards the Noncovalent Functionalization of Graphene. *Angew. Chem. Int. Ed.* **2014,** *53*, 10060-10066.
39. Weck, M.; Jackiw, J. J.; Rossi, R. R.; Weiss, P. S.; Grubbs, R. H. Ring-Opening Metathesis Polymerization from Surfaces. *J. Am. Chem. Soc.* **1999,** *121*, 4088-4089.
40. Kim, N. Y.; Jeon, N. L.; Choi, I. S.; Takami, S.; Harada, Y.; Finnie, K. R.; Girolami, G. S.; Nuzzo, R. G.; Whitesides, G. M.; Laibinis, P. E. Surface-Initiated Ring-Opening Metathesis Polymerization on Si/SiO_2. *Macromolecules* **2000,** *33*, 2793-2795.
41. Hentschke, R.; Schürmann, B. L.; Rabe, J. P. Molecular Dynamics Simulations of Ordered Alkane Chains Physisorbed on Graphite. *J. Chem. Phys.* **1992,** *96*, 6213-6221.
42. Lei, S.; Surin, M.; Tahara, K.; Adisoejoso, J.; Lazzaroni, R.; Tobe, Y.; De Feyter, S. Programmable Hierarchical Three-Component 2D Assembly at a Liquid-Solid Interface: Recognition, Selection, and Transformation. *Nano Lett.* **2008,** *8*, 2541-2546.
43. Ivasenko, O.; Perepichka, D. F. Mastering Fundamentals of Supramolecular Design with Carboxylic Acids. Common Lessons from X-Ray Crystallography and Scanning Tunneling Microscopy. *Chem. Soc. Rev.* **2011,** *40*, 191-206.
44. MacLeod, J. M.; Ben Chaouch, Z.; Perepichka, D. F.; Rosei, F. Two-Dimensional Self-Assembly of a Symmetry-Reduced Tricarboxylic Acid. *Langmuir* **2013,** *29*, 7318-7324.
45. Fu, C.; Rosei, F.; Perepichka, D. F. 2D Self-Assembly of Fused Oligothiophenes: Molecular Control of Morphology. *ACS Nano* **2012,** *6*, 7973-7980.

46. Nath, K. G.; Ivasenko, O.; MacLeod, J. M.; Miwa, J. A.; Wuest, J. D.; Nanci, A.; Perepichka, D. F.; Rosei, F. Crystal Engineering in Two Dimensions: An Approach to Molecular Nanopatterning. *J. Phys. Chem. C* **2007,** *111*, 16996-17007.
47. Langner, A.; Tait, S. L.; Lin, N. A.; Chandrasekar, R.; Meded, V.; Fink, K.; Ruben, M.; Kern, K. Selective Coordination Bonding in Metallo-Supramolecular Systems on Surfaces. *Angew. Chem. Int. Ed.* **2012,** *51*, 4327-4331.
48. Skomski, D.; Tempas, C. D.; Smith, K. A.; Tait, S. L. Redox-Active On-Surface Assembly of Metal–Organic Chains with Single-Site Pt(II). *J. Am. Chem. Soc.* **2014,** *136*, 9862-9865.
49. Gutzler, R.; Fu, C.; Dadvand, A.; Hua, Y.; MacLeod, J. M.; Rosei, F.; Perepichka, D. F. Halogen Bonds in 2D Supramolecular Self-Assembly of Organic Semiconductors. *Nanoscale* **2012,** *4*, 5965-5971.
50. Zheng, Q.-N.; Liu, X.-H.; Chen, T.; Yan, H.-J.; Cook, T.; Wang, D.; Stang, P. J.; Wan, L.-J. Formation of Halogen Bond-Based 2D Supramolecular Assemblies by Electric Manipulation. *J. Am. Chem. Soc.* **2015,** *137*, 6128-6131.
51. Yang, X.; Wang, F.; Chen, Q.; Wang, L.; Wang, Z. Halogen Bonded Two-Dimensional Supramolecular Assemblies Studied by High Resolution Scanning Tunneling Microscopy. *Chin. Sci. Bull.* **2007,** *52*, 1856-1859.
52. Kim, M. K.; Xue, Y.; Paskova, T.; Zimmt, M. B. Monolayer Patterning Using Ketone Dipoles. *Phys. Chem. Chem. Phys.* **2013,** *15*, 12466-12474.
53. Tong, W.; Wei, Y.; Armbrust, K. W.; Zimmt, M. B. Dipolar Side Chain Control of Monolayer Morphology: Symmetrically Substituted 1,5-(Mono- and diether) Anthracenes at the Solution−HOPG Interface. *Langmuir* **2009,** *25*, 2913-2923.
54. Wei, Y.; Tong, W.; Wise, C.; Wei, X.; Armbrust, K.; Zimmt, M. Dipolar Control of Monolayer Morphology: Spontaneous SAM Patterning. *J. Am. Chem. Soc.* **2006,** *128*, 13362-13363.
55. Adisoejoso, J.; Tahara, K.; Okuhata, S.; Lei, S.; Tobe, Y.; De Feyter, S. Two-Dimensional Crystal Engineering: A Four-Component Architecture at a Liquid-Solid Interface. *Angew. Chem. Int. Ed.* **2009,** *48*, 7353-7357.
56. Xu, W.; E. A. Kelly, R.; Otero, R.; Schöck, M.; Lægsgaard, E.; Stensgaard, I.; Kantorovich, L. N.; Besenbacher, F. Probing the Hierarchy of Thymine–Thymine Interactions in Self-Assembled Structures by Manipulation with Scanning Tunneling Microscopy. *Small* **2007,** *3*, 2011-2014.
57. Shen, C.; Cramer, J. R.; Jacobsen, M. F.; Liu, L.; Zhang, S.; Dong, M.; Gothelf, K. V.; Besenbacher, F. Steering Supramolecular Patterns by Nucleobase-Terminated Molecules. *Chem. Commun.* **2013,** *49*, 508-510.
58. Liu, L.; Zhang, L.; Mao, X.; Niu, L.; Yang, Y.; Wang, C. Chaperon-Mediated Single Molecular Approach Toward Modulating Aβ Peptide Aggregation. *Nano Lett.* **2009,** *9*, 4066-4072.
59. Liu, L.; Niu, L.; Xu, M.; Han, Q.; Duan, H.; Dong, M.; Besenbacher, F.; Wang, C.; Yang, Y. Molecular Tethering Effect of C-Terminus of Amyloid Peptide Aβ42. *ACS Nano* **2014,** *8*, 9503-9510.
60. Yugay, D.; Goronzy, D. P.; Kawakami, L. M.; Claridge, S. A.; Song, T.-B.; Yan, Z.; Xie, Y.-H.; Gilles, J.; Yang, Y.; Weiss, P. S. Copper Ion Binding Site in β-Amyloid Peptide. *Nano Lett.* **2016,** *16*, 6282-6289.
61. Rauschenbach, S.; Rinke, G.; Gutzler, R.; Abb, S.; Albarghash, A.; Le, D.; Rahman, T. S.; Dürr, M.; Harnau, L.; Kern, K. Two-Dimensional Folding of Polypeptides into Molecular Nanostructures at Surfaces. *ACS Nano* **2017,** *11*, 2420-2427.
62. Abb, S.; Harnau, L.; Gutzler, R.; Rauschenbach, S.; Kern, K. Two-Dimensional Honeycomb Network through Sequence-Controlled Self-Assembly of Oligopeptides. *Nat. Commun.* **2016,** *7*, 10335-10361.
63. Niu, L.; Liu, L.; Xi, W.; Han, Q.; Li, Q.; Yu, Y.; Huang, Q.; Qu, F.; Xu, M.; Li, Y.; Du, H.; Yang, R.; Cramer, J.; Gothelf, K. V.; Dong, M.; Besenbacher, F.; Zeng, Q.; Wang, C.; Wei, G.; Yang, Y. Synergistic Inhibitory Effect of Peptide–Organic Coassemblies on Amyloid Aggregation. *ACS Nano* **2016,** *10*, 4143-4153.

64. Wiltzius, J. J. W.; Landau, M.; Nelson, R.; Sawaya, M. R.; Apostol, M. I.; Goldschmidt, L.; Soriaga, A. B.; Cascio, D.; Rajashankar, K.; Eisenberg, D. Molecular Mechanisms for Protein-Encoded Inheritance. *Nat. Struct. Mol. Biol.* **2009,** *16*, 973-978.
65. Tartaglia, G. G.; Pawar, A. P.; Campioni, S.; Dobson, C. M.; Chiti, F.; Vendruscolo, M. Prediction of Aggregation-Prone Regions in Structured Proteins. *J. Mol. Biol.* **2008,** *380*, 425-436.
66. Xu, W.; Wang, J. G.; Jacobsen, M. F.; Mura, M.; Yu, M.; Kelly, R. E.; Meng, Q. Q.; Laegsgaard, E.; Stensgaard, I.; Linderoth, T. R.; Kjems, J.; Kantorovich, L. N.; Gothelf, K. V.; Besenbacher, F. Supramolecular Porous Network Formed by Molecular Recognition Between Chemically Modified Nucleobases Guanine and Cytosine. *Angew. Chem. Int. Ed.* **2010,** *49*, 9373-9377.
67. Otero, R.; Xu, W.; Lukas, M.; Kelly, R. E. A.; Lægsgaard, E.; Stensgaard, I.; Kjems, J.; Kantorovich, L. N.; Besenbacher, F. Specificity of Watson–Crick Base Pairing on a Solid Surface Studied at the Atomic Scale. *Angew. Chem. Int. Ed.* **2008,** *47*, 9673-9676.
68. Mao, X.; Guo, Y.; Luo, Y.; Niu, L.; Liu, L.; Ma, X.; Wang, H.; Yang, Y.; Wei, G.; Wang, C. Sequence Effects on Peptide Assembly Characteristics Observed by Using Scanning Tunneling Microscopy. *J. Am. Chem. Soc.* **2013,** *135*, 2181-2187.
69. Claridge, S. A.; Thomas, J. C.; Silverman, M. A.; Schwartz, J. J.; Yang, Y.; Wang, C.; Weiss, P. S. Differentiating Amino Acid Residues and Side Chain Orientations in Peptides Using Scanning Tunneling Microscopy. *J. Am. Chem. Soc.* **2013,** *135*, 18528-18535.
70. Yang, Y.; Wang, C. Single-Molecule Studies on Individual Peptides and Peptide Assemblies on Surfaces. *Philos. Trans. R. Soc., A* **2013,** *371*, 20120311-20120320.
71. Pieta, P.; Mirza, J.; Lipkowski, J. Direct Visualization of the Alamethicin Pore Formed in a Planar Phospholipid Matrix. *Proc. Natl. Acad. Sci. USA* **2012,** *109*, 21223-21227.
72. Wang, Y.; Niu, L.; Li, Y.; Mao, X.; Yang, Y.; Wang, C. Single Molecule Studies of Cyclic Peptides Using Molecular Matrix at Liquid/Solid Interface by Scanning Tunneling Microscopy. *Langmuir* **2010,** *26*, 16305-16311.
73. Chen, Y.; Deng, K.; Qiu, X.; Wang, C. Visualizing Cyclic Peptide Hydration at the Single-Molecule Level. *Sci. Rep.* **2013,** *3*, 2461-2467.
74. Kisiday, J.; Jin, M.; Kurz, B.; Hung, H.; Semino, C.; Zhang, S.; Grodzinsky, A. J. Self-Assembling Peptide Hydrogel Fosters Chondrocyte Extracellular Matrix Production and Cell Division: Implications for Cartilage Tissue Repair. *Proc. Natl. Acad. Sci. U. S. A.* **2002,** *99*, 9996-10001.
75. Ulijn, R. V.; Smith, A. M. Designing Peptide Based Nanomaterials. *Chem. Soc. Rev.* **2008,** *37*, 664-675.
76. Niu, L.; Liu, L.; Xu, M.; Cramer, J.; Gothelf, K. V.; Dong, M.; Besenbacher, F.; Zeng, Q.; Yang, Y.; Wang, C. Transformation of β-sheet Structures of the Amyloid Peptide Induced by Molecular Modulators. *Chem. Commun.* **2014,** *50*, 8923-8926.
77. Tomba, G.; Lingenfelder, M.; Costantini, G.; Kern, K.; Klappenberger, F.; Barth, J. V.; Ciacchi, L. C.; Vita, A. D. Structure and Energetics of Diphenylalanine Self-Assembling on Cu(110). *J. Phys. Chem. A* **2007,** *111*, 12740-12748.
78. Peyrot, D.; Silly, F. On-Surface Synthesis of Two-Dimensional Covalent Organic Structures *versus* Halogen-Bonded Self-Assembly: Competing Formation of Organic Nanoarchitectures. *ACS Nano* **2016,** *10*, 5490-5498.
79. Pham, T. A.; Song, F.; Nguyen, M.-T.; Stöhr, M. Self-Assembly of Pyrene Derivatives on Au(111): Substituent Effects on Intermolecular Interactions. *Chem. Commun.* **2014,** *50*, 14089-14092.
80. Gatti, R.; MacLeod, J. M.; Lipton-Duffin, J. A.; Moiseev, A. G.; Perepichka, D. F.; Rosei, F. Substrate, Molecular Structure, and Solvent Effects in 2D Self-Assembly *via* Hydrogen and Halogen Bonding. *J. Phys. Chem. C* **2014,** *118*, 25505-25516.
81. Song, W.; Martsinovich, N.; Heckl, W. M.; Lackinger, M. Thermodynamics of Halogen Bonded Monolayer Self-Assembly at the Liquid-Solid Interface. *Chem. Commun.* **2014,** *50*, 13465-13468.

82. Chung, K.-H.; Park, J.; Kim, K. Y.; Yoon, J. K.; Kim, H.; Han, S.; Kahng, S.-J. Polymorphic Porous Supramolecular Networks Mediated by Halogen Bonds on Ag(111). *Chem. Commun.* **2011,** *47*, 11492-11494.
83. Cavallo, G.; Metrangolo, P.; Milani, R.; Pilati, T.; Priimagi, A.; Resnati, G.; Terraneo, G. The Halogen Bond. *Chem. Rev.* **2016,** *116*, 2478-2601.
84. Baber, A. E.; Jensen, S. C.; Sykes, E. C. H. Dipole-Driven Ferroelectric Assembly of Styrene on Au{111}. *J. Am. Chem. Soc.* **2007,** *129*, 6368-6369.
85. Xu, L.; Miao, X.; Ying, X.; Deng, W. Two-Dimensional Self-Assembled Molecular Structures Formed by the Competition of van der Waals Forces and Dipole–Dipole Interactions. *J. Phys. Chem. C* **2012,** *116*, 1061-1069.
86. Yokoyama, T.; Takahashi, T.; Shinozaki, K.; Okamoto, M. Quantitative Analysis of Long-Range Interactions Between Adsorbed Dipolar Molecules on Cu(111). *Phys. Rev. Lett.* **2007,** *98*, 206102-206105.
87. Mezour, M. A.; Voznyy, O.; Sargent, E. H.; Lennox, R. B.; Perepichka, D. F. Controlling C60 Organization through Dipole-Induced Band Alignment at Self-Assembled Monolayer Interfaces. *Chem. Mater.* **2016,** *28*, 8322-8329.
88. Schwartz, J. J.; Mendoza, A. M.; Wattanatorn, N.; Zhao, Y.; Nguyen, V. T.; Spokoyny, A. M.; Mirkin, C. A.; Baše, T.; Weiss, P. S. Surface Dipole Control of Liquid Crystal Alignment. *J. Am. Chem. Soc.* **2016,** *138*, 5957-5967.
89. Kim, J.; Rim, Y. S.; Liu, Y.; Serino, A. C.; Thomas, J. C.; Chen, H.; Yang, Y.; Weiss, P. S. Interface Control in Organic Electronics Using Mixed Monolayers of Carboranethiol Isomers. *Nano Lett.* **2014,** *14*, 2946-2951.
90. Serino, A. C.; Anderson, M. E.; Saleh, L. M. A.; Dziedzic, R. M.; Mills, H.; Heidenreich, L. K.; Spokoyny, A. M.; Weiss, P. S. Work Function Control of Germanium through Carborane-Carboxylic Acid Surface Passivation. *ACS Appl. Mater. Interfaces* **2017,** *9*, 34592-34596.
91. Stepanow, S.; Lingenfelder, M.; Dmitriev, A.; Spillmann, H.; Delvigne, E.; Lin, N.; Deng, X. B.; Cai, C. Z.; Barth, J. V.; Kern, K. Steering Molecular Organization and Host-Guest Interactions Using Two-Dimensional Nanoporous Coordination Systems. *Nat. Mater.* **2004,** *3*, 229-233.
92. Skomski, D.; Abb, S.; Tait, S. L. Robust Surface Nano-Architecture by Alkali-Carboxylate Ionic Bonding. *J. Am. Chem. Soc.* **2012,** *134*, 14165-14171.
93. Skomski, D.; Tait, S. L. Ordered and Robust Ionic Surface Networks from Weakly Interacting Carboxyl Building Blocks. *J. Phys. Chem. C* **2013,** *117*, 2959-2965.
94. Skomski, D.; Tempas, C. D.; Bukowski, G. S.; Smith, K. A.; Tait, S. L. Redox-Active On-Surface Polymerization of Single-Site Divalent Cations from Pure Metals by a Ketone-Functionalized Phenanthroline. *J. Chem. Phys.* **2015,** *142*, 101913-101918.
95. Skomski, D.; Tempas, C. D.; Cook, B. J.; Polezhaev, A. V.; Smith, K. A.; Caulton, K. G.; Tait, S. L. Two and Three Electron Oxidation of Single-Site Vanadium Centers at Surfaces by Ligand Design. *J. Am. Chem. Soc.* **2015,** *137*, 7898-7902.
96. Abdurakhmanova, N.; Floris, A.; Tseng, T.-C.; Comisso, A.; Stepanow, S.; De Vita, A.; Kern, K. Stereoselectivity and Electrostatics in Charge-Transfer Mn- and Cs-TCNQ4 Networks on Ag(100). *Nat. Commun.* **2012,** *3*, 940-946.
97. Tait, S. L.; Langner, A.; Lin, N.; Stepanow, S.; Rajadurai, C.; Ruben, M.; Kern, K. One-Dimensional Self-Assembled Molecular Chains on Cu(100): Interplay Between Surface-Assisted Coordination Chemistry and Substrate Commensurability. *J. Phys. Chem. C* **2007,** *111*, 10982-10987.
98. Lin, N.; Langner, A.; Tait, S. L.; Rajadurai, C.; Ruben, M.; Kern, K. Template-Directed Supramolecular Self-Assembly of Coordination Dumbells at Surfaces. *Chem. Commun.* **2007**, 4860-4862.
99. Langner, A.; Tait, S. L.; Lin, N.; Rajadurai, C.; Ruben, M.; Kern, K. Self-Recognition and Self-Selection in Multicomponent Supramolecular Coordination Networks on Surfaces. *Proc. Natl. Acad. Sci. U. S. A.* **2007,** *104*, 17927-17930.

100. Tait, S. L.; Wang, Y.; Costantini, G.; Lin, N.; Baraldi, A.; Esch, F.; Petaccia, L.; Lizzit, S.; Kern, K. Metal-Organic Coordination Interactions in Fe-Terephthalic Acid Networks on Cu(100). *J. Am. Chem. Soc.* **2008,** *130*, 2108-2113.
101. Williams, C. G.; Wang, M.; Skomski, D.; Tempas, C. D.; Kesmodel, L. L.; Tait, S. L. Metal–Ligand Complexation through Redox Assembly at Surfaces Characterized by Vibrational Spectroscopy. *J. Phys. Chem. C* **2017,** *121*, 13183-13190.
102. Tempas, C. D.; Morris, T.; Wisman, D. L.; Le, D.; Din, N. U.; Williams, C. G.; Wang, M.; Polezhaev, A. V.; Rahman, T. S.; Caulton, K. G.; Tait, S. L. Redox-Active Ligand Controlled Selectivity of Vanadium Oxidation on Au(100). *Chem. Sci.* **2018,** *9*, 1674-1685.
103. Le, D.; Rahman, T. S. Pt-Dipyridyl Tetrazine Metal-Organic Network on the Au(100) Surface: Insights from First Principles Calculations. *Faraday Discuss.* **2017,** *204*, 83-95.
104. Wasio, N. A.; Quardokus, R. C.; Forrest, R. P.; Lent, C. S.; Corcelli, S. A.; Christie, J. A.; Henderson, K. W.; Kandel, S. A. Self-Assembly of Hydrogen-Bonded Two-Dimensional Quasicrystals. *Nature* **2014,** *507*, 86-89.
105. Hirsch, B. E.; Lee, S.; Qiao, B.; Chen, C.-H.; McDonald, K. P.; Tait, S. L.; Flood, A. H. Anion-Induced Dimerization of 5-Fold Symmetric Cyanostars in 3D Crystalline Solids and 2D Self-Assembled Crystals. *Chem. Commun.* **2014,** *50*, 9827-9830.
106. Hohman, J. N.; Zhang, P.; Morin, E. I.; Han, P.; Kim, M.; Kurland, A. R.; McClanahan, P. D.; Balema, V. P.; Weiss, P. S. Self-Assembly of Carboranethiol Isomers on Au{111}: Intermolecular Interactions Determined by Molecular Dipole Orientations. *ACS Nano* **2009,** *3*, 527-536.
107. Fabris, S.; Stepanow, S.; Lin, N.; Gambardella, P.; Dmitriev, A.; Honolka, J.; Baroni, S.; Kern, K. Oxygen Dissociation by Concerted Action of Di-Iron Centers in Metal–Organic Coordination Networks at Surfaces: Modeling Non-Heme Iron Enzymes. *Nano Lett.* **2011,** *11*, 5414-5420.
108. Wurster, B.; Grumelli, D.; Hötger, D.; Gutzler, R.; Kern, K. Driving the Oxygen Evolution Reaction by Nonlinear Cooperativity in Bimetallic Coordination Catalysts. *J. Am. Chem. Soc.* **2016,** *138*, 3623-3626.
109. Kamna, M. M.; Stranick, S. J.; Weiss, P. S. Imaging Substrate-Mediated Interactions. *Isr. J. Chem.* **1996,** *36*, 59-62.
110. Kamna, M. M.; Stranick, S. J.; Weiss, P. S. Imaging Substrate-Mediated Interactions. *Science* **1996,** *274*, 118-119.
111. Weiss, P. S.; Kamna, M. M.; Graham, T. M.; Stranick, S. J. Imaging Benzene Molecules and Phenyl Radicals on Cu{111}. *Langmuir* **1998,** *14*, 1284-1289.
112. Kamna, M. M.; Graham, T. M.; Love, J. C.; Weiss, P. S. Strong Electronic Perturbation of the Cu{111} Surface by 7,7′,8,8′-Tetracyanoquinonedimethane. *Surf. Sci.* **1998,** *419*, 12-23.
113. Sykes, E. C. H.; Han, P.; Kandel, S. A.; Kelly, K. F.; McCarty, G. S.; Weiss, P. S. Substrate-Mediated Interactions and Intermolecular Forces Between Molecules Adsorbed on Surfaces. *Acc. Chem. Res.* **2003,** *36*, 945-953.
114. Sykes, E. C. H.; Mantooth, B. A.; Han, P.; Donhauser, Z. J.; Weiss, P. S. Substrate-Mediated Intermolecular Interactions: A Quantitative Single Molecule Analysis. *J. Am. Chem. Soc.* **2005,** *127*, 7255-7260.
115. Han, P.; Weiss, P. S. Electronic Substrate-Mediated Interactions. *Surf. Sci. Rep.* **2012,** *67*, 19-81.
116. Chilukuri, B.; Mazur, U.; Hipps, K. W. Effect of Dispersion on Surface Interactions of Cobalt(II) Octaethylporphyrin Monolayer on Au(111) and HOPG(0001) Substrates: A Comparative First Principles Study. *Phys. Chem. Chem. Phys.* **2014,** *16*, 14096-14107.
117. Monti, O. L. A. Understanding Interfacial Electronic Structure and Charge Transfer: An Electrostatic Perspective. *J. Phys. Chem. Lett.* **2012,** *3*, 2342-2351.
118. Flores, F.; Ortega, J.; Vazquez, H. Modelling Energy Level Alignment at Organic Interfaces and Density Functional Theory. *Phys. Chem. Chem. Phys.* **2009,** *11*, 8658-8675.

119. Tseng, T.-C.; Urban, C.; Wang, Y.; Otero, R.; Tait, S. L.; Alcamí, M.; Écija, D.; Trelka, M.; Gallego, J. M.; Lin, N.; Konuma, M.; Starke, U.; Nefedov, A.; Langner, A.; Wöll, C.; Herranz, M. Á.; Martín, F.; Martín, N.; Kern, K.; Miranda, R. Charge-Transfer-Induced Structural Rearrangements at Both Sides of Organic/Metal Interfaces. *Nat. Chem.* **2010,** *2*, 374-379.
120. Stranick, S. J.; Kamna, M. M.; Weiss, P. S. Interactions and Dynamics of Benzene on Cu{111} at Low Temperature. *Surf. Sci.* **1995,** *338*, 41-59.
121. Blowey, P. J.; Rochford, L. A.; Duncan, D. A.; Warr, D. A.; Lee, T. L.; Woodruff, D. P.; Costantini, G. Probing the Interplay Between Geometric and Electronic Structure in a Two-Dimensional K-TCNQ Charge Transfer Network. *Faraday Discuss.* **2017,** *204*, 97-110.
122. Della Pia, A.; Riello, M.; Floris, A.; Stassen, D.; Jones, T. S.; Bonifazi, D.; De Vita, A.; Costantini, G. Anomalous Coarsening Driven by Reversible Charge Transfer at Metal–Organic Interfaces. *ACS Nano* **2014,** *8*, 12356-12364.
123. Maughan, B.; Zahl, P.; Sutter, P.; Monti, O. L. A. Selective Cooperative Self-Assembly Between an Organic Semiconductor and Native Adatoms on Cu(110). *J. Phys. Chem. C* **2015,** *119*, 27416-27425.
124. Smoluchowski, R. Anisotropy of the Electronic Work Function of Metals. *Physical Review* **1941,** *60*, 661-674.
125. Gruenewald, M.; Schirra, L. K.; Winget, P.; Kozlik, M.; Ndione, P. F.; Sigdel, A. K.; Berry, J. J.; Forker, R.; Brédas, J.-L.; Fritz, T.; Monti, O. L. A. Integer Charge Transfer and Hybridization at an Organic Semiconductor/Conductive Oxide Interface. *J. Phys. Chem. C* **2015,** *119*, 4865-4873.
126. Rohlfing, M.; Temirov, R.; Tautz, F. S. Adsorption Structure and Scanning Tunneling Data of a Prototype Organic-Inorganic Interface: PTCDA on Ag(111). *Phys. Rev. B* **2007,** *76*, 115421-115436.
127. Huber, F.; Matencio, S.; Weymouth, A. J.; Ocal, C.; Barrena, E.; Giessibl, F. J. Intramolecular Force Contrast and Dynamic Current-Distance Measurements at Room Temperature. *Phys. Rev. Lett.* **2015,** *115*, 066101-066104.
128. Bairagi, K.; Bellec, A.; Chumakov, R. G.; Menshikov, K. A.; Lagoute, J.; Chacon, C.; Girard, Y.; Rousset, S.; Repain, V.; Lebedev, A. M.; Sukhanov, L. P.; Svechnikov, N. Y.; Stankevich, V. G. STM Study of $C_{60}F_{18}$ High Dipole Moment Molecules on Au(111). *Surf. Sci.* **2015,** *641*, 248-251.
129. MacLeod, J. M.; Ivasenko, O.; Fu, C.; Taerum, T.; Rosei, F.; Perepichka, D. F. Supramolecular Ordering in Oligothiophene−Fullerene Monolayers. *J. Am. Chem. Soc.* **2009,** *131*, 16844-16850.
130. Ma, W.; Xu, L.; de Moura, A. F.; Wu, X.; Kuang, H.; Xu, C.; Kotov, N. A. Chiral Inorganic Nanostructures. *Chem. Rev.* **2017,** *117*, 8041-8093.
131. Fasel, R.; Parschau, M.; Ernst, K.-H. Amplification of Chirality in Two-Dimensional Enantiomorphous Lattices. *Nature* **2006,** *439*, 449-452.
132. Parschau, M.; Ernst, K. H. Disappearing Enantiomorphs: Single Handedness in Racemate Crystals. *Angew. Chem. Int. Ed.* **2015,** *54*, 14422-14426.
133. Chen, T.; Yang, W.-H.; Wang, D.; Wan, L.-J. Globally Homochiral Assembly of Two-Dimensional Molecular Networks Triggered by Co-Absorbers. *Nat. Commun.* **2013,** *4*, 1389-1396.
134. Fang, Y.; Ghijsens, E.; Ivasenko, O.; Cao, H.; Noguchi, A.; Mali, K. S.; Tahara, K.; Tobe, Y.; De Feyter, S. Dynamic Control Over Supramolecular Handedness by Selecting Chiral Induction Pathways at the Solution–Solid Interface. *Nat. Chem.* **2016,** *8*, 711-717.
135. Katsonis, N.; Xu, H.; Haak Robert , M.; Kudernac, T.; Tomović, Ž.; George, S.; Van der Auweraer, M.; Schenning Albert , P. H. J.; Meijer, E. W.; Feringa Ben , L.; De Feyter, S. Emerging Solvent-Induced Homochirality by the Confinement of Achiral Molecules Against a Solid Surface. *Angew. Chem. Int. Ed.* **2008,** *47*, 4997-5001.
136. Destoop, I.; Minoia, A.; Ivasenko, O.; Noguchi, A.; Tahara, K.; Tobe, Y.; Lazzaroni, R.; De Feyter, S. Transfer of Chiral Information from a Chiral Solvent to a Two-Dimensional Network. *Faraday Discuss.* **2017,** *204*, 215-231.

137. Lei, S.; Tahara, K.; De Schryver Frans , C.; Van der Auweraer, M.; Tobe, Y.; De Feyter, S. One Building Block, Two Different Supramolecular Surface-Confined Patterns: Concentration in Control at the Solid–Liquid Interface. *Angew. Chem. Int. Ed.* **2008,** *47*, 2964-2968.
138. Gutzler, R.; Cardenas, L.; Rosei, F. Kinetics and Thermodynamics in Surface-Confined Molecular Self-Assembly. *Chem. Sci.* **2011,** *2*, 2290-2300.
139. Stranick, S. J.; Parikh, A. N.; Tao, Y. T.; Allara, D. L.; Weiss, P. S. Phase Separation of Mixed-Composition Self-Assembled Monolayers into Nanometer Scale Molecular Domains. *J. Phys. Chem.* **1994,** *98*, 7636-7646.
140. Hipps, K. W.; Mazur, U. Kinetic and Thermodynamic Control in Porphyrin and Phthalocyanine Self-Assembled Monolayers. *Langmuir* **2018,** *34*, 3-17.
141. Bhattarai, A.; Mazur, U.; Hipps, K. W. A Single Molecule Level Study of the Temperature-Dependent Kinetics for the Formation of Metal Porphyrin Monolayers on Au(111) from Solution. *J. Am. Chem. Soc.* **2014,** *136*, 2142-2148.
142. Whitesides, G. M.; Grzybowski, B. Self-Assembly at All Scales. *Science* **2002,** *295*, 2418-2421.
143. Héctor, M. S.; Thomas, J. M.; Pengpeng, Z.; Daniel, C. D.; Shelley, A. C.; Paul, S. W. Hybrid Strategies in Nanolithography. *Rep. Prog. Phys.* **2010,** *73*, 036501-036540.
144. Hipps, K. W.; Scudiero, L.; Barlow, D. E.; Cooke, M. P. A Self-Organized 2-Dimensional Bifunctional Structure Formed by Supramolecular Design. *J. Am. Chem. Soc.* **2002,** *124*, 2126-2127.
145. Xue, Y.; Zimmt, M. B. Patterned Monolayer Self-Assembly Programmed by Side Chain Shape: Four-Component Gratings. *J. Am. Chem. Soc.* **2012,** *134*, 4513-4516.
146. Tahara, K.; Kaneko, K.; Katayama, K.; Itano, S.; Nguyen, C. H.; Amorim, D. D. D.; De Feyter, S.; Tobe, Y. Formation of Multicomponent Star Structures at the Liquid/Solid Interface. *Langmuir* **2015,** *31*, 7032-7040.
147. Velpula, G.; Takeda, T.; Adisoejoso, J.; Inukai, K.; Tahara, K.; Mali, K. S.; Tobe, Y.; De Feyter, S. On the Formation of Concentric 2D Multicomponent Assemblies at the Solution-Solid Interface. *Chem. Commun.* **2017,** *53*, 1108-1111.
148. Shen, Y.-T.; Deng, K.; Zhang, X.-M.; Feng, W.; Zeng, Q.-D.; Wang, C.; Gong, J. R. Switchable Ternary Nanoporous Supramolecular Network on Photo-Regulation. *Nano Lett.* **2011,** *11*, 3245-3250.
149. Yokoyama, S.; Hirose, T.; Matsuda, K. Photoinduced Four-State Three-Step Ordering Transformation of Photochromic Terthiophene at a Liquid/Solid Interface Based on Two Principles: Photochromism and Polymorphism. *Langmuir* **2015,** *31*, 6404-6414.
150. Maeda, N.; Hirose, T.; Yokoyama, S.; Matsuda, K. Rational Design of Highly Photoresponsive Surface-Confined Self-Assembly of Diarylethenes: Reversible Three-State Photoswitching at the Liquid/Solid Interface. *J. Phys. Chem. C* **2016,** *120*, 9317-9325.
151. Böckmann, H.; Liu, S.; Mielke, J.; Gawinkowski, S.; Waluk, J.; Grill, L.; Wolf, M.; Kumagai, T. Direct Observation of Photoinduced Tautomerization in Single Molecules at a Metal Surface. *Nano Lett.* **2016,** *16*, 1034-1041.
152. Gopakumar, T. G.; Müller, F.; Hietschold, M. Scanning Tunneling Microscopy and Scanning Tunneling Spectroscopy Studies of Planar and Nonplanar Naphthalocyanines on Graphite (0001). Part 1: Effect of Nonplanarity on the Adlayer Structure and Voltage-induced Flipping of Nonplanar Tin−Naphthalocyanine. *J. Phys. Chem. B* **2006,** *110*, 6051-6059.
153. Yang, Y.-L.; Chan, Q.-L.; Ma, X.-J.; Deng, K.; Shen, Y.-T.; Feng, X.-Z.; Wang, C. Electrical Conformational Bistability of Dimesogen Molecules with a Molecular Chord Structure. *Angew. Chem. Int. Ed.* **2006,** *45*, 6889-6893.
154. Lei, S.-B.; Deng, K.; Yang, Y.-L.; Zeng, Q.-D.; Wang, C.; Jiang, J.-Z. Electric Driven Molecular Switching of Asymmetric Tris(phthalocyaninato) Lutetium Triple-Decker Complex at the Liquid/Solid Interface. *Nano Lett.* **2008,** *8*, 1836-1843.

155. Alemani, M.; Peters, M. V.; Hecht, S.; Rieder, K.-H.; Moresco, F.; Grill, L. Electric Field-Induced Isomerization of Azobenzene by STM. *J. Am. Chem. Soc.* **2006,** *128*, 14446-14447.
156. Cometto, F. P.; Kern, K.; Lingenfelder, M. Local Conformational Switching of Supramolecular Networks at the Solid/Liquid Interface. *ACS Nano* **2015,** *9*, 5544-5550.
157. Nanayakkara, S. U.; Sykes, E. C. H.; Fernández-Torres, L. C.; Blake, M. M.; Weiss, P. S. Long-Range Electronic Interactions at a High Temperature: Bromine Adatom Islands on Cu(111). *Phys. Rev. Lett.* **2007,** *98*, 206108-206111.
158. Tsong, T. T. Direct Observation of Interactions Between Individual Atoms on Tungsten Surfaces. *Phys. Rev. B* **1972,** *6*, 417-426.
159. Lau, K. H.; Kohn, W. Indirect Long-Range Oscillatory Interaction Between Adsorbed Atoms. *Surf. Sci.* **1978,** *75*, 69-85.
160. Repp, J.; Moresco, F.; Meyer, G.; Rieder, K.-H.; Hyldgaard, P.; Persson, M. Substrate Mediated Long-Range Oscillatory Interaction Between Adatoms: Cu /Cu(111). *Phys. Rev. Lett.* **2000,** *85*, 2981-2984.
161. Knorr, N.; Brune, H.; Epple, M.; Hirstein, A.; Schneider, M. A.; Kern, K. Long-Range Adsorbate Interactions Mediated by a Two-Dimensional Electron Gas. *Phys. Rev. B* **2002,** *65*, 115420-115424.
162. Grimley, T. B. The Indirect Interaction Between Atoms or Molecules Adsorbed on Metals. *Proc. Phys. Soc.* **1967,** *90*, 751-764.
163. Einstein, T. L. Theory of Indirect Interaction Between Chemisorbed Atoms. *Crit. Rev. Solid State Mater. Sci.* **1978,** *7*, 261-288.
164. Li, M.; Deng, K.; Yang, Y.-L.; Zeng, Q.-D.; He, M.; Wang, C. Electronically Engineered Interface Molecular Superlattices: STM Study of Aromatic Molecules on Graphite. *Phys. Rev. B* **2007,** *76*, 155438-155442.
165. Cui, K.; Mali, K. S.; Ivasenko, O.; Wu, D.; Feng, X.; Walter, M.; Müllen, K.; De Feyter, S.; Mertens, S. F. L. Squeezing, Then Stacking: From Breathing Pores to Three-Dimensional Ionic Self-Assembly Under Electrochemical Control. *Angew. Chem. Int. Ed.* **2014,** *53*, 12951-12954.
166. Thomas, J. C.; Schwartz, J. J.; Hohman, J. N.; Claridge, S. A.; Auluck, H. S.; Serino, A. C.; Spokoyny, A. M.; Tran, G.; Kelly, K. F.; Mirkin, C. A.; Gilles, J.; Osher, S. J.; Weiss, P. S. Defect-Tolerant Aligned Dipoles within Two-Dimensional Plastic Lattices. *ACS Nano* **2015,** *9*, 4734-4742.
167. Gutzler, R.; Stepanow, S.; Grumelli, D.; Lingenfelder, M.; Kern, K. Mimicking Enzymatic Active Sites on Surfaces for Energy Conversion Chemistry. *Acc. Chem. Res.* **2015,** *48*, 2132-2139.
168. Donhauser, Z. J.; Mantooth, B. A.; Kelly, K. F.; Bumm, L. A.; Monnell, J. D.; Stapleton, J. J.; Price, D. W.; Rawlett, A. M.; Allara, D. L.; Tour, J. M.; Weiss, P. S. Conductance Switching in Single Molecules through Conformational Changes. *Science* **2001,** *292*, 2303-2307.
169. Lewis, P. A.; Inman, C. E.; Yao, Y.; Tour, J. M.; Hutchison, J. E.; Weiss, P. S. Mediating Stochastic Switching of Single Molecules Using Chemical Functionality. *J. Am. Chem. Soc.* **2004,** *126*, 12214-12215.
170. Weiss, P. S. Functional Molecules and Assemblies in Controlled Environments: Formation and Measurements. *Acc. Chem. Res.* **2008,** *41*, 1772-1781.
171. Kumagai, T.; Hanke, F.; Gawinkowski, S.; Sharp, J.; Kotsis, K.; Waluk, J.; Persson, M.; Grill, L. Controlling Intramolecular Hydrogen Transfer in a Porphycene Molecule with Single Atoms or Molecules Located Nearby. *Nat. Chem.* **2014,** *6*, 41-46.
172. Zheng, Y. B.; Pathem, B. K.; Hohman, J. N.; Thomas, J. C.; Kim, M.; Weiss, P. S. Photoresponsive Molecules in Well-Defined Nanoscale Environments. *Adv. Mater.* **2013,** *25*, 302-312.
173. Abendroth, J. M.; Bushuyev, O. S.; Weiss, P. S.; Barrett, C. J. Controlling Motion at the Nanoscale: Rise of the Molecular Machines. *ACS Nano* **2015,** *9*, 7746-7768.
174. Cheng, C.; McGonigal, P. R.; Stoddart, J. F.; Astumian, R. D. Design and Synthesis of Nonequilibrium Systems. *ACS Nano* **2015,** *9*, 8672-8688.
175. Madueno, R.; Raisanen, M. T.; Silien, C.; Buck, M. Functionalizing Hydrogen-Bonded Surface Networks with Self-Assembled Monolayers. *Nature* **2008,** *454*, 618-621.

176. Ivasenko, O.; MacLeod, J. M.; Chernichenko, K. Y.; Balenkova, E. S.; Shpanchenko, R. V.; Nenajdenko, V. G.; Rosei, F.; Perepichka, D. F. Supramolecular Assembly of Heterocirculenes in 2D and 3D. *Chem. Commun.* **2009**, 1192-1194.
177. Raisanen, M. T.; Slater, A. G.; Champness, N. R.; Buck, M. Effects of Pore Modification on the Templating of Guest Molecules in a 2D Honeycomb Network. *Chem. Sci.* **2012,** *3*, 84-92.
178. Theobald, J. A.; Oxtoby, N. S.; Phillips, M. A.; Champness, N. R.; Beton, P. H. Controlling Molecular Deposition and Layer Structure with Supramolecular Surface Assemblies. *Nature* **2003,** *424*, 1029-1031.
179. Spillmann, H.; Kiebele, A.; Stöhr, M.; Jung, T. A.; Bonifazi, D.; Cheng, F.; Diederich, F. A Two-Dimensional Porphyrin-Based Porous Network Featuring Communicating Cavities for the Templated Complexation of Fullerenes. *Adv. Mater.* **2006,** *18*, 275-279.
180. Li, M.; Deng, K.; Lei, S.-B.; Yang, Y.-L.; Wang, T.-S.; Shen, Y.-T.; Wang, C.-R.; Zeng, Q.-D.; Wang, C. Site-Selective Fabrication of Two-Dimensional Fullerene Arrays by Using a Supramolecular Template at the Liquid-Solid Interface. *Angew. Chem. Int. Ed.* **2008,** *120*, 6819-6823.
181. MacLeod, J. M.; Ivasenko, O.; Perepichka, D. F.; Rosei, F. Stabilization of Exotic Minority Phases in a Multicomponent Self-Assembled Molecular Network. *Nanotechnology* **2007,** *18*, 424031-424039.
182. Blunt, M. O.; Russell, J. C.; Gimenez-Lopez, M. d. C.; Taleb, N.; Lin, X.; Schröder, M.; Champness, N. R.; Beton, P. H. Guest-Induced Growth of a Surface-Based Supramolecular Bilayer. *Nat. Chem.* **2011,** *3*, 74-78.
183. Lee, S.; Hirsch, B. E.; Liu, Y.; Dobscha, J. R.; Burke, D. W.; Tait, S. L.; Flood, A. H. Multifunctional Tricarbazolo Triazolophane Macrocycles: One-Pot Preparation, Anion Binding, and Hierarchical Self-Organization of Multilayers. *Chem. Eur. J.* **2016,** *22*, 560-569.
184. Skomski, D.; Jo, J.; Tempas, C. D.; Kim, S.; Lee, D.; Tait, S. L. High-Fidelity Self-Assembly of Crystalline and Parallel-Oriented Organic Thin Films by π-π Stacking from a Metal Surface. *Langmuir* **2014,** *30*, 10050-10056.
185. Wang, Y.; Kröger, J.; Berndt, R.; Hofer, W. Structural and Electronic Properties of Ultrathin Tin–Phthalocyanine Films on Ag(111) at the Single-Molecule Level. *Angew. Chem. Int. Ed.* **2009,** *121*, 1287-1291.
186. Stöhr, M.; Gabriel, M.; Möller, R. Investigation of the Growth of PTCDA on Cu(110): An STM Study. *Surf. Sci.* **2002,** *507-510*, 330-334.
187. Cui, D.; MacLeod, J. M.; Ebrahimi, M.; Perepichka, D. F.; Rosei, F. Solution and Air Stable Host/Guest Architectures from a Single Layer Covalent Organic Framework. *Chem. Commun.* **2015,** *51*, 16510-16513.
188. Cote, A. P. Porous, Crystalline, Covalent Organic Frameworks. *Science* **2005,** *310*, 1166-1170.
189. Feng, X.; Ding, X.; Jiang, D. Covalent Organic Frameworks. *Chem. Soc. Rev.* **2012,** *41*, 6010-6022.
190. Ding, S.-Y.; Wang, W. Covalent Organic Frameworks (COFs): From Design to Applications. *Chem. Soc. Rev.* **2013,** *42*, 548-568.
191. Plas, J.; Ivasenko, O.; Martsinovich, N.; Lackinger, M.; De Feyter, S. Nanopatterning of a Covalent Organic Framework Host–Guest System. *Chem. Commun.* **2016,** *52*, 68-71.
192. Cui, D.; Ebrahimi, M.; Rosei, F.; Macleod, J. M. Control of Fullerene Crystallization from 2D to 3D through Combined Solvent and Template Effects. *J. Am. Chem. Soc.* **2017,** *139*, 16732-16740.
193. Mezour, M. A.; Perepichka, I. I.; Zhu, J.; Lennox, R. B.; Perepichka, D. F. Directing the Assembly of Gold Nanoparticles with Two-Dimensional Molecular Networks. *ACS Nano* **2014,** *8*, 2214-2222.
194. Rosei, F. Nanostructured Surfaces: Challenges and Frontiers in Nanotechnology. *J. Phys.: Condens. Matter* **2004,** *16*, S1373-S1436.
195. Rosei, F.; Schunack, M.; Naitoh, Y.; Jiang, P.; Gourdon, A.; Laegsgaard, E.; Stensgaard, I.; Joachim, C.; Besenbacher, F. Properties of Large Organic Molecules on Metal Surfaces. *Prog. Surf. Sci.* **2003,** *71*, 95-146.

196. Joachim, C.; Gimzewski, J. K.; Aviram, A. Electronics Using Hybrid-Molecular and Mono-Molecular Devices. *Nature* **2000,** *408*, 541-548.
197. Lu, W.; Lieber, C. M. Nanoelectronics from the Bottom Up. *Nat. Mater.* **2007,** *6*, 841-850.
198. Nerngchamnong, N.; Yuan, L.; Qi, D.-C.; Li, J.; Thompson, D.; Nijhuis, C. A. The Role of Van der Waals Forces in the Performance of Molecular Diodes. *Nat. Nanotechnol.* **2013,** *8*, 113-118.
199. Yuan, L.; Franco, C.; Crivillers, N.; Mas-Torrent, M.; Cao, L.; Sangeeth, C. S. S.; Rovira, C.; Veciana, J.; Nijhuis, C. A. Chemical Control Over the Energy-Level Alignment in a Two-Terminal Junction. *Nat. Commun.* **2016,** *7*, 12066-12075.
200. Tour, J. M. *Molecular Electronics: Commercial Insights, Chemistry, Devices, Architecture and Programming*. World Scientific: New Jersey, 2003.
201. Santato, C.; Rosei, F. Organic/Metal Interfaces: Seeing Both Sides. *Nat. Chem.* **2010,** *2*, 344-345.
202. Han, T.-H.; Lee, Y.; Choi, M.-R.; Woo, S.-H.; Bae, S.-H.; Hong, B. H.; Ahn, J.-H.; Lee, T.-W. Extremely Efficient Flexible Organic Light-Emitting Diodes with Modified Graphene Anode. *Nat. Photonics* **2012,** *6*, 105-110.
203. Torsi, L.; Magliulo, M.; Manoli, K.; Palazzo, G. Organic Field-Effect Transistor Sensors: A Tutorial Review. *Chem. Soc. Rev.* **2013,** *42*, 8612-8628.
204. Guo, Y.; Yu, G.; Liu, Y. Functional Organic Field-Effect Transistors. *Adv. Mater.* **2010,** *22*, 4427-4447.
205. Zhao, A.; Tan, S.; Li, B.; Wang, B.; Yang, J.; Hou, J. G. STM Tip-Assisted Single Molecule Chemistry. *Phys. Chem. Chem. Phys.* **2013,** *15*, 12428-12441.
206. Harikumar, K. R.; McNab, I. R.; Polanyi, J. C.; Zabet-Khosousi, A.; Hofer, W. A. Imprinting Self-Assembled Patterns of Lines at a Semiconductor Surface, Using Heat, Light, or Electrons. *Proc. Natl. Acad. Sci. U. S. A.* **2010,** *108*, 950-955.
207. Li, Z.; Li, B.; Yang, J.; Hou, J. G. Single-Molecule Chemistry of Metal Phthalocyanine on Noble Metal Surfaces. *Acc. Chem. Res.* **2010,** *43*, 954-962.
208. Sloan, P. A.; Palmer, R. E. Two-Electron Dissociation of Single Molecules by Atomic Manipulation at Room Temperature. *Nature* **2005,** *434*, 367-371.
209. Hla, S.-W.; Bartels, L.; Meyer, G.; Rieder, K.-H. Inducing All Steps of a Chemical Reaction with the Scanning Tunneling Microscope Tip: Towards Single Molecule Engineering. *Phys. Rev. Lett.* **2000,** *85*, 2777-2780.
210. Jiang, Y.; Huan, Q.; Fabris, L.; Bazan, G. C.; Ho, W. Submolecular Control, Spectroscopy, and Imaging of Bond-Selective Chemistry in Single Functionalized Molecules. *Nat. Chem.* **2012,** *5*, 36-41.
211. Chen, L.; Li, H.; Wee, A. T. S. Nonlocal Chemical Reactivity at Organic−Metal Interfaces. *ACS Nano* **2009,** *3*, 3684-3690.
212. Maier, S.; Fendt, L.-A.; Zimmerli, L.; Glatzel, T.; Pfeiffer, O.; Diederich, F.; Meyer, E. Nanoscale Engineering of Molecular Porphyrin Wires on Insulating Surfaces. *Small* **2008,** *4*, 1115-1118.
213. Rahe, P.; Kittelmann, M.; Neff, J. L.; Nimmrich, M.; Reichling, M.; Maass, P.; Kühnle, A. Tuning Molecular Self-Assembly on Bulk Insulator Surfaces by Anchoring of the Organic Building Blocks. *Adv. Mater.* **2013,** *25*, 3948-3956.
214. Burke, S. A.; Mativetsky, J. M.; Fostner, S.; Grütter, P. C_{60} on Alkali Halides: Epitaxy and Morphology Studied by Noncontact AFM. *Phys. Rev. B* **2007,** *76*, 035419-035427.
215. Gaberle, J.; Gao, D. Z.; Shluger, A. L.; Amrous, A.; Bocquet, F.; Nony, L.; Para, F.; Loppacher, C.; Lamare, S.; Cherioux, F. Morphology and Growth Mechanisms of Self-Assembled Films on Insulating Substrates: Role of Molecular Flexibility and Entropy. *J. Phys. Chem. C* **2017,** *121*, 4393-4403.
216. Burke, S. A.; Ji, W.; Mativetsky, J. M.; Topple, J. M.; Fostner, S.; Gao, H. J.; Guo, H.; Grütter, P. Strain Induced Dewetting of a Molecular System: Bimodal Growth of PTCDA on NaCl. *Phys. Rev. Lett.* **2008,** *100*, 186104-186107.
217. Tautz, F. S. Structure and Bonding of Large Aromatic Molecules on Noble Metal Surfaces: The Example of PTCDA. *Prog. Surf. Sci.* **2007,** *82*, 479-520.

218. Geim, A. K.; Grigorieva, I. V. Van der Waals Heterostructures. *Nature* **2013,** *499*, 419-425.
219. Corso, M.; Auwärter, W.; Muntwiler, M.; Tamai, A.; Greber, T.; Osterwalder, J. Boron Nitride Nanomesh. *Science* **2004,** *303*, 217-220.
220. Dil, H.; Lobo-Checa, J.; Laskowski, R.; Blaha, P.; Berner, S.; Osterwalder, J.; Greber, T. Surface Trapping of Atoms and Molecules with Dipole Rings. *Science* **2008,** *319*, 1824-1826.
221. Natterer, F. D.; Patthey, F.; Brune, H. Ring State for Single Transition Metal Atoms on Boron Nitride on Rh(111). *Phys. Rev. Lett.* **2012,** *109*, 066101-066104.
222. Brihuega, I.; Michaelis, C. H.; Zhang, J.; Bose, S.; Sessi, V.; Honolka, J.; Alexander Schneider, M.; Enders, A.; Kern, K. Electronic Decoupling and Templating of Co Nanocluster Arrays on the Boron Nitride Nanomesh. *Surf. Sci.* **2008,** *602*, L95-L99.
223. Kahle, S.; Deng, Z.; Malinowski, N.; Tonnoir, C.; Forment-Aliaga, A.; Thontasen, N.; Rinke, G.; Le, D.; Turkowski, V.; Rahman, T. S.; Rauschenbach, S.; Ternes, M.; Kern, K. The Quantum Magnetism of Individual Manganese-12-Acetate Molecular Magnets Anchored at Surfaces. *Nano Lett.* **2012,** *12*, 518-521.
224. Iannuzzi, M.; Tran, F.; Widmer, R.; Dienel, T.; Radican, K.; Ding, Y.; Hutter, J.; Groning, O. Site-Selective Adsorption of Phthalocyanine on h-BN/Rh(111) Nanomesh. *Phys. Chem. Chem. Phys.* **2014,** *16*, 12374-12384.
225. Joshi, S.; Bischoff, F.; Koitz, R.; Ecija, D.; Seufert, K.; Seitsonen, A. P.; Hutter, J.; Diller, K.; Urgel, J. I.; Sachdev, H.; Barth, J. V.; Auwärter, W. Control of Molecular Organization and Energy Level Alignment by an Electronically Nanopatterned Boron Nitride Template. *ACS Nano* **2014,** *8*, 430-442.
226. Korolkov, V. V.; Baldoni, M.; Watanabe, K.; Taniguchi, T.; Besley, E.; Beton, P. H. Supramolecular Heterostructures Formed by Sequential Epitaxial Deposition of Two-Dimensional Hydrogen-Bonded Arrays. *Nat. Chem.* **2017,** *9*, 1191-1197.
227. Korolkov, V. V.; Svatek, S. A.; Summerfield, A.; Kerfoot, J.; Yang, L.; Taniguchi, T.; Watanabe, K.; Champness, N. R.; Besley, N. A.; Beton, P. H. Van der Waals-Induced Chromatic Shifts in Hydrogen-Bonded Two-Dimensional Porphyrin Arrays on Boron Nitride. *ACS Nano* **2015,** *9*, 10347-10355.
228. Lee, C. H.; Schiros, T.; Santos, E. J. G.; Kim, B.; Yager, K. G.; Kang, S. J.; Lee, S.; Yu, J.; Watanabe, K.; Taniguchi, T.; Hone, J.; Kaxiras, E.; Nuckolls, C.; Kim, P. Epitaxial Growth of Molecular Crystals on van der Waals Substrates for High‐Performance Organic Electronics. *Adv. Mater.* **2014,** *26*, 2812-2817.
229. He, D.; Zhang, Y.; Wu, Q.; Xu, R.; Nan, H.; Liu, J.; Yao, J.; Wang, Z.; Yuan, S.; Li, Y.; Shi, Y.; Wang, J.; Ni, Z.; He, L.; Miao, F.; Song, F.; Xu, H.; Watanabe, K.; Taniguchi, T.; Xu, J.-B.*, et al.* Two-Dimensional Quasi-Freestanding Molecular Crystals for High-Performance Organic Field-Effect Transistors. *Nat. Commun.* **2014,** *5*, 5162-5168.
230. Zhang, Y.; Qiao, J.; Gao, S.; Hu, F.; He, D.; Wu, B.; Yang, Z.; Xu, B.; Li, Y.; Shi, Y.; Ji, W.; Wang, P.; Wang, X.; Xiao, M.; Xu, H.; Xu, J.-B.; Wang, X. Probing Carrier Transport and Structure-Property Relationship of Highly Ordered Organic Semiconductors at the Two-Dimensional Limit. *Phys. Rev. Lett.* **2016,** *116*, 0166020-0166025.
231. Korolkov, V. V.; Svatek, S. A.; Allen, S.; Roberts, C. J.; Tendler, S. J. B.; Taniguchi, T.; Watanabe, K.; Champness, N. R.; Beton, P. H. Bimolecular Porous Supramolecular Networks Deposited from Solution on lLayered Materials: Graphite, Boron Nitride, and Molybdenum Disulphide. *Chem. Commun.* **2014,** *50*, 8882-8885.
232. Muller, M.; Paulheim, A.; Eisfeld, A.; Sokolowski, M. Finite Size Line Broadening and Superradiance of Optical Transitions in Two Dimensional Long-Range Ordered Molecular Aggregates. *J. Chem. Phys.* **2013,** *139*, 044302-044310.
233. Eisfeld, A.; Marquardt, C.; Paulheim, A.; Sokolowski, M. Superradiance from Two Dimensional Brick-Wall Aggregates of Dye Molecules: The Role of Size and Shape for the Temperature Dependence. *Phys. Rev. Lett.* **2017,** *119*, 097402-097406.
234. Imada, H.; Miwa, K.; Imai-Imada, M.; Kawahara, S.; Kimura, K.; Kim, Y. Real-Space Investigation of Energy Transfer in Heterogeneous Molecular Dimers. *Nature* **2016,** *538*, 364-367.

235. Zhang, Y.; Luo, Y.; Zhang, Y.; Yu, Y.-J.; Kuang, Y.-M.; Zhang, L.; Meng, Q.-S.; Luo, Y.; Yang, J.-L.; Dong, Z.-C.; Hou, J. G. Visualizing Coherent Intermolecular Dipole–Dipole Coupling in Real Space. *Nature* **2016,** *531*, 623-627.
236. Rahe, P.; Lindner, R.; Kittelmann, M.; Nimmrich, M.; Kuhnle, A. From Dewetting to Wetting Molecular Layers: C_{60} on CaCO3(1014) as a Case Study. *Phys. Chem. Chem. Phys.* **2012,** *14*, 6544-6548.
237. Jaekel, S.; Richter, A.; Lindner, R.; Bechstein, R.; Nacci, C.; Hecht, S.; Kühnle, A.; Grill, L. Reversible and Efficient Light-Induced Molecular Switching on an Insulator Surface. *ACS Nano* **2018,** *12*, 1821-1828.
238. Kim, M.; Hohman, J. N.; Cao, Y.; Houk, K. N.; Ma, H.; Jen, A. K.-Y.; Weiss, P. S. Creating Favorable Geometries for Directing Organic Photoreactions in Alkanethiolate Monolayers. *Science* **2011,** *331*, 1312-1315.
239. Grim, P. C. M.; De Feyter, S.; Gesquière, A.; Vanoppen, P.; Rüker, M.; Valiyaveettil, S.; Moessner, G.; Müllen, K.; De Schryver, F. C. Submolecularly Resolved Polymerization of Diacetylene Molecules on the Graphite Surface Observed with Scanning Tunneling Microscopy. *Angew. Chem. Int. Ed. Engl.* **1997,** *36*, 2601-2603.
240. Takami, T.; Ozaki, H.; Kasuga, M.; Tsuchiya, T.; Ogawa, A.; Mazaki, Y.; Fukushi, D.; Uda, M.; Aono, M. Periodic Structure of a Single Sheet of a Clothlike Macromolecule (Atomic Cloth) Studied by Scanning Tunneling Microscopy. *Angew. Chem. Int. Ed. Engl.* **1997,** *36*, 2755-2757.
241. Okawa, Y.; Aono, M. Nanoscale Control of Chain Polymerization. *Nature* **2001,** *409*, 683-684.
242. Sakaguchi, H.; Matsumura, H.; Gong, H. Electrochemical Epitaxial Polymerization of Single-Molecular Wires. *Nat. Mater.* **2004,** *3*, 551-557.
243. Sakaguchi, H.; Matsumura, H.; Gong, H.; Abouelwafa, A. M. Direct Visualization of the Formation of Single-Molecule Conjugated Copolymers. *Science* **2005,** *310*, 1002-1006.
244. McCarty, G. S.; Weiss, P. S. Formation and Manipulation of Protopolymer Chains. *J. Am. Chem. Soc.* **2004,** *126*, 16772-16776.
245. Lipton-Duffin, J. A.; Ivasenko, O.; Perepichka, D. F.; Rosei, F. Synthesis of Polyphenylene Molecular Wires by Surface-Confined Polymerization. *Small* **2009,** *5*, 592-597.
246. Grill, L.; Dyer, M.; Lafferentz, L.; Persson, M.; Peters, M. V.; Hecht, S. Nano-Architectures by Covalent Assembly of Molecular Building Blocks. *Nat. Nanotechnol.* **2007,** *2*, 687-691.
247. Cardenas, L.; Gutzler, R.; Lipton-Duffin, J.; Fu, C.; Brusso, J. L.; Dinca, L. E.; Vondráček, M.; Fagot-Revurat, Y.; Malterre, D.; Rosei, F.; Perepichka, D. F. Synthesis and Electronic Structure of a Two Dimensional π-Conjugated Polythiophene. *Chem. Sci.* **2013,** *4*, 3263-3268.
248. Bieri, M.; Nguyen, M.-T.; Gröning, O.; Cai, J.; Treier, M.; Aït-Mansour, K.; Ruffieux, P.; Pignedoli, C. A.; Passerone, D.; Kastler, M.; Müllen, K.; Fasel, R. Two-Dimensional Polymer Formation on Surfaces: Insight into the Roles of Precursor Mobility and Reactivity. *J. Am. Chem. Soc.* **2010,** *132*, 16669-16676.
249. Bieri, M.; Blankenburg, S.; Kivala, M.; Pignedoli, C. A.; Ruffieux, P.; Mullen, K.; Fasel, R. Surface-Supported 2D Heterotriangulene Polymers. *Chem. Commun.* **2011,** *47*, 10239-10241.
250. Gutzler, R.; Walch, H.; Eder, G.; Kloft, S.; Heckl, W. M.; Lackinger, M. Surface Mediated Synthesis of 2D Covalent Organic Frameworks: 1,3,5-Tris(4-bromophenyl)benzene on Graphite(001), Cu(111), and Ag(110). *Chem. Commun.* **2009**, 4456-4458.
251. Heimel, G.; Duhm, S.; Salzmann, I.; Gerlach, A.; Strozecka, A.; Niederhausen, J.; Bürker, C.; Hosokai, T.; Fernandez-Torrente, I.; Schulze, G.; Winkler, S.; Wilke, A.; Schlesinger, R.; Frisch, J.; Bröker, B.; Vollmer, A.; Detlefs, B.; Pflaum, J.; Kera, S.; Franke, K. J*., et al.* Charged and Metallic Molecular Monolayers Through Surface-Induced Aromatic Stabilization. *Nat. Chem.* **2013,** *5*, 187-194.
252. Han, P.; Mantooth, B. A.; Sykes, E. C. H.; Donhauser, Z. J.; Weiss, P. S. Benzene on Au{111} at 4 K: Monolayer Growth and Tip-Induced Molecular Cascades. *J. Am. Chem. Soc.* **2004,** *126*, 10787-10793.
253. Vasseur, G.; Fagot-Revurat, Y.; Sicot, M.; Kierren, B.; Moreau, L.; Malterre, D.; Cardenas, L.; Galeotti, G.; Lipton-Duffin, J.; Rosei, F.; Di Giovannantonio, M.; Contini, G.; Le Fèvre, P.; Bertran, F.; Liang,

L.; Meunier, V.; Perepichka, D. F. Quasi One-Dimensional Band Dispersion and Surface Metallization in Long-Range Ordered Polymeric Wires. *Nat. Commun.* **2016,** *7*, 10235-10243.
254. Di Giovannantonio, M.; El Garah, M.; Lipton-Duffin, J.; Meunier, V.; Cardenas, L.; Fagot Revurat, Y.; Cossaro, A.; Verdini, A.; Perepichka, D. F.; Rosei, F.; Contini, G. Insight into Organometallic Intermediate and Its Evolution to Covalent Bonding in Surface-Confined Ullmann Polymerization. *ACS Nano* **2013,** *7*, 8190-8198.
255. Di Giovannantonio, M.; Tomellini, M.; Lipton-Duffin, J.; Galeotti, G.; Ebrahimi, M.; Cossaro, A.; Verdini, A.; Kharche, N.; Meunier, V.; Vasseur, G.; Fagot-Revurat, Y.; Perepichka, D. F.; Rosei, F.; Contini, G. Mechanistic Picture and Kinetic Analysis of Surface-Confined Ullmann Polymerization. *J. Am. Chem. Soc.* **2016,** *138*, 16696-16702.
256. Björk, J.; Hanke, F.; Stafström, S. Mechanisms of Halogen-Based Covalent Self-Assembly on Metal Surfaces. *J. Am. Chem. Soc.* **2013,** *135*, 5768-5775.
257. Shi, K. J.; Yuan, D. W.; Wang, C. X.; Shu, C. H.; Li, D. Y.; Shi, Z. L.; Wu, X. Y.; Liu, P. N. Ullmann Reaction of Aryl Chlorides on Various Surfaces and the Application in Stepwise Growth of 2D Covalent Organic Frameworks. *Org. Lett.* **2016,** *18*, 1282-1285.
258. Galeotti, G.; Di Giovannantonio, M.; Lipton-Duffin, J.; Ebrahimi, M.; Tebi, S.; Verdini, A.; Floreano, L.; Fagot-Revurat, Y.; Perepichka, D.; Rosei, F.; Contini, G. The Role of Halogens in On-Surface Ullmann Polymerization. *Faraday Discuss.* **2017,** *204*, 453-469.
259. Lafferentz, L.; Eberhardt, V.; Dri, C.; Africh, C.; Comelli, G.; Esch, F.; Hecht, S.; Grill, L. Controlling On-Surface Polymerization by Hierarchical and Substrate-Directed Growth. *Nat. Chem.* **2012,** *4*, 215-220.
260. Blake, M. M.; Nanayakkara, S. U.; Claridge, S. A.; Fernández-Torres, L. C.; Sykes, E. C. H.; Weiss, P. S. Identifying Reactive Intermediates in the Ullmann Coupling Reaction by Scanning Tunneling Microscopy and Spectroscopy. *J. Phys. Chem. A* **2009,** *113*, 13167-13172.
261. Kamna, M. M. Atomic-Scale Views of Surface Chemistry: Structures, Interactions, and Intermediates. Ph. D. Thesis, The Pennsylvania State University, University Park, Pennsylvania, 1997.
262. Zhang, H.; Lin, H.; Sun, K.; Chen, L.; Zagranyarski, Y.; Aghdassi, N.; Duhm, S.; Li, Q.; Zhong, D.; Li, Y.; Müllen, K.; Fuchs, H.; Chi, L. On-Surface Synthesis of Rylene-Type Graphene Nanoribbons. *J. Am. Chem. Soc.* **2015,** *137*, 4022-4025.
263. Gutzler, R.; Perepichka, D. F. π-Electron Conjugation in Two Dimensions. *J. Am. Chem. Soc.* **2013,** *135*, 16585-16594.
264. Sun, Q.; Cai, L.; Ma, H.; Yuan, C.; Xu, W. Dehalogenative Homocoupling of Terminal Alkynyl Bromides on Au(111): Incorporation of Acetylenic Scaffolding into Surface Nanostructures. *ACS Nano* **2016,** *10*, 7023-7030.
265. Sun, Q.; Tran, B. V.; Cai, L.; Ma, H.; Yu, X.; Yuan, C.; Stöhr, M.; Xu, W. On-Surface Formation of Cumulene by Dehalogenative Homocoupling of Alkenyl *gem*-Dibromides. *Angew. Chem. Int. Ed.* **2017,** *56*, 12165-12169.
266. Sun, Q.; Cai, L.; Ding, Y.; Ma, H.; Yuan, C.; Xu, W. Single-Molecule Insight into Wurtz Reactions on Metal Surfaces. *Phys. Chem. Chem. Phys.* **2016,** *18*, 2730-2735.
267. Gao, H.-Y.; Held, P. A.; Knor, M.; Mück-Lichtenfeld, C.; Neugebauer, J.; Studer, A.; Fuchs, H. Decarboxylative Polymerization of 2,6-Naphthalenedicarboxylic Acid at Surfaces. *J. Am. Chem. Soc.* **2014,** *136*, 9658-9663.
268. In't Veld, M.; Iavicoli, P.; Haq, S.; Amabilino, D. B.; Raval, R. Unique Intermolecular Reaction of Simple Porphyrins at a Metal Surface Gives Covalent Nanostructures. *Chem. Commun.* **2008**, 1536-1538.
269. Cirera, B.; Giménez-Agulló, N.; Björk, J.; Martínez-Peña, F.; Martin-Jimenez, A.; Rodriguez-Fernandez, J.; Pizarro, A. M.; Otero, R.; Gallego, J. M.; Ballester, P.; Galan-Mascaros, J. R.; Ecija, D. Thermal Selectivity of Intermolecular *versus* Intramolecular Reactions on Surfaces. *Nat. Commun.* **2016,** *7*, 11002-11009.

270. Zhong, D.; Franke, J.-H.; Podiyanachari, S. K.; Blömker, T.; Zhang, H.; Kehr, G.; Erker, G.; Fuchs, H.; Chi, L. Linear Alkane Polymerization on a Gold Surface. *Science* **2011,** *334*, 213-216.
271. Gao, H.-Y.; Wagner, H.; Zhong, D.; Franke, J.-H.; Studer, A.; Fuchs, H. Glaser Coupling at Metal Surfaces. *Angew. Chem. Int. Ed.* **2013,** *52*, 4024-4028.
272. Zhang, Y.-Q.; Kepčija, N.; Kleinschrodt, M.; Diller, K.; Fischer, S.; Papageorgiou, A. C.; Allegretti, F.; Björk, J.; Klyatskaya, S.; Klappenberger, F.; Ruben, M.; Barth, J. V. Homo-Coupling of Terminal Alkynes on a Noble Metal Surface. *Nat. Commun.* **2012,** *3*, 1286-1293.
273. Saywell, A.; Browning, A. S.; Rahe, P.; Anderson, H. L.; Beton, P. H. Organisation and Ordering of 1D Porphyrin Polymers Synthesised by On-Surface Glaser Coupling. *Chem. Commun.* **2016,** *52*, 10342-10345.
274. Klappenberger, F.; Zhang, Y.-Q.; Björk, J.; Klyatskaya, S.; Ruben, M.; Barth, J. V. On-Surface Synthesis of Carbon-Based Scaffolds and Nanomaterials Using Terminal Alkynes. *Acc. Chem. Res.* **2015,** *48*, 2140-2150.
275. Dinca, L. E.; MacLeod, J. M.; Lipton-Duffin, J.; Fu, C.; Ma, D.; Perepichka, D. F.; Rosei, F. Tip-Induced C-H Activation and Oligomerization of Thienoanthracenes. *Chem. Commun.* **2014,** *50*, 8791-8793.
276. Treier, M.; Pignedoli, C. A.; Laino, T.; Rieger, R.; Müllen, K.; Passerone, D.; Fasel, R. Surface-Assisted Cyclodehydrogenation Provides a Synthetic Route Towards Easily Processable and Chemically Tailored Nanographenes. *Nat. Chem.* **2011,** *3*, 61-67.
277. Sun, Q.; Zhang, C.; Kong, H.; Tan, Q.; Xu, W. On-Surface Aryl-Aryl Coupling *via* Selective C-H Activation. *Chem. Commun.* **2014,** *50*, 11825-11828.
278. Sun, Q.; Zhang, C.; Cai, L.; Xie, L.; Tan, Q.; Xu, W. On-Surface Formation of Two-Dimensional Polymer *via* Direct C-H Activation of Metal Phthalocyanine. *Chem. Commun.* **2015,** *51*, 2836-2839.
279. Li, Q.; Yang, B.; Lin, H.; Aghdassi, N.; Miao, K.; Zhang, J.; Zhang, H.; Li, Y.; Duhm, S.; Fan, J.; Chi, L. Surface-Controlled Mono/Diselective *ortho* C–H Bond Activation. *J. Am. Chem. Soc.* **2016,** *138*, 2809-2814.
280. Cote, A. P.; Benin, A. I.; Ockwig, N. W.; O'Keeffe, M.; Matzger, A. J.; Yaghi, O. M. Porous, Crystalline, Covalent Organic Frameworks. *Science* **2005,** *310*, 1166-1170.
281. Zwaneveld, N. A. A.; Pawlak, R.; Abel, M.; Catalin, D.; Gigmes, D.; Bertin, D.; Porte, L. Organized Formation of 2D Extended Covalent Organic Frameworks at Surfaces. *J. Am. Chem. Soc.* **2008,** *130*, 6678-6679.
282. Dienstmaier, J. F.; Gigler, A. M.; Goetz, A. J.; Knochel, P.; Bein, T.; Lyapin, A.; Reichlmaier, S.; Heckl, W. M.; Lackinger, M. Synthesis of Well-Ordered COF Monolayers: Surface Growth of Nanocrystalline Precursors *versus* Direct On-Surface Polycondensation. *ACS Nano* **2011,** *5*, 9737-9745.
283. Guan, C.-Z.; Wang, D.; Wan, L.-J. Construction and Repair of Highly Ordered 2D Covalent Networks by Chemical Equilibrium Regulation. *Chem. Commun.* **2012,** *48*, 2943-2945.
284. Yu, L.; Li, Z. B.; Wang, D. Construction of Boronate Ester Based Single-Layered Covalent Organic Frameworks. *Chem. Commun.* **2016,** *52*, 13771-13774.
285. Liu, C. H.; Yu, Y. X.; Zhang, W.; Zeng, Q. D.; Lei, S. B. Room-Temperature Synthesis of Covalent Organic Frameworks with a Boronic Ester Linkage at the Liquid/Solid Interface. *Chem. Eur. J.* **2016,** *22*, 18412-18418.
286. Spitzer, S.; Rastgoo-Lahrood, A.; Macknapp, K.; Ritter, V.; Sotier, S.; Hecklab, W. M.; Lackinger, M. Solvent-Free On-Surface Synthesis of Boroxine COF Monolayers. *Chem. Commun.* **2017,** *53*, 5147-5150.
287. Tanoue, R.; Higuchi, R.; Enoki, N.; Miyasato, Y.; Uemura, S.; Kimizuka, N.; Stieg, A. Z.; Gimzewski, J. K.; Kunitake, M. Thermodynamically Controlled Self-Assembly of Covalent Nanoarchitectures in Aqueous Solution. *ACS Nano* **2011,** *5*, 3923-3929.
288. Liu, X. H.; Guan, C. Z.; Ding, S. Y.; Wang, W.; Yan, H. J.; Wang, D.; Wan, L. J. On-Surface Synthesis of Single-Layered Two-Dimensional Covalent Organic Frameworks *via* Solid-Vapor Interface Reactions. *J. Am. Chem. Soc.* **2013,** *135*, 10470-10474.

289. Yu, Y.; Lin, J.; Wang, Y.; Zeng, Q.; Lei, S. Room Temperature On-Surface Synthesis of Two-Dimensional Imine Polymers at the Solid/Liquid Interface: Concentration Takes Control. *Chem. Commun.* **2016,** *52*, 6609-6612.
290. Yue, J. Y.; Mo, Y. P.; Li, S. Y.; Dong, W. L.; Chen, T.; Wang, D. Simultaneous Construction of Two Linkages for the On-Surface Synthesis of Imine-Boroxine Hybrid Covalent Organic Frameworks. *Chem. Sci.* **2017,** *8*, 2169-2174.
291. Ciesielski, A.; El Garah, M.; Haar, S.; Kovaricek, P.; Lehn, J. M.; Samori, P. Dynamic Covalent Chemistry of Bisimines at the Solid/Liquid Interface Monitored by Scanning Tunnelling Microscopy. *Nat. Chem.* **2014,** *6*, 1017-1023.
292. Mo, Y.-P.; Liu, X.-H.; Wang, D. Concentration-Directed Polymorphic Surface Covalent Organic Frameworks: Rhombus, Parallelogram, and Kagome. *ACS Nano* **2017,** *11*, 11694-11700.
293. Son, Y.-W.; Cohen, M. L.; Louie, S. G. Energy Gaps in Graphene Nanoribbons. *Phys. Rev. Lett.* **2006,** *97*, 216803-216806.
294. Han, M. Y.; Özyilmaz, B.; Zhang, Y.; Kim, P. Energy Band-Gap Engineering of Graphene Nanoribbons. *Phys. Rev. Lett.* **2007,** *98*, 206805-206808.
295. Wei, D.; Xie, L.; Lee, K. K.; Hu, Z.; Tan, S.; Chen, W.; Sow, C. H.; Chen, K.; Liu, Y.; Wee, A. T. S. Controllable Unzipping for Intramolecular Junctions of Graphene Nanoribbons and Single-Walled Carbon Nanotubes. *Nat. Commun.* **2013,** *4*, 1374-1382.
296. Kawai, S.; Benassi, A.; Gnecco, E.; Söde, H.; Pawlak, R.; Feng, X.; Müllen, K.; Passerone, D.; Pignedoli, C. A.; Ruffieux, P.; Fasel, R.; Meyer, E. Superlubricity of Graphene Nanoribbons on Gold Surfaces. *Science* **2016,** *351*, 957-961.
297. Nakada, K.; Fujita, M.; Dresselhaus, G.; Dresselhaus, M. S. Edge State in Graphene Ribbons: Nanometer Size Effect and Edge Shape Dependence. *Phys. Rev. B* **1996,** *54*, 17954-17961.
298. Chen, L.; Hernandez, Y.; Feng, X.; Müllen, K. From Nanographene and Graphene Nanoribbons to Graphene Sheets: Chemical Synthesis. *Angew. Chem. Int. Ed.* **2012,** *51*, 7640-7654.
299. Son, Y.-W.; Cohen, M. L.; Louie, S. G. Half-Metallic Graphene Nanoribbons. *Nature* **2006,** *444*, 347-349.
300. Cai, J.; Ruffieux, P.; Jaafar, R.; Bieri, M.; Braun, T.; Blankenburg, S.; Muoth, M.; Seitsonen, A. P.; Saleh, M.; Feng, X.; Mullen, K.; Fasel, R. Atomically Precise Bottom-Up Fabrication of Graphene Nanoribbons. *Nature* **2010,** *466*, 470-473.
301. Chen, Y.-C.; de Oteyza, D. G.; Pedramrazi, Z.; Chen, C.; Fischer, F. R.; Crommie, M. F. Tuning the Band Gap of Graphene Nanoribbons Synthesized from Molecular Precursors. *ACS Nano* **2013,** *7*, 6123-6128.
302. Han, P.; Akagi, K.; Federici Canova, F.; Mutoh, H.; Shiraki, S.; Iwaya, K.; Weiss, P. S.; Asao, N.; Hitosugi, T. Bottom-Up Graphene-Nanoribbon Fabrication Reveals Chiral Edges and Enantioselectivity. *ACS Nano* **2014,** *8*, 9181-9187.
303. Chen, Y.-C.; Cao, T.; Chen, C.; Pedramrazi, Z.; Haberer, D.; de Oteyza, D. G.; Fischer, F. R.; Louie, S. G.; Crommie, M. F. Molecular Bandgap Engineering of Bottom-Up Synthesized Graphene Nanoribbon Heterojunctions. *Nat. Nanotechnol.* **2015,** *10*, 156-160.
304. Han, P.; Akagi, K.; Federici Canova, F.; Mutoh, H.; Shiraki, S.; Iwaya, K.; Weiss, P. S.; Asao, N.; Hitosugi, T. Reply to "Comment on 'Bottom-Up Graphene-Nanoribbon Fabrication Reveals Chiral Edges and Enantioselectivity'". *ACS Nano* **2015,** *9*, 3404-3405.
305. Han, P.; Akagi, K.; Federici Canova, F.; Shimizu, R.; Oguchi, H.; Shiraki, S.; Weiss, P. S.; Asao, N.; Hitosugi, T. Self-Assembly Strategy for Fabricating Connected Graphene Nanoribbons. *ACS Nano* **2015,** *9*, 12035-12044.
306. Sánchez-Sánchez, C.; Dienel, T.; Deniz, O.; Ruffieux, P.; Berger, R.; Feng, X.; Müllen, K.; Fasel, R. Purely Armchair or Partially Chiral: Noncontact Atomic Force Microscopy Characterization of Dibromo-Bianthryl-Based Graphene Nanoribbons Grown on Cu(111). *ACS Nano* **2016,** *10*, 8006-8011.

307. de Oteyza, D. G.; García-Lekue, A.; Vilas-Varela, M.; Merino-Díez, N.; Carbonell-Sanromà, E.; Corso, M.; Vasseur, G.; Rogero, C.; Guitián, E.; Pascual, J. I.; Ortega, J. E.; Wakayama, Y.; Peña, D. Substrate-Independent Growth of Atomically Precise Chiral Graphene Nanoribbons. *ACS Nano* **2016,** *10*, 9000-9008.
308. Bronner, C.; Durr, R. A.; Rizzo, D. J.; Lee, Y.-L.; Marangoni, T.; Kalayjian, A. M.; Rodriguez, H.; Zhao, W.; Louie, S. G.; Fischer, F. R.; Crommie, M. F. Hierarchical On-Surface Synthesis of Graphene Nanoribbon Heterojunctions. *ACS Nano* **2018,** *12*, 2193-2200.
309. Sakaguchi, H.; Kawagoe, Y.; Hirano, Y.; Iruka, T.; Yano, M.; Nakae, T. Width-Controlled Sub-Nanometer Graphene Nanoribbon Films Synthesized by Radical-Polymerized Chemical Vapor Deposition. *Adv. Mater.* **2014,** *26*, 4134-4138.
310. Narita, A.; Feng, X.; Müllen, K. Bottom-Up Synthesis of Chemically Precise Graphene Nanoribbons. *Chem. Rec.* **2015,** *15*, 295-309.
311. Xu, W.; Lee, T.-W. Recent Progress on Fabrication Techniques of Graphene Nanoribbons. *Mater. Horiz.* **2016,** *3*, 186-207.
312. Ruffieux, P.; Wang, S.; Yang, B.; Sánchez-Sánchez, C.; Liu, J.; Dienel, T.; Talirz, L.; Shinde, P.; Pignedoli, C. A.; Passerone, D.; Dumslaff, T.; Feng, X.; Müllen, K.; Fasel, R. On-Surface Synthesis of Graphene Nanoribbons with Zigzag Edge Topology. *Nature* **2016,** *531*, 489-492.
313. Kawai, S.; Saito, S.; Osumi, S.; Yamaguchi, S.; Foster, A. S.; Spijker, P.; Meyer, E. Atomically Controlled Substitutional Boron-Doping of Graphene Nanoribbons. *Nat. Commun.* **2015,** *6*, 8098-8103.
314. Simonov, K. A.; Vinogradov, N. A.; Vinogradov, A. S.; Generalov, A. V.; Zagrebina, E. M.; Svirskiy, G. I.; Cafolla, A. A.; Carpy, T.; Cunniffe, J. P.; Taketsugu, T.; Lyalin, A.; Mårtensson, N.; Preobrajenski, A. B. From Graphene Nanoribbons on Cu(111) to Nanographene on Cu(110): Critical Role of Substrate Structure in the Bottom-Up Fabrication Strategy. *ACS Nano* **2015,** *9*, 8997-9011.
315. Huang, H.; Wei, D.; Sun, J.; Wong, S. L.; Feng, Y. P.; Neto, A. H. C.; Wee, A. T. S. Spatially Resolved Electronic Structures of Atomically Precise Armchair Graphene Nanoribbons. *Sci. Rep.* **2012,** *2*, 983-989.
316. Bronner, C.; Stremlau, S.; Gille, M.; Braußе, F.; Haase, A.; Hecht, S.; Tegeder, P. Aligning the Band Gap of Graphene Nanoribbons by Monomer Doping. *Angew. Chem. Int. Ed.* **2013,** *52*, 4422-4425.
317. Cai, J.; Pignedoli, C. A.; Talirz, L.; Ruffieux, P.; Söde, H.; Liang, L.; Meunier, V.; Berger, R.; Li, R.; Feng, X.; Müllen, K.; Fasel, R. Graphene Nanoribbon Heterojunctions. *Nat. Nano.* **2014,** *9*, 896-900.
318. Nguyen, G. D.; Tsai, H.-Z.; Omrani, A. A.; Marangoni, T.; Wu, M.; Rizzo, D. J.; Rodgers, G. F.; Cloke, R. R.; Durr, R. A.; Sakai, Y.; Liou, F.; Aikawa, A. S.; Chelikowsky, J. R.; Louie, S. G.; Fischer, F. R.; Crommie, M. F. Atomically Precise Graphene Nanoribbon Heterojunctions from a Single Molecular Precursor. *Nat. Nanotechnol.* **2017,** *12*, 1077-1083.
319. Simonov, K. A.; Vinogradov, N. A.; Vinogradov, A. S.; Generalov, A. V.; Zagrebina, E. M.; Mårtensson, N.; Cafolla, A. A.; Carpy, T.; Cunniffe, J. P.; Preobrajenski, A. B. Comment on "Bottom-Up Graphene-Nanoribbon Fabrication Reveals Chiral Edges and Enantioselectivity". *ACS Nano* **2015,** *9*, 3399-3403.
320. Dinca, L. E.; Fu, C.; MacLeod, J. M.; Lipton-Duffin, J.; Brusso, J. L.; Szakacs, C. E.; Ma, D.; Perepichka, D. F.; Rosei, F. Unprecedented Transformation of Tetrathienoanthracene into Pentacene on Ni(111). *ACS Nano* **2013,** *7*, 1652-1657.
321. Dinca, L. E.; MacLeod, J. M.; Lipton-Duffin, J.; Fu, C.; Ma, D.; Perepichka, D. F.; Rosei, F. Tailoring the Reaction Path in the On-Surface Chemistry of Thienoacenes. *J. Phys. Chem. C* **2015,** *119*, 22432-22438.
322. Zugermeier, M.; Gruber, M.; Schmid, M.; Klein, B. P.; Ruppenthal, L.; Muller, P.; Einholz, R.; Hieringer, W.; Berndt, R.; Bettinger, H. F.; Gottfried, J. M. On-Surface Synthesis of Heptacene and its Interaction with a Metal Surface. *Nanoscale* **2017,** *9*, 12461-12469.
323. Zuzak, R.; Dorel, R.; Krawiec, M.; Such, B.; Kolmer, M.; Szymonski, M.; Echavarren, A. M.; Godlewski, S. Nonacene Generated by On-Surface Dehydrogenation. *ACS Nano* **2017,** *11*, 9321-9329.
324. Justus, K.; Fátima, G.; Frank, E.; Dmitry, S.; M., A. J.; Enrique, G.; Dolores, P.; Gianaurelio, C.; Francesca, M.; Diego, P. Decacene: On-Surface Generation. *Angew. Chem. Int. Ed.* **2017,** *56*, 11945-11948.

325. Pavliček, N.; Mistry, A.; Majzik, Z.; Moll, N.; Meyer, G.; Fox, D. J.; Gross, L. Synthesis and Characterization of Triangulene. *Nat. Nanotechnol.* **2017,** *12*, 308-311.
326. de Oteyza, D. G.; Gorman, P.; Chen, Y.-C.; Wickenburg, S.; Riss, A.; Mowbray, D. J.; Etkin, G.; Pedramrazi, Z.; Tsai, H.-Z.; Rubio, A.; Crommie, M. F.; Fischer, F. R. Direct Imaging of Covalent Bond Structure in Single-Molecule Chemical Reactions. *Science* **2013,** *340*, 1434-1437.
327. Polanyi, J. C.; Wong, W. H. Location of Energy Barriers. I. Effect on the Dynamics of Reactions A + BC. *J. Chem. Phys.* **1969,** *51*, 1439-1450.
328. Mok, M. H.; Polanyi, J. C. Location of Energy Barriers. II. Correlation with Barrier Height. *J. Chem. Phys.* **1969,** *51*, 1451-1469.
329. Polanyi, J. C. Some Concepts in Reaction Dynamics. *Science* **1987,** *236*, 680-690.
330. Ebrahimi, M.; Guo, S. Y.; McNab, I. R.; Polanyi, J. C. "Early" and "Late" Barriers in Dissociative Attachment: Steering Surface Reaction. *J. Phys. Chem. Lett.* **2010,** *1*, 2600-2605.
331. Leung, L.; Lim, T.; Polanyi, J. C.; Hofer, W. A. Molecular Calipers Control Atomic Separation at a Metal Surface. *Nano Lett.* **2011,** *11*, 4113-4117.
332. Eisenstein, A.; Leung, L.; Lim, T.; Ning, Z.; Polanyi, J. C. Reaction Dynamics at a Metal Surface; Halogenation of Cu(110). *Faraday Discuss.* **2012,** *157*, 337-353.
333. Chatterjee, A.; Cheng, F.; Leung, L.; Luo, M.; Ning, Z.; Polanyi, J. C. Molecular Dynamics of the Electron-Induced Reaction of Diiodomethane on Cu(110). *J. Phys. Chem. C* **2014,** *118*, 25525-25533.
334. Rastgoo-Lahrood, A.; Björk, J.; Lischka, M.; Eichhorn, J.; Kloft, S.; Fritton, M.; Strunskus, T.; Samanta, D.; Schmittel, M.; Heckl, W. M.; Lackinger, M. Post-Synthetic Decoupling of On-Surface-Synthesized Covalent Nanostructures from Ag(111). *Angew. Chem. Int. Ed.* **2016,** *55*, 7650-7654.
335. Kittelmann, M.; Rahe, P.; Nimmrich, M.; Hauke, C. M.; Gourdon, A.; Kühnle, A. On-Surface Covalent Linking of Organic Building Blocks on a Bulk Insulator. *ACS Nano* **2011,** *5*, 8420-8425.
336. Kolmer, M.; Zuzak, R.; Zebari, A. A. A.; Godlewski, S.; Prauzner-Bechcicki, J. S.; Piskorz, W.; Zasada, F.; Sojka, Z.; Bléger, D.; Hecht, S.; Szymonski, M. On-Surface Polymerization on a Semiconducting Oxide: Aryl Halide Coupling Controlled by Surface Hydroxyl Groups on Rutile TiO_2(011). *Chem. Commun.* **2015,** *51*, 11276-11279.
337. Vasseur, G.; Abadia, M.; Miccio, L. A.; Brede, J.; Garcia-Lekue, A.; de Oteyza, D. G.; Rogero, C.; Lobo-Checa, J.; Ortega, J. E. Π Band Dispersion along Conjugated Organic Nanowires Synthesized on a Metal Oxide Semiconductor. *J. Am. Chem. Soc.* **2016,** *138*, 5685-5692.
338. Richter, A.; Haapasilta, V.; Venturini, C.; Bechstein, R.; Gourdon, A.; Foster, A. S.; Kuhnle, A. Diacetylene Polymerization on a Bulk Insulator Surface. *Phys. Chem. Chem. Phys.* **2017,** *19*, 15172-15176.
339. Marina, V. M.; Yuji, O.; Elisseos, V.; Kenji, W.; Takashi, T.; Christian, J.; Masakazu, A. Self-Assembled Diacetylene Molecular Wire Polymerization on an Insulating Hexagonal Boron Nitride (0001) Surface. *Nanotechnology* **2016,** *27*, 395303-395310.
340. Verveniotis, E.; Okawa, Y.; Watanabe, K.; Taniguchi, T.; Taniguchi, T.; Osada, M.; Joachim, C.; Aono, M. Self-Sensitization and Photo-Polymerization of Diacetylene Molecules Self-Assembled on a Hexagonal-Boron Nitride Nanosheet. *Polymers* **2018,** *10*, 206-214.
341. Gobbi, M.; Bonacchi, S.; Lian, J. X.; Liu, Y.; Wang, X.-Y.; Stoeckel, M.-A.; Squillaci, M. A.; D'Avino, G.; Narita, A.; Müllen, K.; Feng, X.; Olivier, Y.; Beljonne, D.; Samorì, P.; Orgiu, E. Periodic Potentials in Hybrid van der Waals Heterostructures Formed by Supramolecular Lattices on Graphene. *Nat. Commun.* **2017,** *8*, 14767-14774.
342. Xia, Z.; Leonardi, F.; Gobbi, M.; Liu, Y.; Bellani, V.; Liscio, A.; Kovtun, A.; Li, R.; Feng, X.; Orgiu, E.; Samorì, P.; Treossi, E.; Palermo, V. Electrochemical Functionalization of Graphene at the Nanoscale with Self-Assembling Diazonium Salts. *ACS Nano* **2016,** *10*, 7125-7134.
343. Bragança, A. M.; Greenwood, J.; Ivasenko, O.; Phan, T. H.; Müllen, K.; De Feyter, S. The Impact of Grafted Surface Defects and Their Controlled Removal on Supramolecular Self-Assembly. *Chem. Sci.* **2016,** *7*, 7028-7033.

344. Verstraete, L.; Greenwood, J.; Hirsch, B. E.; De Feyter, S. Self-Assembly under Confinement: Nanocorrals for Understanding Fundamentals of 2D Crystallization. *ACS Nano* **2016,** *10*, 10706-10715.
345. Choi, S. H.; Kim, B.; Frisbie, C. D. Electrical Resistance of Long Conjugated Molecular Wires. *Science* **2008,** *320*, 1482-1486.
346. Perera, U. G. E.; Ample, F.; Kersell, H.; Zhang, Y.; Vives, G.; Echeverria, J.; Grisolia, M.; Rapenne, G.; Joachim, C.; Hla, S. W. Controlled Clockwise and Anticlockwise Rotational Switching of a Molecular Motor. *Nat. Nanotechnol.* **2012,** *8*, 46-51.
347. Dong, Y.; Goubert, G.; Groves, M. N.; Lemay, J.-C.; Hammer, B.; McBreen, P. H. Structure and Dynamics of Individual Diastereomeric Complexes on Platinum: Surface Studies Related to Heterogeneous Enantioselective Catalysis. *Acc. Chem. Res.* **2017,** *50*, 1163-1170.
348. Venkataraman, L.; Klare, J. E.; Nuckolls, C.; Hybertsen, M. S.; Steigerwald, M. L. Dependence of Single-Molecule Junction Conductance on Molecular Conformation. *Nature* **2006,** *442*, 904-907.
349. Tao, N. J. Electron Transport in Molecular Junctions. *Nat. Nanotechnol.* **2006,** *1*, 173-181.
350. Xing, Y.; Park, T.-H.; Venkatramani, R.; Keinan, S.; Beratan, D. N.; Therien, M. J.; Borguet, E. Optimizing Single-Molecule Conductivity of Conjugated Organic Oligomers with Carbodithioate Linkers. *J. Am. Chem. Soc.* **2010,** *132*, 7946-7956.
351. Mishchenko, A.; Vonlanthen, D.; Meded, V.; Bürkle, M.; Li, C.; Pobelov, I. V.; Bagrets, A.; Viljas, J. K.; Pauly, F.; Evers, F.; Mayor, M.; Wandlowski, T. Influence of Conformation on Conductance of Biphenyl-Dithiol Single-Molecule Contacts. *Nano Lett.* **2010,** *10*, 156-163.
352. Arroyo, C. R.; Frederiksen, T.; Rubio-Bollinger, G.; Vélez, M.; Arnau, A.; Sánchez-Portal, D.; Agraït, N. Characterization of Single-Molecule Pentanedithiol Junctions by Inelastic Electron Tunneling Spectroscopy and First-Principles Calculations. *Phys. Rev. B* **2010,** *81*, 075405-075409.
353. Choi, S. H.; Risko, C.; Delgado, M. C. R.; Kim, B.; Brédas, J.-L.; Frisbie, C. D. Transition from Tunneling to Hopping Transport in Long, Conjugated Oligo-imine Wires Connected to Metals. *J. Am. Chem. Soc.* **2010,** *132*, 4358-4368.
354. Koch, M.; Ample, F.; Joachim, C.; Grill, L. Voltage-Dependent Conductance of a Single Graphene Nanoribbon. *Nat. Nanotechnol.* **2012,** *7*, 713-717.
355. Temirov, R.; Lassise, A.; Anders, F. B.; Tautz, F. S. Kondo Effect by Controlled Cleavage of a Single-Molecule Contact. *Nanotechnology* **2008,** *19*, 065401-065413.
356. Reecht, G.; Scheurer, F.; Speisser, V.; Dappe, Y. J.; Mathevet, F.; Schull, G. Electroluminescence of a Polythiophene Molecular Wire Suspended Between a Metallic Surface and the Tip of a Scanning Tunneling Microscope. *Phys. Rev. Lett.* **2014,** *112*, 047403-047407.
357. Lafferentz, L.; Ample, F.; Yu, H.; Hecht, S.; Joachim, C.; Grill, L. Conductance of a Single Conjugated Polymer as a Continuous Function of Its Length. *Science* **2009,** *323*, 1193-1197.
358. Nacci, C.; Ample, F.; Bleger, D.; Hecht, S.; Joachim, C.; Grill, L. Conductance of a Single Flexible Molecular Wire Composed of Alternating Donor and Acceptor Units. *Nat. Commun.* **2015,** *6*, 7397-7404.
359. Thomas, L.; Lionti, F.; Ballou, R.; Gatteschi, D.; Sessoli, R.; Barbara, B. Macroscopic Quantum Tunnelling of Magnetization in a Single Crystal of Nanomagnets. *Nature* **1996,** *383*, 145-147.
360. Mannini, M.; Pineider, F.; Sainctavit, P.; Danieli, C.; Otero, E.; Sciancalepore, C.; Talarico, A. M.; Arrio, M.-A.; Cornia, A.; Gatteschi, D.; Sessoli, R. Magnetic Memory of a Single-Molecule Quantum Magnet Wired to a Gold Surface. *Nat. Mater.* **2009,** *8*, 194-197.
361. Bogani, L.; Wernsdorfer, W. Molecular Spintronics Using Single-Molecule Magnets. *Nat. Mater.* **2008,** *7*, 179-186.
362. Sessoli, R.; Gatteschi, D.; Caneschi, A.; Novak, M. A. Magnetic Bistability in a Metal-Ion Cluster. *Nature* **1993,** *365*, 141-143.
363. Zhao, A.; Li, Q.; Chen, L.; Xiang, H.; Wang, W.; Pan, S.; Wang, B.; Xiao, X.; Yang, J.; Hou, J. G.; Zhu, Q. Controlling the Kondo Effect of an Adsorbed Magnetic Ion through its Chemical Bonding. *Science* **2005,** *309*, 1542-1544.

364. Iancu, V.; Deshpande, A.; Hla, S.-W. Manipulation of the Kondo Effect *via* Two-Dimensional Molecular Assembly. *Phys. Rev. Lett.* **2006,** *97*, 266603-266606.
365. Fu, Y.-S.; Ji, S.-H.; Chen, X.; Ma, X.-C.; Wu, R.; Wang, C.-C.; Duan, W.-H.; Qiu, X.-H.; Sun, B.; Zhang, P.; Jia, J.-F.; Xue, Q.-K. Manipulating the Kondo Resonance through Quantum Size Effects. *Phys. Rev. Lett.* **2007,** *99*, 256601-256604.
366. Tsukahara, N.; Shiraki, S.; Itou, S.; Ohta, N.; Takagi, N.; Kawai, M. Evolution of Kondo Resonance from a Single Impurity Molecule to the Two-Dimensional Lattice. *Phys. Rev. Lett.* **2011,** *106*, 187201-187204.
367. Minamitani, E.; Tsukahara, N.; Matsunaka, D.; Kim, Y.; Takagi, N.; Kawai, M. Symmetry-Driven Novel Kondo Effect in a Molecule. *Phys. Rev. Lett.* **2012,** *109*, 086602-086606.
368. Tsukahara, N.; Minamitani, E.; Kim, Y.; Kawai, M.; Takagi, N. Controlling Orbital-Selective Kondo Effects in a Single Molecule through Coordination Chemistry. *J. Chem. Phys.* **2014,** *141*, 054702-054710.
369. Hulsken, B.; Van Hameren, R.; Gerritsen, J. W.; Khoury, T.; Thordarson, P.; Crossley, M. J.; Rowan, A. E.; Nolte, R. J. M.; Elemans, J. A. A. W.; Speller, S. Real-Time Single-Molecule Imaging of Oxidation Catalysis at a Liquid–Solid Interface. *Nat. Nanotechnol.* **2007,** *2*, 285-289.
370. den Boer, D.; Li, M.; Habets, T.; Iavicoli, P.; Rowan, A. E.; Nolte, R. J. M.; Speller, S.; Amabilino, D. B.; De Feyter, S.; Elemans, J. A. A. W. Detection of Different Oxidation States of Individual Manganese Porphyrins During Their Reaction with Oxygen at a Solid/Liquid Interface. *Nat. Chem.* **2013,** *5*, 621-627.
371. Li, M.; den Boer, D.; Iavicoli, P.; Adisoejoso, J.; Uji-i, H.; Van der Auweraer, M.; Amabilino, D. B.; Elemans, J. A. A. W.; De Feyter, S. Tip-Induced Chemical Manipulation of Metal Porphyrins at a Liquid/Solid Interface. *J. Am. Chem. Soc.* **2014,** *136*, 17418-17421.
372. Schuler, B.; Meyer, G.; Peña, D.; Mullins, O. C.; Gross, L. Unraveling the Molecular Structures of Asphaltenes by Atomic Force Microscopy. *J. Am. Chem. Soc.* **2015,** *137*, 9870-9876.
373. Amabilino, D. B.; Tait, S. Complex Molecular Surfaces and Interfaces: Concluding Remarks. *Faraday Discuss.* **2017,** *204*, 487-502.
374. Bonnell, D. A.; Basov, D. N.; Bode, M.; Diebold, U.; Kalinin, S. V.; Madhavan, V.; Novotny, L.; Salmeron, M.; Schwarz, U. D.; Weiss, P. S. Imaging Physical Phenomena with Local Probes: From Electrons to Photons. *Rev. Mod. Phys.* **2012,** *84*, 1343-1381.
375. Jiang, N.; Kurouski, D.; Pozzi, E. A.; Chiang, N.; Hersam, M. C.; Van Duyne, R. P. Tip-Enhanced Raman Spectroscopy: From Concepts to Practical Applications. *Chem. Phys. Lett.* **2016,** *659*, 16-24.
376. Pavliček, N.; Gross, L. Generation, Manipulation and Characterization of Molecules by Atomic Force Microscopy. *Nat. Rev. Chem.* **2017,** *1*, 5-15.
377. MacLean, O.; Huang, K.; Leung, L.; Polanyi, J. C. Direct and Delayed Dynamics in Electron-Induced Surface Reaction. *J. Am. Chem. Soc.* **2017,** *139*, 17368-17375.
378. Gallardo, R.; Ramakers, M.; De Smet, F.; Claes, F.; Khodaparast, L.; Khodaparast, L.; Couceiro, J. R.; Langenberg, T.; Siemons, M.; Nyström, S.; Young, L. J.; Laine, R. F.; Young, L.; Radaelli, E.; Benilova, I.; Kumar, M.; Staes, A.; Desager, M.; Beerens, M.; Vandervoort, P.*, et al. De Novo* Design of a Biologically Active Amyloid. *Science* **2016,** *354*, aah4949-aah4957.
379. Feng, M.; Sun, H.; Zhao, J.; Petek, H. Self-Catalyzed Carbon Dioxide Adsorption by Metal–Organic Chains on Gold Surfaces. *ACS Nano* **2014,** *8*, 8644-8652.
380. Jahanbekam, A.; Chilukuri, B.; Mazur, U.; Hipps, K. W. Kinetically Trapped Two-Component Self-Assembled Adlayer. *J. Phys. Chem. C* **2015,** *119*, 25364-25376.
381. Gobbi, M.; Orgiu, E.; Samorì, P. When 2D Materials Meet Molecules: Opportunities and Challenges of Hybrid Organic/Inorganic van der Waals Heterostructures. *Adv. Mater.* **2018,** *30*, 1706103-1706122.
382. Song, Z.; Schultz, T.; Ding, Z.; Lei, B.; Han, C.; Amsalem, P.; Lin, T.; Chi, D.; Wong, S. L.; Zheng, Y. J.; Li, M.-Y.; Li, L.-J.; Chen, W.; Koch, N.; Huang, Y. L.; Wee, A. T. S. Electronic Properties of a 1D Intrinsic/p-Doped Heterojunction in a 2D Transition Metal Dichalcogenide Semiconductor. *ACS Nano* **2017,** *11*, 9128-9135.

383. Hammer, B.; Norskov, J. K. Why Gold is the Noblest of All the Metals. *Nature* **1995,** *376*, 238-240.
384. Llinas, J. P.; Fairbrother, A.; Borin Barin, G.; Shi, W.; Lee, K.; Wu, S.; Yong Choi, B.; Braganza, R.; Lear, J.; Kau, N.; Choi, W.; Chen, C.; Pedramrazi, Z.; Dumslaff, T.; Narita, A.; Feng, X.; Müllen, K.; Fischer, F.; Zettl, A.; Ruffieux, P*., et al.* Short-Channel Field-Effect Transistors with 9-Atom and 13-Atom Wide Graphene Nanoribbons. *Nat. Commun.* **2017,** *8*, 633-638.
385. Service, R. F. Next-Generation Technology Hits an Early Midlife Crisis. *Science* **2003,** *302*, 556-559.

Suggested pull-out quotes:

- Two-dimensional nanostructures with remarkable structural complexity, and rationally tuned symmetry and periodicity have been created.
- The chiral outcome of self-assembly can be tuned and controlled, leading to homochiral surfaces of opposite chirality under optimized conditions
- Understanding the roles of kinetics is therefore essential to control the outcome of self-assembly
- Multi-component assembly … could greatly expand the fabrication of functional molecular nanostructures.
- Due to the inherently different structures and chemistry of the constituent moieties, it should be possible to tune the networks' energetics and kinetics by temperature, intermolecular interaction strength, and other environmental stimuli.
- Tunable symmetry, periodicity, and interactions of self-assembled molecular networks make them attractive as nanoscale templates for patterning functional materials on surfaces.
- The game-changing reaction that has enabled much of the explosive growth of the field of on-surface polymerization is Ullmann coupling, which links halogenated aromatic rings with a C–C bond.
- Despite significant progress in improving the order of on-surface synthesized covalent networks, their structural quality is limited … Dynamic covalent chemistry offers a possible solution to this problem.
- Scanning probe microscopy studies of molecules adsorbed on reactive surfaces have also led to the discovery of new reactions.
- Once molecular systems adsorb on surfaces, their intrinsic electronic and optical properties are modified by their interactions with the substrate.